

# PRACTICAL CHEMICAL KINETICS IN SOLUTION

OMAR A. EL SEOUD, WILHELM J. BAADER, AND ERICK L. BASTOS

*Department of Fundamental Chemistry, Institute of Chemistry, University of São Paulo, São Paulo, SP, Brazil*

## 1 INTRODUCTION AND SCOPE

Most of the information about reaction mechanism came and still comes from chemical kinetics; therefore, all science students have had contact with the subject. While there are many excellent textbooks on the theory of chemical kinetics, the information on practical kinetics in solution is dispersed in the literature; only those with some experience can find the information sought. The need for a concise text on practical kinetics has become critical in view of the universal use of computers in teaching and research. Thanks to this fact, data acquisition and subsequent calculations have become somewhat “boring” routine. Consequently, it is sometimes tempting to fall into the “black-box trap”: push buttons in order to mix the reagents, acquire the experimental data, and carry out the calculations. The problem is that, due to several experimental pitfalls, for example, not paying attention to the quality of the data acquired; poor control of reaction conditions; using software without understanding how it works, one may end up with rate constants that appear to be in order if examined for a single run. The problem may appear later, however, when the data from several runs are examined collectively, for example, the dependence of observed rate constant,  $k_{\text{obs}}$ , on [catalyst], or  $\log k_2$  (second-order rate constant) on  $1/T$  may show scatter. The person feels frustrated; rightly so.

We wrote the present overview with this background in mind. After listing the equations that describe simple and complex reactions, we address the question of obtaining quality kinetic data, first by describing the advantages and limitations of the techniques most frequently employed in chemical kinetics and how to analyze properly the data obtained. Drawing on practical experience, we considered some of the common pitfalls in kinetics, both in setting up the experiment and in performing the subsequent calculations. This concise account should be helpful to neophytes or occasional users of chemical kinetics, as

well as those who need to refresh/update their information on the subject. We have limited our discussion to reactions in solution. The kinetics of gas-phase reactions merits a separate account, in view of the distinctly different experimental setup.

## 2 FUNDAMENTALS OF CHEMICAL KINETICS

### 2.1 Basic Terminology

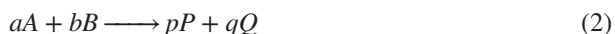
An important prelude to the discussion of chemical kinetics is the definition of terminology [1]. The following text summarizes some of the basic terms related to the kinetic study of chemical reactions, according to IUPAC recommendations [2]. More in-depth analysis is available elsewhere [2–22].

**2.1.1 Amount Concentration** Consider a chemical reaction occurring in a dilute and homogeneous system whose volume is constant. Under these conditions, the concentration can be employed instead of activity, as expressed by Equation 1 (*in what follows, unless specified otherwise, we assume the constant volume condition*):

$$[A] = \frac{n_A}{V} \quad (1)$$

where  $[A]$  indicates the concentration of species  $A$ ,  $V$  is solution volume, and  $n_A$  indicates the amount of ( $A$ ) present in that volume (i.e., the number of moles of  $A$ ). The units commonly employed are mole per cubic decimeter ( $\text{mol dm}^{-3}$ ) or mole per liter ( $\text{mol L}^{-1}$ ), the latter unit is sometimes denoted by ( $M$ ) a symbol that is now regarded as obsolete by IUPAC.

**2.1.2 Rate of Reaction ( $\nu$ )** For the general chemical reaction shown in Equation 2:



assuming that the reaction is essentially irreversible, that is, any intermediates formed are reactive and do not accumulate, then the reaction rate (usually referred by the symbols  $r$  or  $\nu$ ) is related to the rate of disappearance of reactants or formation of products by Equation 3.

$$\text{Rate} = -\frac{1}{a} \frac{d[A]}{dt} = -\frac{1}{b} \frac{d[B]}{dt} = \frac{1}{p} \frac{d[P]}{dt} = \frac{1}{q} \frac{d[Q]}{dt} \quad (3)$$

where the symbols within the brackets denote concentrations, ( $a$ ,  $b$ ,  $p$ ,  $q$ ) are the stoichiometric coefficients. In practice, it is usual to define the rate only in terms of the species whose concentration is being monitored. When the use of concentration is inconvenient, for example, under conditions of varying volume, the rate of conversion should be used instead of  $\nu$ .

**2.1.3 Rate Law** The empirical differential rate equation (or simply the rate law) is determined experimentally and is defined as the expression for the rate of reaction in terms of concentrations of chemical species as indicated by Equation 4:

$$\text{Rate} = k[A]^m[B]^n \quad (4)$$

where  $k$  is the rate constant (or rate coefficient) and the exponents ( $m$ ) and ( $n$ ) are determined experimentally and can be a whole number (positive or negative) or, in complex reactions, fractions. Note that these exponents are independent of concentration and time: their values are not necessarily the same as the stoichiometric coefficients ( $a$ ) and ( $b$ ) of Equation 2. The reaction rate equation (RRE) contains concentration terms for all species that interact *up to and including* the rate-limiting step (RLS, see below) [23]. Therefore, RRE does not contain concentration terms for species that are consumed in the reaction, but whose participation occurs after the RLS. An example is the acid- or base-catalyzed halogenation of acetone. The RLS is the enolization of the ketone; hence, the RRE does not contain a halogen concentration term. Therefore, under identical experimental conditions, the rates of chlorination and bromination of acetone are equal. The RRE may contain terms for chemical species that do not appear in the balanced chemical equation (such as the catalyst concentration, for example) and may be the sum of several terms for different reaction pathways (as in radical chain reactions).

**2.1.4 Order of Reaction** The order of reaction (or order of the rate law) is the sum of the exponents in the rate law, that is, the sum of the partial orders with respect to individual reagents, for example, ( $m + n$ ) of Equation 4. However, Zuman and Patel stressed that: “with more complex reactions the overall kinetic order loses its meaning, since the reaction rates are not simple functions of concentration. In such cases, systematically planned experiments enabling the verification of the complete RRE are necessary” [3].

**2.1.5 Molecularity** Molecularity is the number of colliding molecular entities that are involved in a single reaction step. While the order of a reaction is derived experimentally, the molecularity is a theoretical concept and can only be applied to elementary reactions. In elementary reactions, the reaction order, the molecularity, and the stoichiometric coefficient are numerically the same but represent different concepts. Thus, a reaction involving one molecular entity is called unimolecular, whereas a bimolecular reaction involves two molecular entities. A reaction involving three molecular entities is called termolecular or trimolecular; these reactions are rare because of the improbability of three molecular entities colliding simultaneously. However, the term termolecular is also used to refer to three-body association via consecutive reactions of the type shown in Equations 5 and 6.



Therefore, the relationship between molecularity and overall kinetic order of a reaction depends on the mechanism. For example, the (one step)  $S_N2$  reactions are both bimolecular and second order.

**2.1.6 Rate Constant** The rate constant,  $k$ , is the proportionality constant that relates the reaction rate to the concentration (or activity or pressure, for example) of the reacting substances, as shown in Equation 4. Consider a first-order reaction of a reagent ( $1.0 \text{ mol L}^{-1}$ ) whose  $k = 0.01 \text{ s}^{-1}$ . This means that each second,  $0.01 \text{ mol L}^{-1}$  of the reactant, is transformed into products. The value of  $k$  for two reactions of different orders (e.g., first, second) cannot be compared directly because their units are different.

**2.1.7 Rate-Controlling Step** A rate-controlling (rate-determining or rate-limiting) step is the slowest step of a chemical reaction that determines the rate of the overall reaction. In a simplified model, it can be compared to the neck of a funnel. The rate at which water flows through a funnel is limited/determined roughly by the width of the neck of the funnel and not by the rate at which the water is poured into the funnel. For any multistep reaction, the RLS is taken as the “most sensitive” step, or the step, which, if perturbed, causes the largest change in overall rate.

*Note on diffusion-limited rate coefficients:* In very fast reactions, every encounter of the reactants leads to chemical transformation. Therefore, the diffusion of the reactants through the solution is the rate-limiting process [24].

**2.1.8 Reaction Half-Life ( $t_{1/2}$ )** The half-life (or half-time,  $t_{1/2}$ ) of a reaction is the time required for the concentration of a given reactant to reach a value that is the arithmetic mean of its initial and final, or equilibrium, values. For a reactant that is entirely consumed, it is the time required for the reactant concentration to fall to one-half of its initial value. This term is used to convey a qualitative idea of the timescale for the reaction. It has a quantitative relationship to the rate constant in simple cases. For example, an irreversible first-order reaction is practically complete after five  $t_{1/2}$ , corresponding to 96.9% reactant transformation.

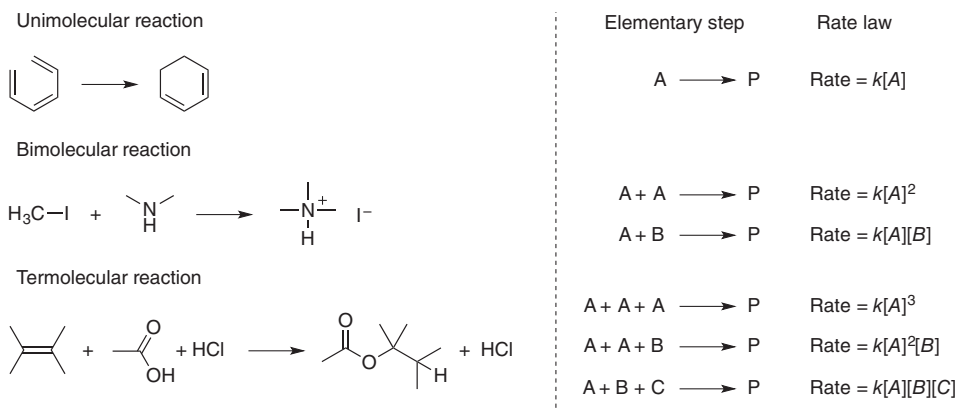
The half-life of a reaction has an exact quantitative meaning only in the following cases: (i) for a first-order reaction, where the half-life of the reactant may be called the half-life of the reaction; (ii) for a reaction involving more than one reactant, with their concentrations in their stoichiometric ratios. In this case, the half-life of each reactant is the same and may be called the half-life of the reaction. If the concentrations of reactants are not in their stoichiometric ratios, the half-lives for the different reactants are not the same and use of the term half-life of the reaction is not warranted.

**2.1.9 Lifetime ( $\tau$ )** For a molecular entity that is reacting by first-order kinetics, ( $\tau$ ) is the time required for its concentration to decrease to  $1/e$  ( $\approx 0.37$ ) of its initial value. Statistically, it represents the life “expectancy” of the entity. It is equal to the reciprocal of the sum of the first-order rate constants of all processes causing the decay of the molecular entity. This term is commonly used in the so-called lifetime methods, such as NMR, in relaxation methods, such as temperature jump, and in the kinetics of decay of electronically excited states.

**2.1.10 Elementary Reactions and Mechanisms** If a chemical reaction can be described as an *individual* molecular event, that is, occurs in a single step and passes through a single transition state, then it is referred to as an elementary reaction. In this case, the rate law can be deduced from the stoichiometry. Scheme 1 shows several examples of bimolecular elementary reactions and less common uni- and termolecular reactions.

The following are the criteria for considering a reaction as elementary [4]:

1. it should be part of van't Hoff's “natural classification,” that is, the reaction is assumed to be uni-, bi-, or termolecular;
2. its rate is governed by the mass-action law;
3. it occurs by overcoming one energetic barrier according to the principle “one energetic barrier, one elementary reaction” [20, 25].



**Scheme 1** Examples of elementary reactions.

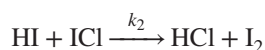
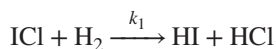
Kinetic studies are employed to determine the sequence of elementary reactions that makes up the overall reaction, that is, the *reaction mechanism* [6]. Consider the hydrogenation of iodine monochloride:



If one assumes that the reaction occurs in one elementary step (the bimolecular reaction between  $\text{ICl}$  and  $\text{H}_2$ ), then the derived rate law would be

$$\frac{1}{2} \frac{d[\text{HCl}]}{dt} = k[\text{ICl}][\text{H}_2] \quad (7)$$

However, the reaction may also occur in a stepwise manner:



resulting in a rate law that cannot be directly inferred from reaction stoichiometry. Clearly, the rate law must be determined experimentally. A kinetic study provides information about the change of the concentration of a given reactant or product as a function of time, allowing the determination of the rate law and providing evidence to support/reject a reaction mechanism that is not in agreement with the experimental result [26–29].

## 2.2 Empirical Reaction Rate Equations and Approximations

In this section, we discuss some examples of chemical reactions in solution, classified according to their reaction order. These examples introduce the most common approximations used for the analysis of kinetic data [5, 30].

### 2.2.1 Simple, Irreversible Reactions

*First-Order Reactions* The simplest chemical reaction is the first-order one, for which the rate is directly proportional to the concentration of a single species [31]. For the following reaction,



the reaction rate is given by:

$$\text{Rate} = -\frac{d[A]}{dt} = \frac{d[B]}{dt} = k_1[A] \quad (9)$$

Rearrangement of Equation 9 in terms of the concentration of the reactant ( $A$ ) and integration from  $t=0$  (initial concentration  $A_0$ ) to time  $t$  (concentration  $A_t$ ) gives

$$\frac{d[A]}{[A]} = -k_1 dt \quad (10)$$

$$\int_{[A]_0}^{[A]_t} \frac{1}{[A]} d[A] = -\int_0^t k_1 dt \quad (11)$$

We can write the integrated equation in the following forms that are more convenient:

$$\ln [A]_t = \ln [A]_0 - k_1 t \quad (12)$$

$$[A]_t = [A]_0 e^{-k_1 t} \quad (13)$$

where  $[A]_t = [A]_0 - x$  and  $[B]_t = x$ . Therefore, at any time ( $t$ ), the sum of the concentrations of ( $A$ ) and the product ( $B$ ) is equal to  $[A]_0$ .

The value of  $[B]_t$ , the concentration of ( $B$ ) at time  $t$ , is related to  $[A]_0$  by

$$[B]_t = [A]_0 \{1 - e^{-k_1 t}\} \quad (14)$$

Figure 1 shows the effects of  $[A]_0$  or the rate constant  $k_1$  on the concentration–time profiles for the disappearance of ( $A$ ) and production of ( $B$ ) according to Equation 8.

Inspection of parts (a) and (b) of Figure 1 shows that  $d[A]/d(t)$  or  $d[B]/d(t)$  are the same, that is,  $k_1$  is independent of  $[A]_0$ . On the other hand, parts (c) and (d) show that we can describe the dependence of  $t_{1/2}$  on  $k_1$  by a simple exponential decay equation.

The half-life of the reaction,  $t_{1/2}$ , at which  $[A] = [B] = [A]_0/2$ , is given by

$$t_{1/2} = \frac{\ln 2}{k_1} = \frac{0.693}{k_1} = 0.693\tau \quad (15)$$

Therefore, the half-life is independent of the initial concentration. This simple conclusion has many important practical consequences:

1. Knowledge of the concentration of a reactant or a product is not necessary for the calculation of a first-order rate constant. It also means that using highly pure reagent is not a must, provided that the impurity present, for example, a carboxylic acid formed by partial ester hydrolysis, does not affect the kinetics;

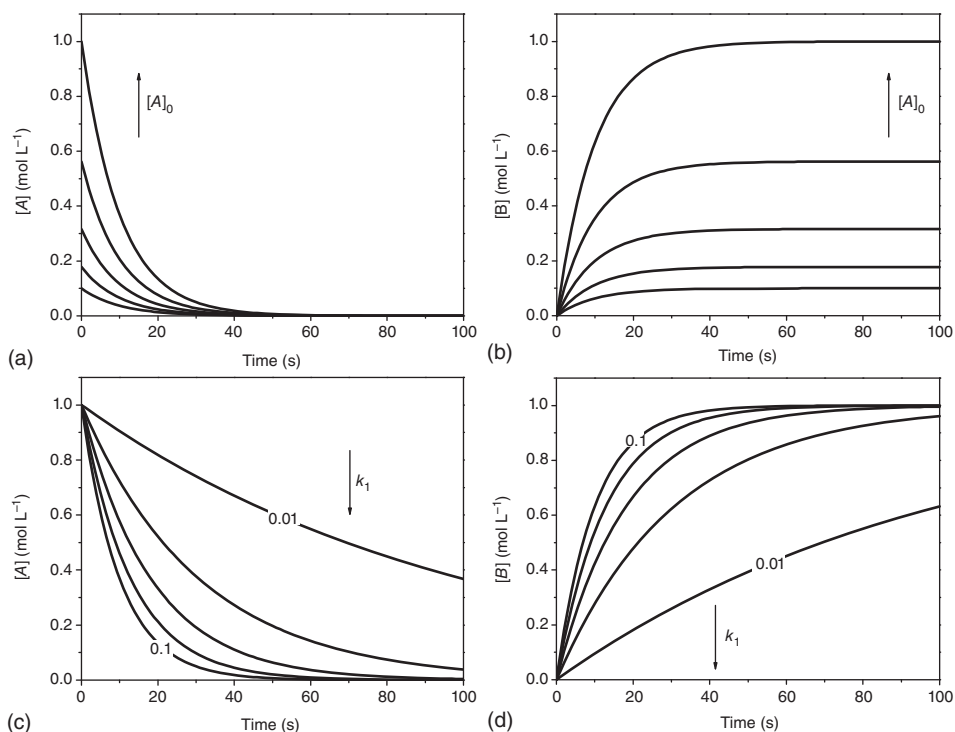


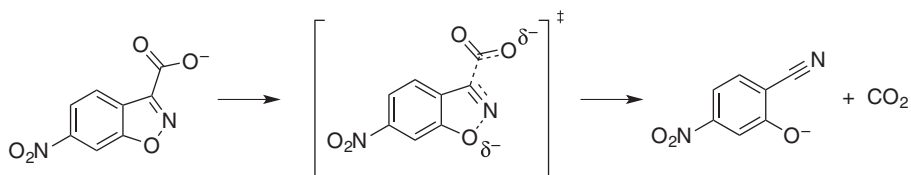
**Figure 1** Effects of experimental variables on the concentration–time profiles for first-order reactions. Parts (a) and (b) show the effect of increasing  $[A]_0$  ( $= 0.10, 0.18, 0.32, 0.56,$  and  $1.0 \text{ mol L}^{-1}$ ) on the curves of the reactant, and product, respectively, for  $k_1 = 0.1 \text{ s}^{-1}$ . Parts (c) and (d) show the effect of the value of  $k_1$  ( $0.01, 0.03, 0.05, 0.08,$  and  $0.10 \text{ s}^{-1}$ ) on the transformation of  $1.0 \text{ mol L}^{-1}$  of (A) into (B).

2. A corollary is that the change in *any* physicochemical property of the solution that is a function of concentration change can be plotted directly versus time to calculate the rate constant. Examples are UV–vis absorbance, solution conductivity, IR, NMR, and HPLC peak areas, changes in solution temperature and volume, and so on. *This convenient feature is the reason why most researchers study higher order reactions under pseudo-first-order conditions.*

An example of a first-order reaction is the thermal decomposition of 6-nitro-3-carboxy benzo[*d*]isoxazole shown in Scheme 2. This example is particularly illustrative of the effects of solvents on reactivity because it is a spontaneous decomposition reaction, that is, not subject to acid- or base-catalysis. The values of  $t_{1/2}$  of this reaction in hexamethylphosphotriamide, acetonitrile, and water are 0.001 s, 11.6 min, and about 24 h, respectively [32–34].

**Second-Order Reactions** The simplest form of a second-order reaction is one in which the rate is proportional to the square of the concentration of a single component according to the following reaction:





**Scheme 2** Spontaneous decomposition of 6-nitro-3-carboxybenzo[*d*]isoxazole.

the reaction rate law is described by

$$\text{Rate} = -\frac{d[A]}{dt} = k_2[A]^2 \quad (17)$$

Rearrangement and integration from  $[A_0]$  at  $t=0$ , to  $[A_t]$  at time  $t$ , leads to

$$\frac{d[A]}{[A]^2} = -k_2 dt \quad (18)$$

$$\int_{[A]_0}^{[A]_t} \frac{d[A]}{[A]^2} = -\int_0^t k_2 dt \quad (19)$$

$$\frac{1}{[A]_t} = \frac{1}{[A]_0} + k_2 t \quad (20)$$

Therefore, the half-time is defined by

$$t_{1/2} = \frac{1}{k_2[A]_0} \quad (21)$$

A more common case is, however, an irreversible second-order reaction between two reactants:



If (A) and (B) react stoichiometrically, the rate law is described by

$$\text{Rate} = -\frac{d[A]}{dt} = -\frac{d[B]}{dt} = k_2[A][B] \quad (23)$$

Considering that  $[A]_0 - [A]_t = [B]_0 - [B]_t$  and integration gives

$$\frac{1}{([A]_0 - [B]_0)} \ln \left( \frac{[A]_t[B]_0}{[A]_0[B]_t} \right) = k_2 t \quad (24)$$

or in a more convenient form:

$$\frac{[A]_t}{[B]_t} = \frac{[A]_0}{[B]_0} e^{([A]_0 - [B]_0)k_2 t} \quad (25)$$

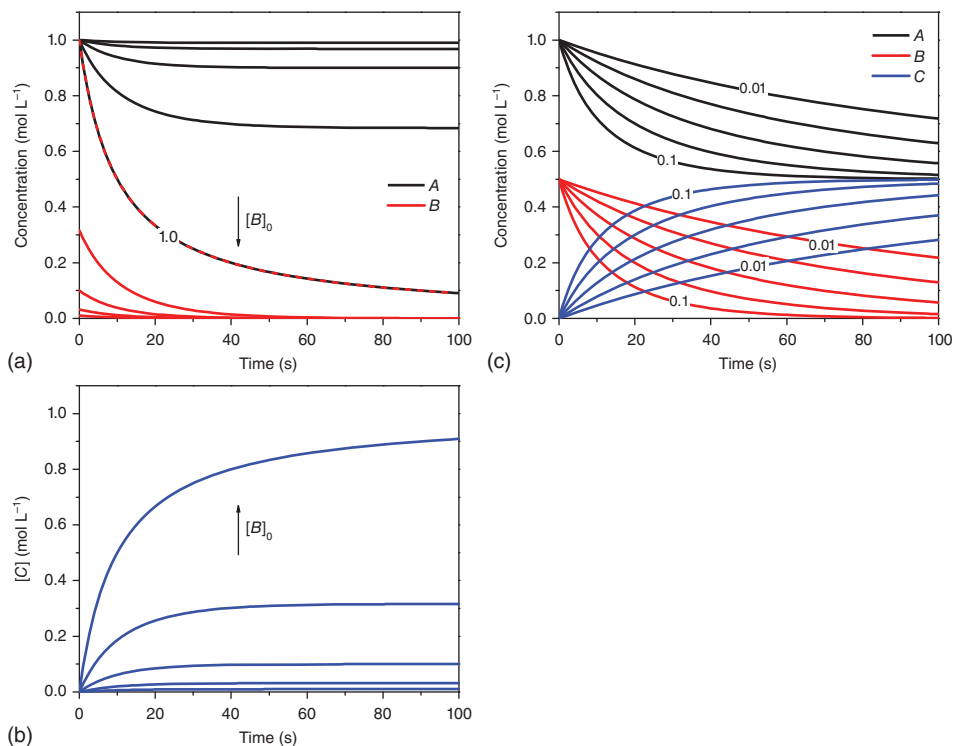


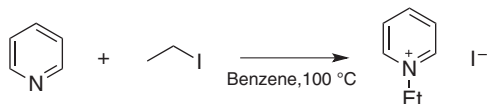
**Figure 2** Effects of experimental variables on the concentration–time profiles of the irreversible second-order reaction shown in Equation 22. Parts (a) and (b) are for  $k_2 = 0.1 \text{ L mol}^{-1} \text{ s}^{-1}$  and depict the effect of  $[B]_0$  ( $0.01\text{--}1 \text{ mol L}^{-1}$ ) on the disappearance of A ( $1 \text{ mol L}^{-1}$ ) and appearance of C, respectively. Part (c) shows the effect of the value of  $k_2$  ( $0.01, 0.03, 0.05, 0.08,$  and  $0.1 \text{ L mol}^{-1} \text{ s}^{-1}$ ) on the disappearance of the reagents A and B ( $[A]_0 = 1.0 \text{ mol L}^{-1}$  and  $[B]_0 = 0.5 \text{ mol L}^{-1}$ ) and appearance of the product (C).

Obviously, this deduction is adequate when  $[A]_0 \neq [B]_0$ ; in case  $[A]_0 = [B]_0$ , the 1 : 1 stoichiometry implies that for any time  $t$ ,  $[A] = [B]$  and the rate law will be

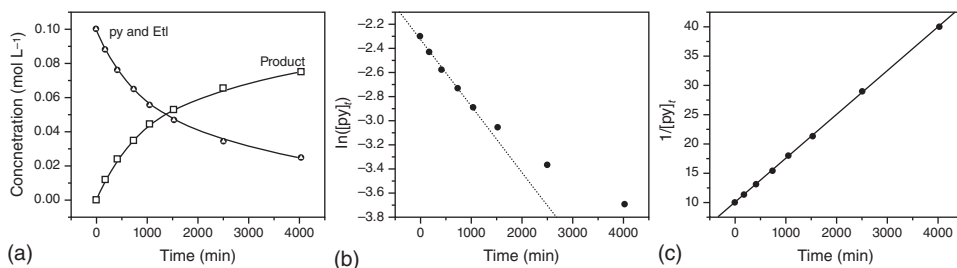
$$\text{rate} = k[A][B] = k[A][A] = k[A]^2 \quad (26)$$

Figure 2 shows the effects of experimental variables on the concentration–time profiles of the second-order reaction of Equation 22.

Examples of kinetic studies of second-order reactions are abundant [35–39], for example, the bimolecular nucleophilic substitution ( $S_N2$ , or alternatively  $A_ND_N$  mechanism) reaction between pyridine and ethyl iodide (Scheme 3) [40]. Figure 3 shows the disappearance of the reagents and the formation of the pyridinium salt, as well as the result of attempting to fit the data using the first-order kinetic model ( $\ln[\text{py}]$  vs time plot) or using the (adequate) second-order model ( $1/[\text{py}]$  vs time).



**Scheme 3** Alkylation of pyridine with ethyl iodide carried out in a sealed glass tube [40].



**Figure 3**  $S_N2$  reaction of pyridine and ethyl iodide in benzene. (a) Kinetic profile for disappearance of pyridine (py,  $\circ$ ), and formation of ethylpyridinium iodide (product,  $\square$ ). (b) Attempt at fitting a first-order kinetic model to the data. The expected linearity of  $\ln [py]_t$  versus time plot is not observed. (c) Fitting second-order kinetics to the data. As expected for a second-order reaction, a plot of  $1/[py]_t$  versus time is linear;  $k_2 = 1.25 \times 10^{-4} \text{ L mol}^{-1} \text{ s}^{-1}$  [40].

**Third-Order Reactions** Although we will not dwell here on the rare case of third-order reactions [41], it is a special case of a  $n$ th-order reaction, whose integrated rate law is given by

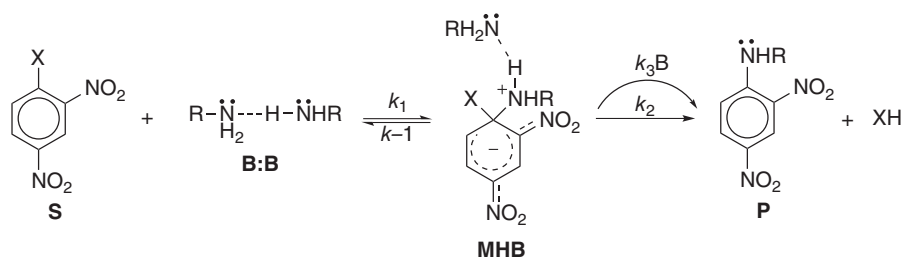
$$\text{rate} = \frac{-d[A]}{dt} = k[A]^n \quad (27)$$

$$\frac{1}{[A]^{n-1}} = \frac{1}{[A]_0^{n-1}} + (n-1)kt \quad (28)$$

For a third-order reaction, that is,  $n = 3$ :

$$\frac{1}{[A]^2} = 2kt + \frac{1}{[A]_0^2} \quad (29)$$

There are reactions where the third-order rate constant still shows a linear dependence on the concentration of one of the reactants. An example is nucleophilic aromatic substitution in aprotic solvents of low polarity, for example, the aminolysis of 2,4-dinitrohalobenzene in toluene. As shown in Scheme 4, the reaction involves attack of the amine *dimer* on the aromatic compound to produce a zwitterionic intermediate. This pre-equilibrium is third order; decomposition of the latter intermediate is rate limiting and is catalyzed by an additional amine molecule, leading to a linear dependence of ( $k_3$ ) on amine concentration [42].



**Scheme 4** Proposed mechanism for the aminolysis of 2,4-dinitrohalobenzene [42].

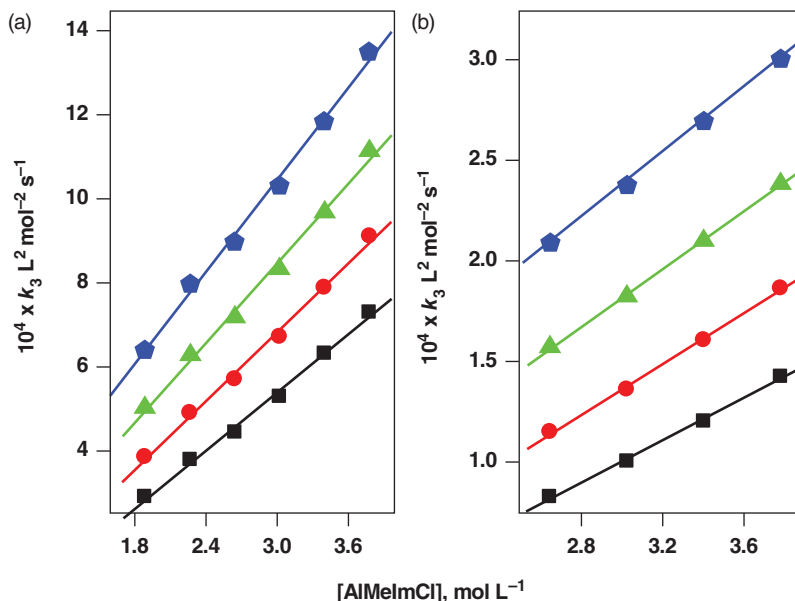


**Figure 4** Dependence of  $k_3$  for the acetylation of cellulose in mixtures of IL and dipolar aprotic solvents. The plots are for the systems IL-DMAC (a) and IL-MeCN (b). Symbols  $\blacksquare$ ,  $\bullet$ ,  $\blacktriangle$ , and  $\blacklozenge$  are for  $k_3$  at 30, 40, 50, and 60 °C, respectively [43].

Another example of third-order reaction is the acetylation of cellulose in a mixture of the ionic liquid (IL) 1-allyl-3-methylimidazolium chloride,  $AlMeImCl$ , and  $N,N$ -dimethylacetamide or acetonitrile (Figure 4). The third-order rate constant (first order in cellulose, IL, and acetic anhydride), however, shows a linear dependence on  $[AlMeImCl]$  because dissolution of cellulose occurs due to its hydrogen bonding to the IL, that is, the reactive form of the biopolymer is not free cellulose but cellulose hydrogen bonded to the IL.

*Simplification of Higher Order Reactions: Pseudo-First-Order Reaction Conditions* An important practical simplification for reactions that are second- or higher order is to convert their kinetics into pseudo-first order, in order to take advantage of the fact that studying first-order reactions is inherently simpler, see above. Consider Equation 22 when  $[B]_0 \gg [A]_0$ . At the end of the reaction, the amount of  $B$  consumed is negligible (relative to  $[B]_0$ ), that is,  $[B]_t \sim [B]_0$ . If the overall rate of reaction is, for example, given by

$$v = k[A]^m[B]^n \quad (30)$$

then the order of the reaction (with respect to time) will be  $(m)$  because  $[B]$  remains constant, and the rate of disappearance of  $(A)$  can be expressed as

$$v_A = k_{\text{obs}}[A]^m \quad (31)$$

The proportionality factor  $k_{\text{obs}}$  deduced from such an experiment is called the *observed rate constant* and it is related to  $k$  by the equation:

$$k_{\text{obs}} = k[B]^n \quad (32)$$

For the common case when  $m = 1$ ,  $k_{\text{obs}}$  is often referred to, incorrectly, as a *pseudo-first-order rate constant* ( $k_1'$ ). The bimolecular rate constant can be determined graphically as the slope of the  $k_{\text{obs}}$  versus  $[B]$  (Figure 5).

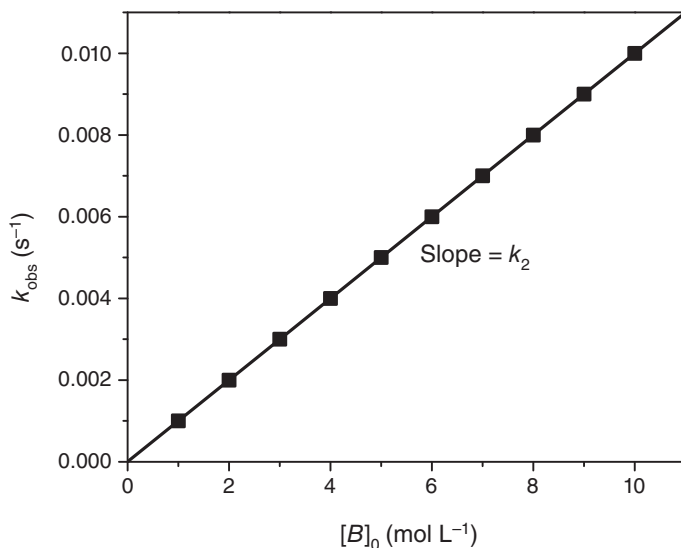


**Figure 5** Graphical calculation of a second-order rate constants ( $k_2$ ). Value of the latter ( $0.001 \text{ mol L}^{-1} \text{ s}^{-1}$ ) is the slope of the plot of  $k_{\text{obs}}$ , obtained under pseudo-first-order conditions versus the initial concentration of the reagent in excess.

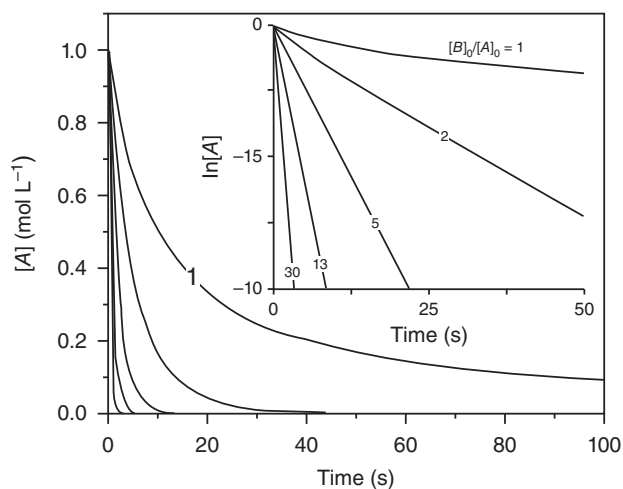
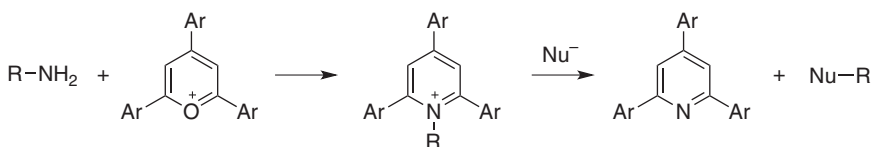


**Figure 6** Effect of  $[B]_0$  on the kinetic profile of reaction 22. The  $[B]_0/[A]_0$  ratio was varied from 1 to 30. The inset plot shows the effect of the  $[B]_0/[A]_0$  ratio on the linearity of the semilogarithmic plot.

In practice, this method can be applied when the initial concentration of one of the reagents is, at least 10 times higher than the other, for example,  $[B]_0 \geq 10[A]_0$ . The convenience of studying a reaction under pseudo-first-order conditions outweighs the fact that the experiment should be repeated at different excess  $[B]_0$  in order to calculate the true (higher order or  $[B]$ -independent) rate constants [44]. Figure 6 shows the effect of the initial concentration of  $B$  on the kinetic profile of the reaction depicted in Equation 22 at a fixed  $[A]_0$ . When  $[B]_0 = [A]_0$ , the typical second-order kinetic profile is observed and the semi-log plot is curved.

$S_N2$  reactions represent a classic example of a second-order reaction that has been extensively studied under pseudo-first-order conditions. For example, Katritzky *et al.* used the reaction between pyrilium salts and nucleophiles to investigate the mechanisms of nucleophilic substitution (Scheme 5; Figure 7) [45].



**Scheme 5** Pyrilium-mediated transformation of amines into other functionalities by a two-step process [45].

*Zero-Order* The rate of a zero-order reaction does not depend on reactant concentration [46]. Enzymatic reactions frequently show zero-order kinetics when the enzyme active site

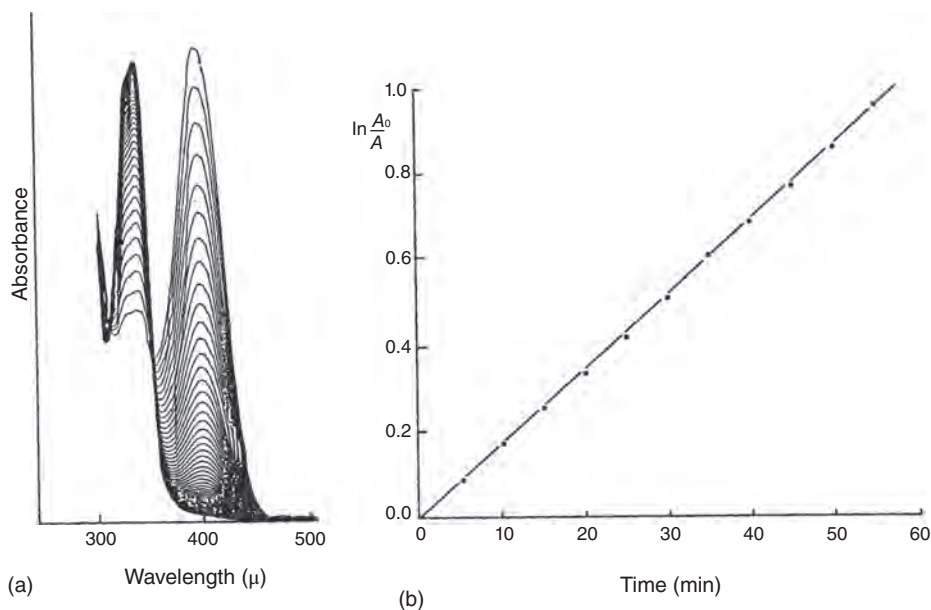


**Figure 7** Kinetics of the reaction between *N-p*-methylbenzyl-5,6,8,9-tetrahydro-7-phenyl-bisbenzo[*a,h*]acridinium tetrafluoroborate ( $5 \times 10^{-5}$  mol L $^{-1}$ ) and piperidine ( $5 \times 10^{-3}$  mol L $^{-1}$ ) in chlorobenzene at 25 °C. (a) Absorption spectra (recorded at 5 min intervals) and (b) first-order plot [45].

is saturated with the substrate. For the general reaction:



the zero-order rate law for the disappearance of (A) is given by

$$\text{Rate} = -\frac{d[A]}{dt} = k[A]^0 = k = \text{constant} \quad (34)$$

Integration over the limits  $[A] = [A]_0$  to  $[A]$  and  $t = 0$  to  $t$

$$\int_{[A]_0}^{[A]} d[A] = -\int_0^t k dt \quad (35)$$

gives

$$[A] = [A]_0 - kt \quad (36)$$

Therefore, a plot of  $[A]$  or  $\Delta[A]$  ( $= [A] - [A]_0$ ) versus time is expected to be linear with a slope of  $k$ . The half-life is

$$t_{1/2} = \frac{[A]_0}{2k} \quad (37)$$

An interesting practical consequence of Equation 37 is that the value of  $t_{1/2}$  decreases with time as (A) is consumed, as shown in Figure 8. As will be shown later, this is in contrast to the more common cases of first- and second-order reactions, where  $t_{1/2}$  is either constant (first order) or inversely proportional to the initial reagent concentration (second order).

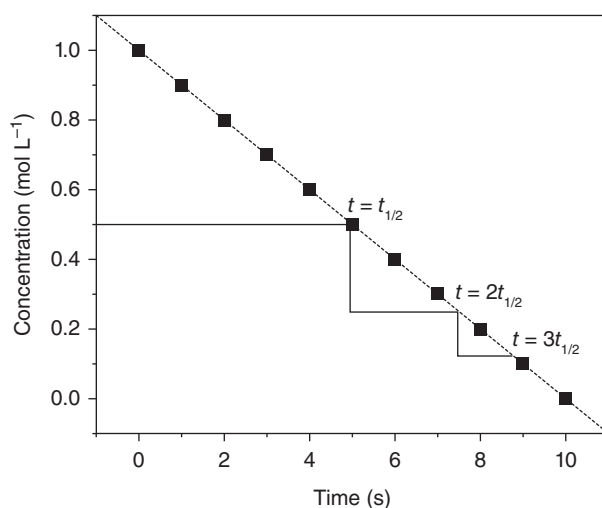
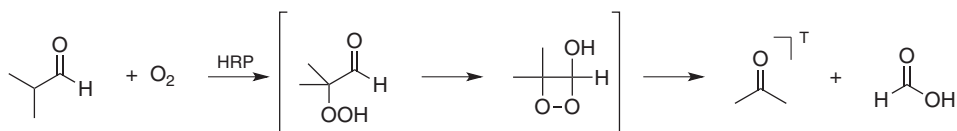


**Figure 8** Kinetic plot of a zero-order reaction, with an initial reagent concentration of  $1.0 \text{ mol L}^{-1}$  and a zero-order rate constant of  $0.1 \text{ mol L}^{-1} \text{ s}^{-1}$ . The dependence of reactant concentration on time is linear, leading to a decrease in the value of  $t_{1/2}$  as the reaction proceeds.

According to Hindmarsh and House [47], “zero-order reactions are chemical kinetics curiosities. In most textbooks, they are only briefly mentioned before rapidly passing to first-order reactions. Examples from organic chemistry are seldom discussed in detail and are hardly ever illustrated by an example.” Ethanol shows a steady-state metabolism, not an exponential metabolism. An average human metabolizes around 13 mL of ethanol per hour and the rate of decay of ethanol is linear, that is, a zero-order reaction. The steady-state metabolism of ethanol is related to the fact that acetaldehyde (the primary decay product of ethanol metabolism) is toxic and must be eliminated before any more ethanol can be processed (by the liver) to avoid acetaldehyde poisoning [48, 49]. Another interesting example, the chemiluminescent reaction of isobutanal (IBAL) with oxygen catalyzed by horseradish peroxidase (HRP) is a zero-order reaction. The reason is that one of the reaction products is light, whose intensity can be monitored [50–52].

The autoxidation of the IBAL produces a peracid that is converted into the cyclic peroxide whose decomposition gives triplet-excited acetone (Scheme 6). The reaction of oxygen with IBAL appears to occur spontaneously in the presence of HRP. Initially, there is a burst in luminescence followed by a steady-state phase in which  $O_2$  is consumed in a zero-order process (Figure 9) [50, 53–55].



**Scheme 6** Chemiluminescent oxidation of isobutanal by oxygen in the presence of HRP.

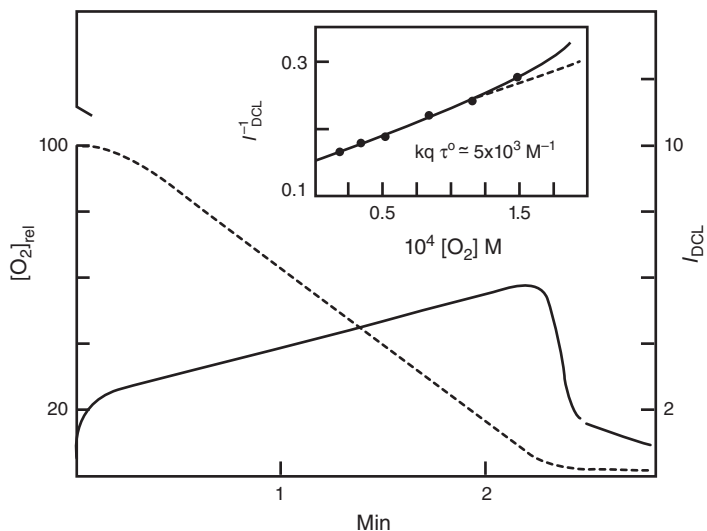


**Figure 9** Oxygen depletion (broken curve, ordinates in the left) and concomitant light emission intensity ( $I_{DCL}$ : direct chemiluminescence intensity) during oxidation of  $42 \text{ mmol L}^{-1}$  isobutyraldehyde catalyzed by  $2.5 \mu\text{mol L}^{-1}$  HRP in  $0.1 \text{ mol L}^{-1}$  phosphate buffer ( $\text{pH} = 7.4$ ) at  $30^\circ\text{C}$  in the presence of EDTA [53].

During this reaction phase, the RLS is the reaction of oxygen with the IBAL enol radical formed by action of the enzyme. The velocity of this transformation, which is formally a radical recombination (enol radical with the biradical triplet oxygen), does not depend on oxygen concentration. Therefore, the reaction rate, as measured by oxygen consumption, does not change (Figure 9). In addition, the intensity of emitted light stays approximately constant during the steady-state phase of the reaction. The slight increase in the direct chemiluminescence (CL) emission intensity is due to the higher emission efficiency of enzyme protected triplet acetone at lower oxygen concentrations due to decreased triplet quenching by oxygen (Figure 9).

Another example of this type of reaction is the oxidation of  $\text{PtCl}_4^{2-}$  by excess of  $\text{S}_2\text{O}_8^{2-}$  in aqueous HCl, which exhibits all the characteristics of a zero-order reaction [56]. Although very little is known about the reaction mechanism, it appears that reactions that involve persulfates have a propensity for zero-order kinetics [56].

**2.2.2 Complex Reactions** In this section, we discuss examples of complex reactions, limiting ourselves to the more representative examples, namely reversible, consecutive, and parallel reactions. Catalysis is not extensively discussed since Blackmond has provided a comprehensive analysis of kinetic data obtained from the study of catalyzed complex reactions [57].

*Reversible First-Order Reactions* We can treat irreversible reactions as a special case of the reversible system in which the rate constant of the forward reaction is much larger than that of the reverse counterpart. Consider the general case:



If  $k_1 \gg k_{-1}$ , the reaction is essentially irreversible and, therefore, the observed rate constant is practically equal to  $k_1$  of Equation 8. For reactions where  $k_1$  and  $k_{-1}$  are comparable, Equation 39 applies

$$-\frac{d[A]}{dt} = \frac{d[B]}{dt} = k_1[A] - k_{-1}[B] \quad (39)$$

At any ( $t$ ), the sum of the transient concentrations of  $[A]_t$  and  $[B]_t$  and the equilibrium concentrations ( $[A]_e$  and  $[B]_e$ ) are equal to the sum of the initial concentrations of both reactants; accordingly

$$[A]_0 + [B]_0 = [A]_t + [B]_t = [A]_e + [B]_e \quad (40)$$

thus,

$$[A]_t = [A]_e + [B]_e - [B]_t \quad (41)$$

Combining Equations 39 and 41:

$$\frac{d[B]_t}{dt} = k_1([A]_e + [B]_e - [B]_t) - k_{-1}[B]_t \quad (42)$$

This equation can be rearranged and its solution with  $[A]_t(t=0) = A_0$  results in the following rate law:

$$\frac{d[B]_t}{dt} = k_1([A]_e + [B]_e) - (k_1 + k_{-1})[B]_t = -k_{\text{obs}}[B]_t + C \quad (43)$$

If the equilibrium constant,  $K_{\text{eq}}$ , is known, or can be determined, then  $k_{\text{obs}}$  can be split into its components ( $k_1$  and  $k_{-1}$ ) since:

$$k_1[A]_{\text{eq}} = k_{-1}[B]_{\text{eq}} \quad (44)$$

$$\frac{[B]_{\text{eq}}}{[A]_{\text{eq}}} = \frac{k_1}{k_{-1}} = K_{\text{eq}} \quad (45)$$

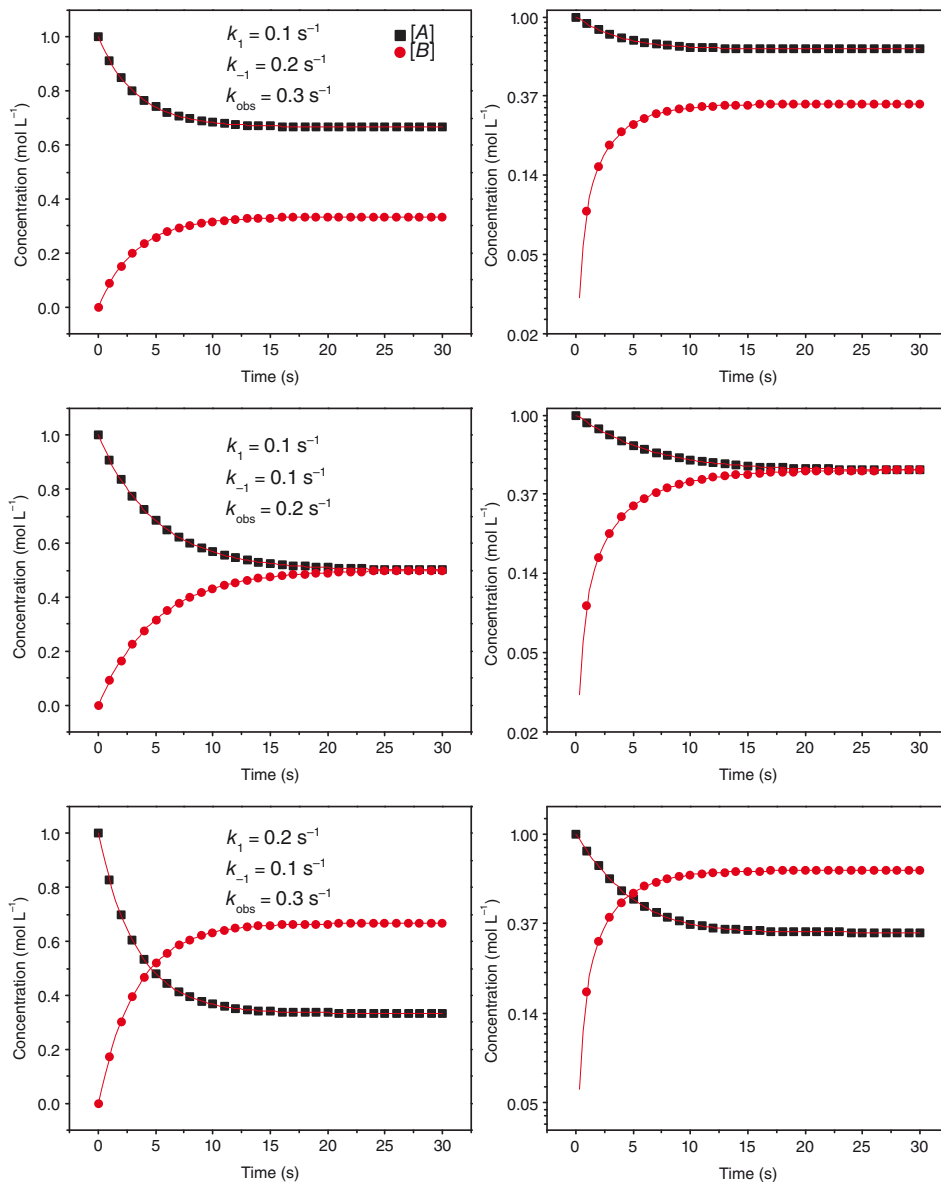


**Figure 10** Dependence of [A] and [B] on time for different ratios of  $k_1$  to  $k_{-1}$ .

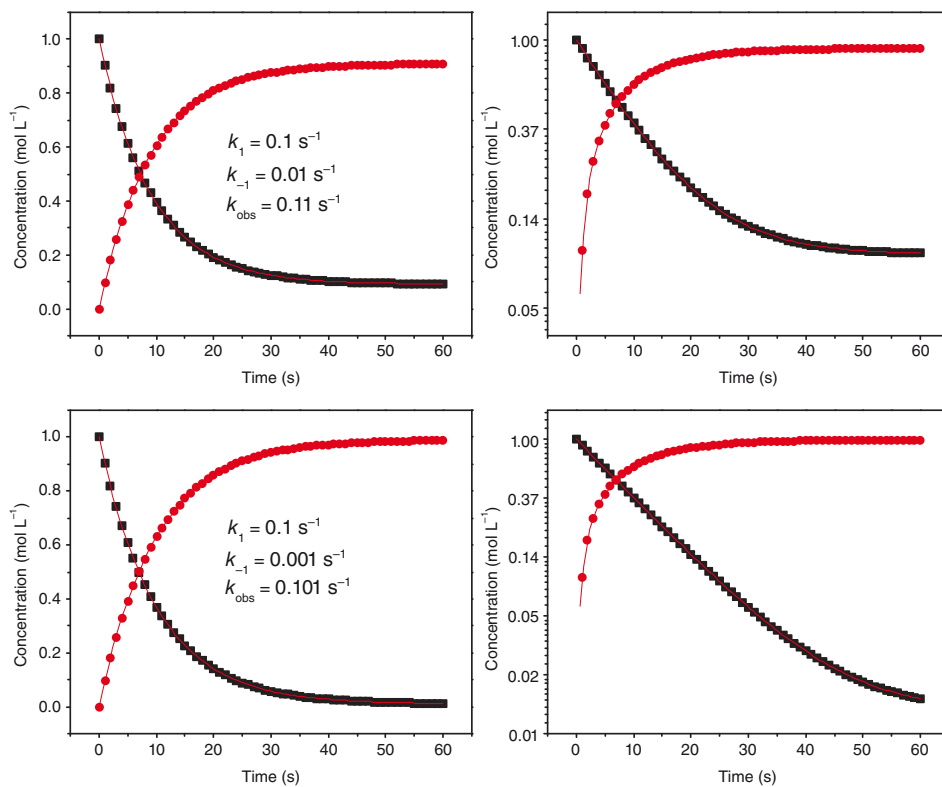


Figure 10 (Continued)

or, in a more convenient form,

$$k_{\text{obs}} = k_{-1}K_{\text{eq}} + k_{-1} = k_{-1}(K_{\text{eq}} + 1) \quad (46)$$

Similar to irreversible first-order reactions, calculation of the rate constants from experimental data does not require that we know the concentrations.

At the half-time,  $t = t_{1/2}$ ,  $[B] = 0.5([B]_{\text{e}} - [B]_0) + [B]_0$  and substitution into Equation 43 gives

$$t_{1/2} = \frac{\ln 2}{k_1 + k_{-1}} = \frac{0.693}{k_1 + k_{-1}} \quad (47)$$

As the ratio  $(k_1/k_{-1})$  becomes progressively large,  $k_1$  approaches  $k_{\text{obs}}$ , that is, the reaction becomes essentially an irreversible first order process, as shown in Figure 10. For each horizontal pair the graph on the right-hand side is equivalent to that on the left-hand side, except that the concentrations in the latter are plotted on a logarithmic scale. As shown,  $\ln(A)$  becomes practically linear when  $k_{-1} \ll k_1$ , leading to  $k_1 \approx k_{\text{obs}}$ .

In summary, Figure 11 depicts a comparison of kinetic profiles of irreversible and reversible unimolecular first-order reactions. This figure shows that the final situation in the system is reached much faster in the reversible reaction, even though the forward rate constant is the same for both cases. This can be intuitively understood by assuming that

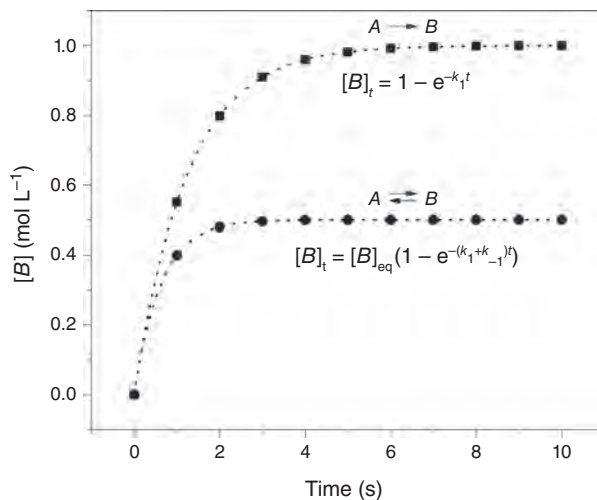


**Figure 11** Temporal dependence of  $[B]$  for the irreversible reaction  $A \xrightarrow{k_1} B$  compared with the reversible reaction  $A \xrightleftharpoons[k_{-1}]{k_1} B$ ;  $k_1 = k_{-1} = 0.8 \text{ s}^{-1}$ ;  $[B]_{\text{eq}} = k_1/(k_1 + k_{-1}) = 0.5$ . (Adapted from Ref. [4].)

both reaction pathways (forward and reverse) sum to reach the equilibrium situation, as indicated also by the integrated rate law (Figure 11).

*Consecutive First-Order Reactions* The simplest case of consecutive reactions is:



For this system, it is possible to derive Equations 49–51.

$$[A] = [A]_0 e^{-k_1 t} \quad (49)$$

$$[B] = \frac{[A]_0 k_1}{k_2 - k_1} (e^{-k_1 t} - e^{-k_2 t}) \quad (50)$$

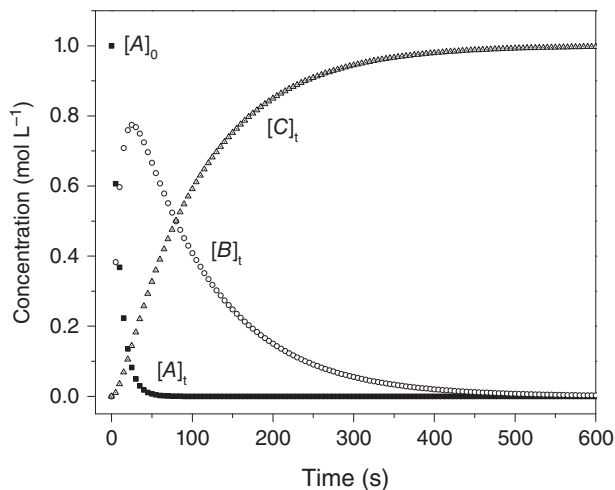
$$[C] = [A]_0 \left\{ 1 + \frac{1}{k_1 - k_2} [k_2 e^{-k_1 t} - k_1 e^{-k_2 t}] \right\} \quad (51)$$

At any time ( $t$ ), the sum of the concentrations is equal to the initial concentration of the reactant.

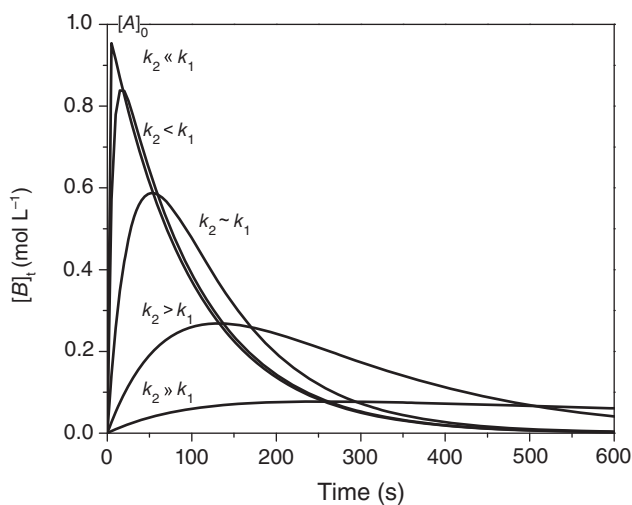
$$[A]_0 = [A] + [B] + [C] \quad (52)$$

Figure 12 shows the kinetic profile for two consecutive first-order reactions where the intermediate ( $B$ ) accumulates ( $k_2 < k_1$ ). The effect of varying the  $k_1/k_2$  ratio on the concentration of ( $B$ ) is shown in Figure 13.

For simplicity, the discussion above has been limited to first-order reactions. Obviously, it applies to second-order reactions carried out under pseudo-first-order conditions; an

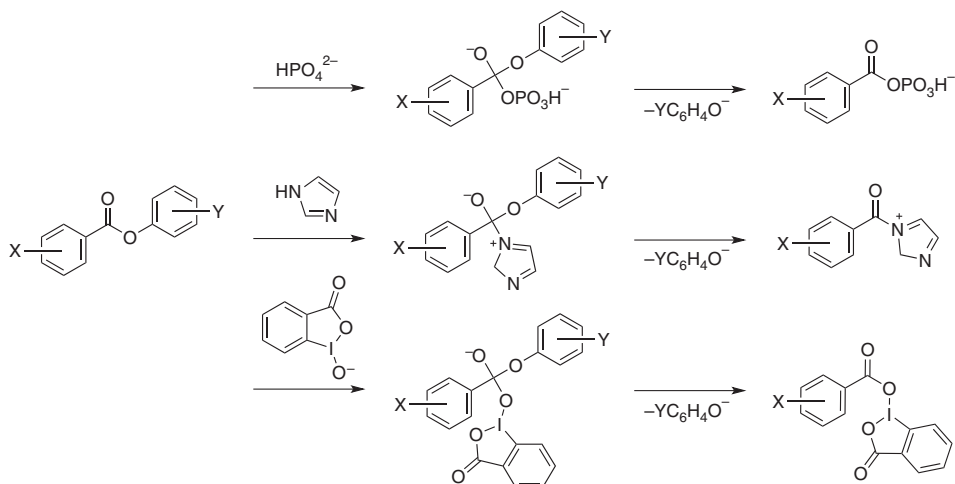


**Figure 12** Dependence of concentration of the reagent ( $A$ ), intermediate ( $B$ ), and product ( $C$ ) on time for a first-order consecutive reaction following Equation 48 with  $k_1 = 0.1 \text{ s}^{-1}$  and  $k_2 = 0.01 \text{ s}^{-1}$ .



**Figure 13** Dependence of the concentration of the intermediate ( $B$ ) on time for two consecutive first-order reactions where the ratio of the rate constants  $k_1$  and  $k_2$  is varied.

example is ester hydrolysis in buffers. The catalysis can be acid–base or, as shown below, nucleophilic, involving the formation of an intermediate that hydrolyzes faster than the parent ester. This is the case for the buffer-catalyzed hydrolysis of esters activated either in the leaving group, 2,4-dinitrophenyl-4- $X$ -benzoate, or in the acyl moiety, 4- $Y$ -phenyl-3,5-dinitrobenzoate, where  $X$  and  $Y$  are substituent groups. Thus, the reaction of both series of esters with phosphate, imidazole, and *o*-iodosobenzoate buffer involves the formation of a mixed carboxylic-phosphoric acid anhydride, an  $N$ -acylimidazole, or a 1-hydro(benzoyloxy)-1,2-benzodioxol-3(1*H*)-one, respectively. These intermediates undergo further hydrolysis with catalyst (hydrogen phosphate, imidazole, and



**Scheme 7** Nucleophilic catalysis of the hydrolysis of activated benzoate esters, catalyzed by phosphate, imidazole, or *o*-iodosobenzoate buffer, respectively [58].

iodosobenzoate, respectively) turn over. All rate constants for these systems have been determined because the intermediates involved were synthesized and their hydrolysis studied (Scheme 7) [58].

*Competitive First Order Reactions* Compounds that undergo reaction via two or more pathways simultaneously are referred to as parallel or competitive (Equation 53).



Although the kinetic equations are easily solved by integration, it is instructive to solve them using chemical intuition, as demonstrated by Fersht [14]. Obviously,  $[A]$  decreases with a rate constant that is the sum of  $k_B$  and  $k_C$ . In addition,  $(B)$  and  $(C)$  are formed in the ratio of the corresponding rate constants,  $k_B$  and  $k_C$ , respectively. Since the rates of formation of  $(B)$  and  $(C)$  should be the same as for the disappearance of the reagent,

$$[A] = [A]_0 e^{-(k_B+k_C)t} \quad (54)$$

$$[B] = \frac{[A]_0 k_B}{k_B + k_C} (1 - e^{-(k_B+k_C)t}) \quad (55)$$

$$[C] = \frac{[A]_0 k_C}{k_B + k_C} (1 - e^{-(k_B+k_C)t}) \quad (56)$$

The situation is similar to reversible reactions where the relaxation time is composed of the sum of the rate constants for the two reactions. On the other hand, in the consecutive mechanism, the concentration of the intermediate goes through a maximum (Figure 12),

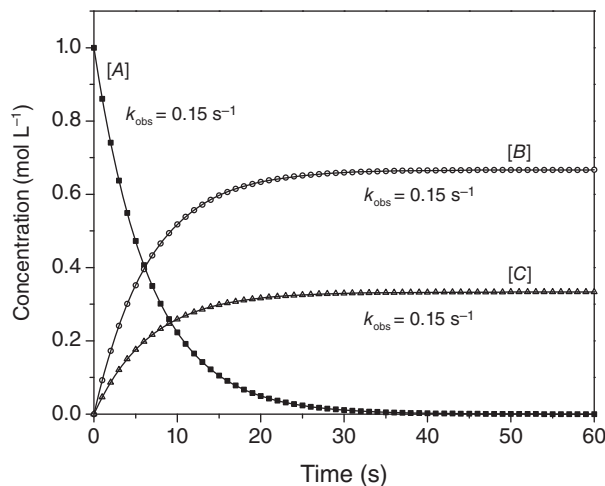


**Figure 14** Simulated data for two parallel first-order reactions (Equation 53) using  $[A]_0 = 1.0 \text{ mol L}^{-1}$ ,  $k_{A \rightarrow B} = 0.1 \text{ s}^{-1}$ , and  $k_{A \rightarrow C} = 0.05 \text{ s}^{-1}$ . Fitting was carried out using the mono-exponential function (Equation 13). Since the rates of formation of (B) and (C) depend on [A]. Note that both (B) and (C) must be formed with the same rate constant as that for the disappearance of (A), in agreement to Equations 54–56 [14].

whereas, in parallel reactions, no intermediate is formed and product formation shows a saturation profile. Interestingly, and surprisingly at least at first glance, both products are formed with the same rate constant, which corresponds to the sum of the two competing reaction rate constants and to the disappearance of the reagent (Figure 14) [4].

*Reversible Competitive First-Order Reactions* In principle, the formation of both kinetic and thermodynamic products is possible for two parallel and reversible reactions, for example:

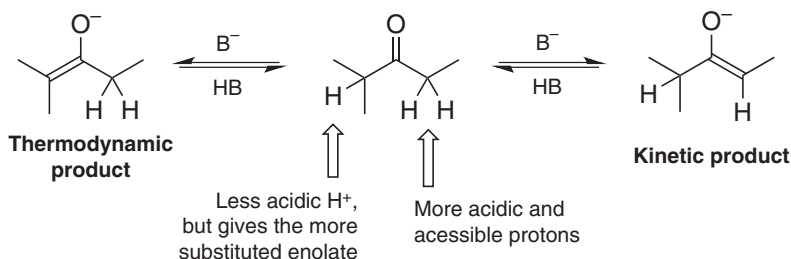


Assuming that (B) and (C) do not interconvert, then

$$\frac{[B]_{\text{eq}}}{[C]_{\text{eq}}} = \frac{[B]_{\text{eq}} [A]_{\text{eq}}}{[A]_{\text{eq}} [C]_{\text{eq}}} = \frac{k_1 k_{-2}}{k_{-1} k_2} = K_{\text{BC}} \quad (59)$$

There are several possibilities for these reactions, depending on the values of the rate and equilibrium constants. If  $k_1 \gg k_{-1}$  and  $k_2 \gg k_{-2}$ , the reactions are essentially irreversible; the ratio  $[B]/[C]$  is proportional to  $k_1/k_2$ . If  $[C]_{\text{eq}} \gg [B]_{\text{eq}}$ , then  $K_{\text{BC}} \ll 1$ , (C) is preferred. On the other hand, if  $k_1 \gg k_2$ , (B) is preferred, and the reaction is kinetically controlled [59].

An illustrative example is the regioselective formation of enolates from ketones (Scheme 8), which depends on the reaction conditions, for example, solvent, base, cation, and temperature. Although the  $\text{p}K_{\text{a}}$  difference between the two sites is only 1–2 units, this



**Scheme 8** Two possibilities for hydrogen abstraction from a carbonyl compound leading to different products, for example, in alkylation.

difference, when combined with the relative steric accessibility of the  $\alpha$ -protons, is usually enough to form selectively the kinetic enolate.

The regioselectivity of this reaction is influenced by the reaction conditions [61, 62]. Aprotic solvents such as tetrahydrofuran (THF) or diethyl ether favor the kinetic product (enolate) because the solvent carries no acidic hydrogen to favor the reverse reaction. Strong, voluminous bases (e.g., lithium di(isopropyl)amide) also favor the kinetic product, as they approach the ketone from the least hindered side and form a weaker acid than the enolate. For the same reaction, the kinetic product is associated with a lower activation energy. Therefore, use of high temperature and long reaction time favor the formation of the thermodynamic product. Further details on thermodynamic and kinetic control and the Curtin–Hammett principle is available elsewhere [63–65].

**2.2.3 Common Approximations** There are several approaches to eliminate the concentration of intermediates from the rate law. This is convenient because many of these intermediates are unstable. The consequence is that their concentrations are difficult or not feasible to be determined. Whenever one or more assumptions about the values of rate coefficients are made, their range of validity should be verified by numerical calculations.

*Steady-State Approximation* For the following reaction:



the rate laws are the following,

$$\frac{d[A]}{dt} = -k_1[A] + k_{-1}[B] \quad (61)$$

$$\frac{d[B]}{dt} = k_1[A] - (k_{-1} + k_2)[B] \quad (62)$$

$$\frac{d[C]}{dt} = k_2[B] \quad (63)$$

In the steady-state (or Bodenstein) approximation (SSA), one assumes that the concentration of (*B*) remains small throughout the reaction since  $(k_{-1} + k_2) > k_1$ . Then the absolute

slope of its concentration will be small compared to other time dependences in the system; consequently, the variation of its concentration with time will be negligible as compared with those of (A) or (C) (Equation 64).

$$\frac{d[B]}{dt} = k_1[A] - (k_{-1} + k_2)[B] \stackrel{\text{SSA}}{\approx} 0 \quad (64)$$

So that,

$$[B] \stackrel{\text{SSA}}{\approx} \frac{k_1[A]}{k_{-1} + k_2} \quad (65)$$

$$\frac{d[C]}{dt} \stackrel{\text{SSA}}{\approx} \frac{k_1 k_2}{k_{-1} + k_2} [A] \quad (66)$$

The validity of the SSA is limited to chemical reactions where the intermediate does not accumulate. This means that the sum of the effective rate coefficients leading to the disappearing of the intermediate should be, at least, greater by a (safe) factor of 50 than that leading to its formation. In addition, a “build-up time,” that is, the time required for the intermediate to reach its steady-state value, should be small in order to reduce errors.

*Rapid Equilibrium Approximation* The condition for the rapid equilibrium approximation (REA) is  $(k_1 + k_{-1}) > k_2$ . Therefore, the system can be reduced to  $A \rightleftharpoons B$ . After  $(t \approx 1/(k_1 + k_{-1}))$ , the reaction will reach approximate equilibrium so that,

$$[B] \approx \frac{k_1}{k_{-1}} [A] \quad (67)$$

Species (A) and (B) will act like a single species that is slowly decaying toward (C), and, consequently,

$$\frac{d[C]}{dt} \stackrel{\text{REA}}{\approx} \frac{k_1 k_2}{k_{-1}} [A] = K k_2 [A] \quad (68)$$

*Equilibrium-Steady-State Case* As shown earlier, the condition for the steady-state case is  $(k_{-1} + k_2) > k_1$ , that for the rapid equilibrium is  $(k_1 + k_{-1}) > k_2$ . If  $k_{-1}$  is the largest rate coefficient in the system, that is,  $k_{-1} > k_1$  (SSA) and  $k_{-1} > k_2$  (REA), then both approximations have a common result, namely the equilibrium-steady-state (EQ-SS) solution [66]. After the time required for the establishment of either the steady state or the rapid equilibrium condition, (C) is produced (in this first-order example) with a simple exponential behavior.

*Comments of the Use of Computer Software to Rationalize Kinetic Data* There are several programs designed to create mathematical models of chemical and biological processes [24]. Together with chemical kinetics databases [67] these software provide a valuable insights in the study of reaction kinetics and mechanisms. Although a comprehensive list of software available for the analysis and simulation of kinetic data is outside the scope of this account, we discuss a representative example. COPASI (acronym for *complex pathway simulator*) is an open-source software application for creating and solving mathematical models of biological processes such as metabolic networks, cell-signaling pathways, regulatory networks, infectious diseases, and many others [68]. Models are defined as chemical

reactions between molecular species and model dynamics is determined by rate laws associated with individual reactions. This software handles steady-state analysis, stoichiometric analysis, metabolic control analysis, computation of Lyapunov exponent, timescale separation, parameter scans, optimization, and parameter estimation.

### 3 INFORMATION DERIVED FROM KINETIC DATA

#### 3.1 Activation Parameters

One of the most important sets of parameters obtained from kinetic studies of chemical reactions are the so-called activation parameters, which indicate the energetic requirements of the reaction. Two general approaches are available to correlate the primary kinetic parameter, rate constants, with reaction temperature, Eyring equation, and empirical Arrhenius rate law [5, 69–71].

In order to understand the derivation of the Eyring equation, we consider the following transformation:



According to the transition state theory, the rate of production of ( $C$ ) is directly proportional to the concentration of the reactants and a rate constant  $k$ , and also to the concentration of the activated complex  $AB^\ddagger$  and the rate constant of its transformation into products,  $k^\ddagger$ :

$$\frac{d[C]}{dt} = k[A][B] \quad (70)$$

$$\frac{d[C]}{dt} = k^\ddagger[[AB]^\ddagger] \quad (71)$$

Because the value of  $k^\ddagger$  is independent of the reaction, we can consider that reactants are in (pseudo) equilibrium with the activated complex. That is, what controls the reaction is the equilibrium between the reactants and the activated complex with the equilibrium constant  $K^\ddagger$  so that:

$$[[AB]^\ddagger] = K^\ddagger[A][B] \quad (72)$$

Eyring equation relates the intrinsic rate constant  $k^\ddagger$  and the intrinsic equilibrium constant  $K^\ddagger$  in terms of activation parameters, that is, activation enthalpy,  $\Delta^\ddagger H$ , entropy,  $\Delta^\ddagger S$ , and Gibbs free energy,  $\Delta^\ddagger G$ :

$$\Delta^\ddagger G = \Delta^\ddagger H - T\Delta^\ddagger S \quad (73)$$

$$k = \kappa \left( \frac{k_B T}{h} \right) e^{(-\Delta^\ddagger G/RT)} \quad (74)$$

where ( $\kappa$ ) is the transmission coefficient (of the activated complex into products  $\approx 1$ ),  $k_B$  the Boltzmann constant, and ( $h$ ) Planck constant. Combining Equations 73 and 74, Equation 75 is obtained.

$$k = \kappa \left( \frac{k_B T}{h} \right) e^{(\Delta^\ddagger S/R)} e^{(-\Delta^\ddagger H/RT)} \quad (75)$$

**TABLE 1** Order of Magnitude of the Kinetic Parameters for First-Order Homogeneous Reactions [4]

Reaction type, rate constant $k$ ( $\text{s}^{-1}$ )	Activation energy, $E_a$ ( $\text{kJ mol}^{-1}$ )
Slow, $<10^{-3}$ to $10^{-2}$	High, $>130$
Moderate, $10^{-2}$ to $10$	Moderate, $20$ – $130$
Fast, $>10$	Low, $<20$

which correlates the experimental rate constant with temperature and thereby allows the experimental determination of the activation parameters ( $\Delta^\ddagger H$  and  $\Delta^\ddagger S$ ) from the temperature dependence of reaction rate. As will be shown in the following discussion, these parameters are very important to understand chemical reactions on the molecular level.

The calculation of the Arrhenius activation energy is achieved by measurement of the rate constants at different temperatures and is valid for most homogeneous elementary reactions as well as complex reactions. The Arrhenius rate law was derived empirically before the development of transition state theory from the observation that the rate of reactions increased exponentially as the absolute temperature increased.

$$k = Ae^{-E_a/RT} \quad (76)$$

where  $A$  is the Arrhenius pre-exponential factor,  $E_a$  the Arrhenius activation energy,  $R$  the gas constant ( $1.987 \text{ cal mol}^{-1} \text{ K}^{-1}$  or  $8.314 \text{ J mol}^{-1} \text{ K}^{-1}$ ), and  $T$  the absolute temperature. Table 1 shows the order of magnitude of the kinetic parameters for first-order reactions. The pre-exponential factor for a monomolecular reaction is about  $10^{13} \text{ s}^{-1}$  [4].

The empirical nature of the Arrhenius equation implies that the *macroscopic* rate constant for a particular conversion is being observed. In other words, it ignores any mechanistic consideration, such as whether one or more intermediates are involved in the overall conversion of the reagent to the product. Eyring equation, on the other hand, analyzes the *microscopic* rate constant for a single-step conversion of a reactant to a product [5]. Therefore, in a multistep process involving intermediates, there is a  $\Delta^\ddagger G$  for every step, whereas the  $E_a$  describes the overall transformation. However, if one considers a *single-step process*, the Arrhenius and Eyring equations are connected and  $E_a$  and  $\Delta^\ddagger H$  are related by

$$E_a = \Delta^\ddagger H + RT \quad (77)$$

and the pre-exponential factor  $A$  is associated with  $\Delta^\ddagger S$ ,

$$\Delta^\ddagger S = 4.576(\log A - 10.753 - \log T) \quad (78)$$

For simplicity, many organic chemistry textbooks discuss reactions in terms of their activation energy; the entropy term occupies a position of secondary importance. Although this is expedient and appropriate for the beginner, the entropy of activation term should never be overlooked because some reactions, in particular those involving strongly solvated ions may be dominated by entropy due, for example, to steric and solvation effects. Thus, reactions of aqueous hydroxide ion are dominated by the entropy term because of the required desolvation of  $\text{HO}^-$  [72, 73]. The following is a brief discussion of the fundamental aspects, the relevance, and the use of the activation parameters:

1. The approach employed to formulate and calculate the activation parameters is modeled after equilibrium thermodynamics. As stated earlier, the reagents are in (pseudo) equilibrium with the activated complex. It follows that equations similar to those of van't Hoff and Gibbs can be applied. This is the reason that the activation parameters are also referred to as *extra-thermodynamic* parameters because they describe pseudo-equilibria [74].
2. Since the largest bond energies in organic molecules are typically in the order of  $300 \text{ kJ mol}^{-1}$ , one can expect the  $E_a$  of bimolecular reactions to be lower than  $300 \text{ kJ mol}^{-1}$ . This upper limit on the activation energy provides a second test for the validity of experimentally determined rate constants assigned to bimolecular reactions. Theoretical considerations lead to the conclusion that the pre-exponential term has an upper limit of about  $10^{13} \text{ s}^{-1}$ , which corresponds to the average vibrational frequency of a bond that is broken in the reaction [19].
3. Reaction rates are controlled by the rate of conversion of the reactants or by non-chemical processes such as the rate of diffusion of reactants or the rate of heat transfer. In the study of chemical kinetics, we will be interested in the rates of chemical change governed by the speed of chemical processes [19].
4. For a chemical reaction, the calculated activation parameters refer to the differences between the reagents and the activated complex for the rate-limiting step.
5. The  $E_a$  calculated from the Arrhenius equation is not a thermodynamic quantity. Fortunately, Arrhenius modeled his equation after van't Hoff's equation, hence  $E_a$  differs from  $\Delta^\ddagger H$  (a thermodynamic quantity) by the simple term  $RT$  (Equation 77).
6. The universality of the Arrhenius equation is remarkable because it has been successfully applied to both solution- and gas-phase reactions. In addition, there are "Arrhenius-type" equations that describe cases where no reaction occurs, for example, the viscous flow of liquids ( $\log$  viscosity vs  $1/T$ ).
7. It has been stated that the activation energy *cannot be negative* and that any data fitting that results in negative  $E_a$  in a rate expression is unacceptable for interpreting the mechanism of the reaction [19]. However, this is strictly true only for elementary reactions or irreversible reactions. Indeed, near zero or negative activation energies have been reported on rare occasions, for example, when an exothermic step (e.g., a pre-equilibrium) occurs prior to the RLS, or in fast reactions that involve radicals and ions [5, 75, 76].
8. The activation enthalpy contains contributions from bonding interactions and is determined by the energetics and degree of synchrony of bonds breaking and forming upon going from the reactants to the transition state. On the other hand, the activation entropy contains contributions from factors that are associated with changes in the degree of freedom of the system (solute plus solvent), on going from the reactant to the transition state. Therefore, the activation entropy is determined primarily by reaction molecularity, whether the reaction is dissociative (e.g., spontaneous decomposition;  $S_N1$ ) or associative (e.g., addition or  $S_N2$ ). In the first case, the degrees of freedom increase on going from the reactant to the transition-state; consequently, there is a gain in entropy and the  $\Delta^\ddagger S$  is expected to be positive. The converse applies to associative reactions, where  $\Delta^\ddagger S$  is expected to be negative. Steric interactions and solvation also affect the reaction entropy. The influence of these parameters on the sign of  $\Delta^\ddagger S$ , however, depends on the reaction considered and if the degrees of freedom increase or decrease [5].

9. Solvation may produce some very interesting effects on reaction mechanism and, consequently, on reaction rates. A textbook example is the Finkelstein isoergonic halide self-exchange reaction between iodomethane and radioactive labeled iodide ion ( $^{131}\text{I}^-$ ) (Scheme 9) [77]. The rate constant for this reaction decreases by a factor of about  $10^4$  upon changing the solvent from (aprotic; less polar) acetone to (protic) water. In some cases, a change of the solvent, for example, from protic to dipolar aprotic, can produce a larger effect than temperature [18].

The solvent effects on rate constant show poor correlation with individual solvent parameters [18], such as the empirical polarity parameter ( $E_T(30)$ ), relative permittivity ( $\epsilon_r$ ), solvent acidity, or basicity, but are better correlated with a linear combination of several solvent descriptors [78, 79].

For many reactions studied as a function of an experimental variable, such as the composition of a binary mixture of solvents, the variation of  $\Delta^\ddagger G$  may be monotonic and deceptive because it is the result of quasi-compensatory changes in the  $\Delta^\ddagger H$  and  $T\Delta^\ddagger S$  terms, as shown in Figure 15. Understanding these changes is relevant to rationalize the complex effect of solvation on chemical reactions.

10. When data are obtained over a sufficiently wide temperature range, the Arrhenius equation often does not describe them accurately; plots of  $\ln k$  versus  $1/T$  are curved; due to  $T$ -dependent  $A$  and  $E_a$ , as illustrated in Figure 16.

Data that show curvature on Arrhenius plots are most often fitted by the equation

$$k(T) = AT^m e^{-E_b/RT} \quad (79)$$

where the three parameters ( $A$ ,  $m$ , and  $E_b$ ) can be varied to fit the data over a wide ( $T$ ) range. A corollary is that obtaining rate constants from the Arrhenius plot by extrapolation to a

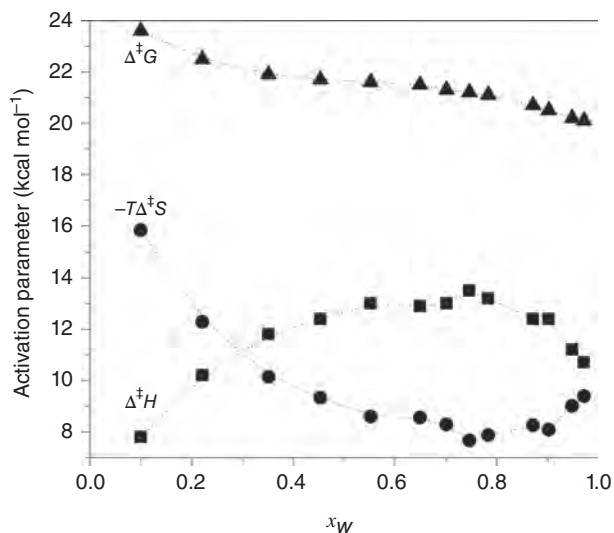
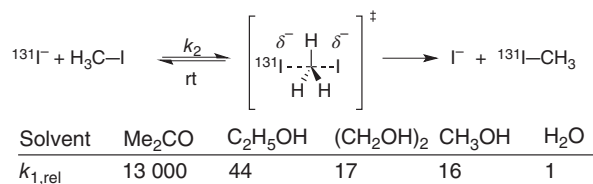


**Figure 15** The complex changes of the activation enthalpy and entropy for the hydrolysis of bis(2,4-dinitrophenyl)carbonate in aqueous acetonitrile as a function of  $\chi_w$ , the mole fraction of water in the medium [60].



**Scheme 9** Iodide self-exchange reaction and solvent effects on relative rate constants.

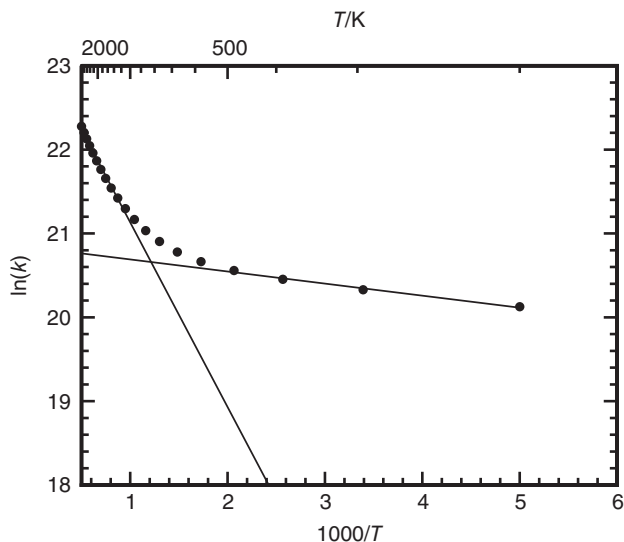


**Figure 16** “Arrhenius plot” for a reaction that does not follow simple Arrhenius behavior [24].

different temperature should be done with care because there is no guarantee, *a priori*, that the plot is linear over a wide ( $T$ ) range. Nonlinear Arrhenius plots may be observed, however, even if the ( $T$ ) range is not large [75, 80–83]. This is especially the case for many biochemical reactions, for example, enzymatic processes and those occurring in membranes. The reason is that different steps of the complex reaction may become rate limiting at different temperatures. Alternatively, there may be  $T$ -induced phase transitions within the membrane. Approaches to analyze the data of these biochemical reactions are known [80–83]. Furthermore, quantum effects, including tunneling, have been reported to influence enzyme kinetics [84].

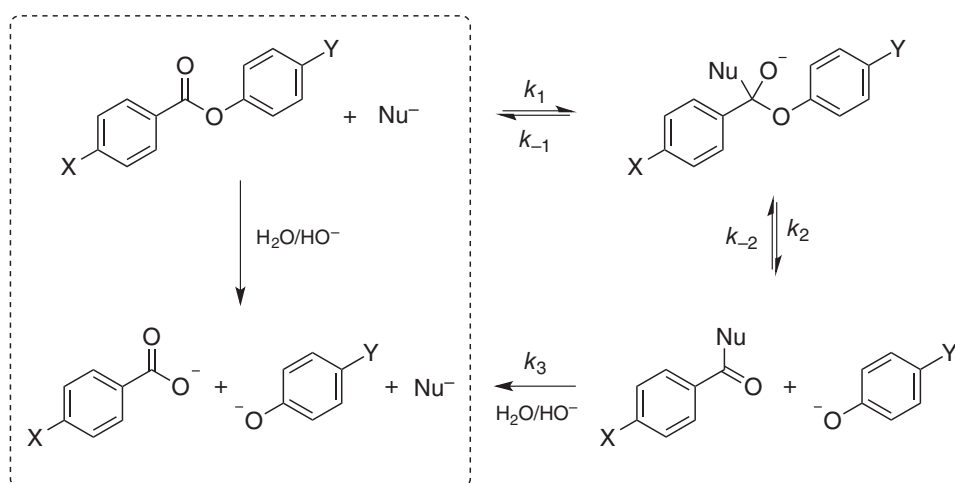
### 3.2 Mechanistic Interpretation

According to Blackmond [57], “Kinetics is one of several languages for describing chemical events. Other possibilities include drawing out a reaction mechanism or construction of an energy diagram. To a synthetic chemist, a chemical reaction is characterized by the singular verdict of its outcome: yield and selectivity at the end of the reaction event are registered as numbers in a table. From a kinetic perspective, a chemical reaction is a journey narrated by the reaction rate law. While reaction progress is evident in an energy diagram with its

“reaction coordinate” axis, surprisingly few chemists realize that they may envision kinetic graphs in this way. Where classical kinetic approaches provide only a bare summary of the journey that the molecules have undertaken, reaction progress kinetic analysis allows much more to be learnt by following the molecules on their journey.” In addition, Wojciechowski and Rice suggested that “Every attempt at identifying the mechanism of a chemical reaction should be preceded by a verification of the fact that rate measurements are being made under conditions where the chemical reaction is the rate governing step. Studies that report no such verification, or present no good argument for chemical reaction being the rate-limiting step, are of little value as archival sources of information and do not deserve to be cited. Moreover, conclusions drawn on the basis of such studies are also dubious” [19].

With this in mind, the calculation of rate constants has many purposes, including the determination of the rate-determining step and effects of structure and the medium on reactivity [3, 57, 85–87]. The few examples in the following illustrate the power of chemical kinetics in probing reaction mechanism.

**3.2.1 Insight into the Nature of the Rate-determining Step** As discussed earlier, the rate-determining step (rds) is the one that, if perturbed, causes the largest change in overall velocity. Therefore, if a reaction is to be optimized, one should determine and try to control its rds. A classic example is base- or nucleophile-catalyzed ester hydrolysis. Many of these acyl-transfer reactions occur by an addition/elimination pathway, via the formation of a tetrahedral intermediate. This raises the question whether the rds is the addition (favored by electron-rich species) or the decomposition of the intermediate (controlled by the efficiency of the leaving group). Only chemical kinetics answers this important question. An example is the nucleophile-catalyzed hydrolysis of a series of phenyl benzoates of the general structure 4-NO<sub>2</sub>PhCO<sub>2</sub>PhX and YPhCO<sub>2</sub>PhNO<sub>2</sub>, where X and Y are substituents (CH<sub>3</sub>O, CH<sub>3</sub>, H, Cl, CN, or NO<sub>2</sub>) (Scheme 10) [88]. The determination of the rate constants and application of Hammett equation allowed the calculation of the corresponding  $\rho$  values [89]. From the experimental values of  $\rho_X$  (1.09) and  $\rho_Y$  (1.59), it was concluded that the reaction is more sensitive to the structure of the leaving group than that of the acyl



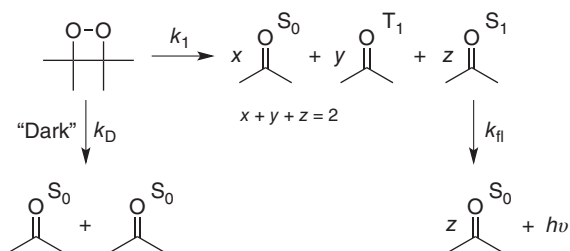
**Scheme 10** Mechanism of the nucleophile-catalyzed hydrolysis of substituted phenyl benzoates.

moiety, that is, rds is the decomposition of the tetrahedral intermediate ( $k_2$  in Scheme 10) [88].

**3.2.2 Probing Catalysis** Green chemistry implies the use, where possible, of efficient catalytic pathways. Therefore, understanding the mechanism of catalysis and comparing the efficiency of catalysts has become a part of the approach to “greener” industrial processes. As an example, consider acyl-transfer reactions, whose industrial importance has increased because of the production of biodiesel [90]. These reactions often occur via the addition/elimination mechanism. There is always the question whether the catalysis is general base (GB; with the base/nucleophile removing a proton from the attacking water or alcohol molecule) or nucleophilic (via the intermediate formation of, e.g., *N*-acylimidazole). Again, several pieces of kinetic-based evidence have been employed in order to answer this question. One is to determine whether the catalytic rate constants for bases of similar  $pK_a$  (e.g.,  $\text{HPO}_4^{2-}$ ; imidazole; the *o*-iodosobenzoate ion) are similar (GB catalysis) or not. In nucleophilic catalysis, the intermediate formed is more reactive than the starting compound; hence, the catalytic rate constants for efficient nucleophiles, for example, imidazole, are much faster than those of GB-catalysts, for example,  $\text{HPO}_4^{2-}$ . In GB catalysis, the catalytic rate constants are expected to obey the Brønsted catalysis law, with slope  $<1$ . Nucleophilic catalysts may still show linear Brønsted-type plots, but the slope can be  $>1$ . Finally, both types of catalysis show distinct kinetic solvent isotope effects (e.g.,  $\text{H}_2\text{O}$  vs.  $\text{D}_2\text{O}$ ): large, and primary for GB catalysis, small and secondary (essentially due to differences in solvation) for the nucleophilic counterpart.

**3.2.3 Understanding Complex Reactions** Chemiluminescence (CL) refers to chemical transformations that occur with the emission of visible light, that is, reaction progress can be followed by measuring the intensity of emitted light. An exothermic transformation can occur with the formation of an intermediate of high-energy content (high-energy intermediate, HEI). If this compound is transformed into products in one elementary step, then one of these products may be formed in its electronically excited state, whose decay to the ground state can be accompanied by light emission [91]. This type of transformation can be conveniently employed to illustrate basic kinetic principles, as shown in the following sections.

**Determination of Activation Parameters** One of the simplest CL transformation is the unimolecular cleavage of 1,2-dioxetanes that can lead to the formation of singlet and triplet excited carbonyl compounds; the singlet excited carbonyls are capable of light emission (Scheme 11). The kinetics of decomposition can be followed by measuring the intensity of emitted light ( $I$ ); mono-exponential decay curves are observed as a function of time



**Scheme 11** Unimolecular 1,2-dioxetane decomposition.

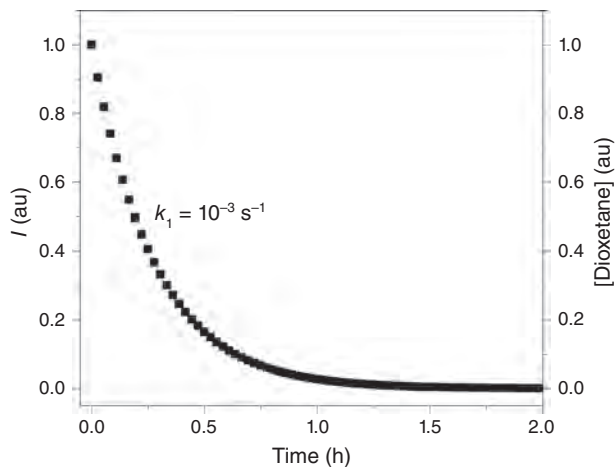


**Figure 17** Temporal profile of the total emission intensity time for the unimolecular 1,2-dioxetane decomposition [91].

(Figure 17). The value of ( $I$ ) at any ( $t$ ) is proportional to the 1,2-dioxetane concentration (Equation 80), that is, the kinetics of 1,2-dioxetane decomposition can be accompanied by measuring the time course of ( $I$ ).

$$I = k[\text{dioxetane}]\Phi_{\text{CL}} \quad (80)$$

On measuring the CL emission intensity at different temperatures, using a condition where the 1,2-dioxetane concentration does not change (relatively low temperature and consequently a low decomposition rate), the activation parameters of the CL process can be determined in a single kinetic run, that is, under nonisothermal conditions [92, 93] (Figure 18). The activation enthalpy ( $\Delta^\ddagger H$ ) and the activation energy ( $E_a$ ) can be obtained by the Eyring and Arrhenius correlations of the emission intensity with the inverse of

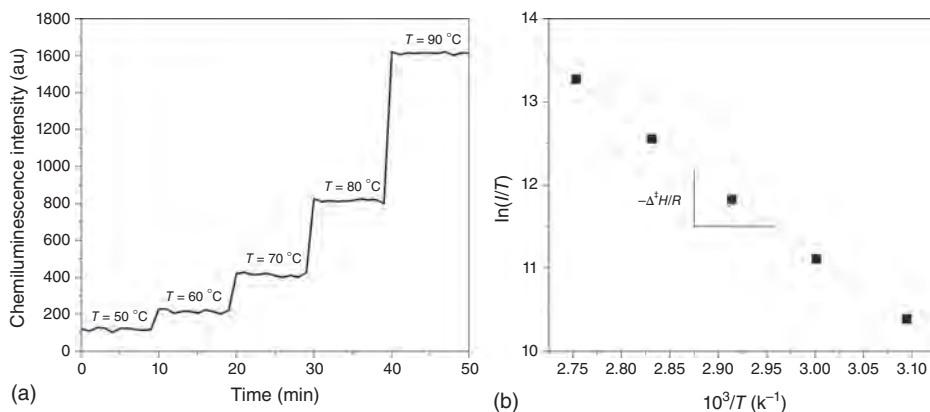
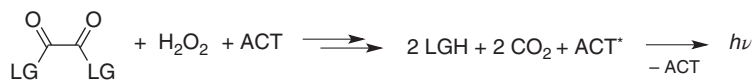


**Figure 18** Emission intensity versus temperature diagram for unimolecular 1,2-dioxetane decomposition. (a) Temperature jump emission intensity profile and (b) the corresponding Eyring plot [91].

temperature, respectively (Figure 18b), since the emission intensity at each temperature is proportional to the rate constant. However, these CL activation parameters correspond to those for the reaction pathway leading to CL emission because the measured intensity arises from this pathway and not from any of the dark decomposition pathways (Scheme 11). Therefore, comparing these CL activation parameters with those obtained by conventional techniques, such as directly following the time course of the dioxetane concentration, allows mechanistic conclusions with respect to the chemiexcitation pathway in these transformations [91].

*Determination of Peroxyoxalate Reaction Mechanism* An important example of a complex chemiluminescent transformation, with various consecutive and parallel reaction steps, is the base-catalyzed reaction of aromatic oxalic esters with hydrogen peroxide [52, 94–105]. This reaction illustrates how rate constants of a multistep complex reaction can be determined from kinetic experiment. This reaction occurs when appropriate oxalic derivatives (e.g., oxalyl chloride, oxalic esters, and amides) are submitted to perhydrolysis in the presence of a base and a fluorescent compound with a low oxidation potential (called an activator, *ACT*) (Scheme 12). Typical kinetic curves obtained for this reaction consist of a fast increase in the emission intensity followed by a considerably slower intensity decrease (Figure 19). The kinetic profile is reminiscent of a system with the formation and decomposition of a reasonably stable intermediate. The kinetic rate constants extracted from these curves correspond to different reaction steps of the complex transformation. Note that ( $k_{\text{obs}}$ ) are generally dependent on the concentrations of the base and the peroxide but not the initial oxalic ester as this is the limiting reagent [103].



**Scheme 12** Base-catalyzed perhydrolysis of oxalic acid derivatives in the presence of fluorescent activators (ACT), resulting in the electronically excitation of the latter and consequently, chemiluminescence emission.

Detailed kinetic studies on the so-called peroxyoxalate reaction have been performed with bis(2,4,6-trichlorophenyl) oxalate (TCPO) using imidazole (IMI-H) as catalyst and 9,10-diphenylanthracene (DPA) as activator. In this case, the reaction kinetics can be followed both by recording the intensity of DPA fluorescence emission and by monitoring the absorption variation caused by the liberation of 2,4,6-trichlorophenol (TCP) (Scheme 13). Note that TCP is liberated from TCPO in the presence of IMI-H alone (no added  $\text{H}_2\text{O}_2$ ) and the rate constants of this transformation are similar to those obtained in the presence of hydrogen peroxide [95, 97]. These and other experimental observations led to the formulation of a reaction mechanism, in which IMI-H acts as nucleophilic catalyst substituting TCP in the TCPO with the formation of a 1,1'-diimidazolyl oxalate (Scheme 13, step 1). Interestingly, two molecules of imidazole appear to participate in this step as indicated by the quadratic dependence of the observed rate constant ( $k_{\text{obs}}$ ) on the [IMI-H] [95]. The  $k_{\text{obs}}$  determined in the absorption experiments is equal to the rate constant extracted from light emission intensity profiles and both these rate constants are independent of the peroxide concentration under certain reaction conditions, consistent with the mechanistic proposal (Scheme 13).

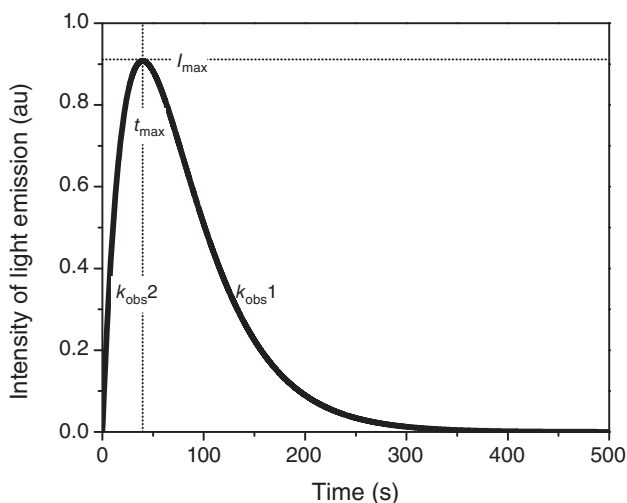
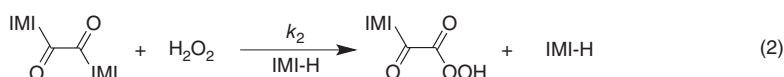
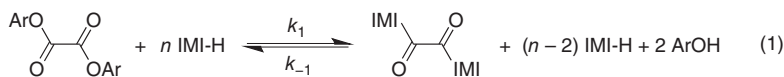
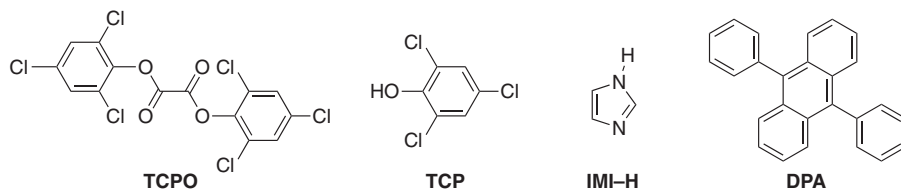


**Figure 19** Emission intensity time course of peroxyoxalate chemiluminescence.  $[\text{TCPO}] = 0.1 \text{ mmol L}^{-1}$ ,  $[\text{H}_2\text{O}_2] = 10 \text{ mmol L}^{-1}$ ,  $[\text{imidazole}] = 1.0 \text{ mmol L}^{-1}$ , and  $[\text{DPA}] = 1 \text{ mmol L}^{-1}$ , in anhydrous ethyl acetate at room temperature [95, 97].

On the other hand, the rate constant extracted from the initial rise of the emission intensity ( $k_{\text{obs}2}$ ) is linearly dependent on  $[\text{H}_2\text{O}_2]$  and  $[\text{IMI-H}]$ , indicating that both reagents participate in the reaction step governing this rate constant. Therefore, the rate constant  $k_{\text{obs}2}$  could be attributed to the nucleophilic attack of peroxide on the 1,1'-diimidazolyl oxalate, catalyzed by imidazole (Scheme 13, step 2). Interestingly, this step can be observed directly by adding  $\text{H}_2\text{O}_2$  after a delay time to the reaction system containing TCPO and imidazole, as well as the ACT [97]. The emission intensity decay rate constants obtained upon such delayed peroxide addition correspond to those derived from the intensity rise of the complete system, further validating the mechanistic proposal (Scheme 13). When  $[\text{H}_2\text{O}_2]$  is increased, the observed rate constant eventually exhibits saturation behavior, indicating a change in the rds (Figure 20). Under these conditions, it appears that the rds is the cyclization of the intermediate peracid derivative to a cyclic peroxide intermediate (Scheme 13, step 3), a transformation that should be independent of  $[\text{H}_2\text{O}_2]$ . However, the maximum rise rate constant ( $k_{\text{obs}2}^{\text{max}}$ ) still depends linearly on  $[\text{IMI-H}]$  (Figure 20), indicating the importance of base catalysis for the efficiency of the intramolecular nucleophilic attack on the carboxyl function of the imidazolide (Scheme 13, step 3).

The cyclic peroxide intermediate formed in the cyclization step is believed to constitute a “HEI” important for all CL transformations [91]. Such intermediates are the “enthalpic sources” that make chemiexcitation energetically feasible. The interaction of this HEI with the ACT leads to the formation of the electronically excited state of the latter, which relaxes to the ground state, accompanied by the emission of fluorescence. Using a Stern–Volmer-like photophysical approach, it was possible to obtain relative values for the rate constants of interaction between the HEI and different ACT [97, 105]. These rate constants correlate with the oxidation potential of the ACT utilized, an indication of the occurrence of an electron transfer from this ACT to the cyclic peroxide. This type of mechanism is quite common in CL systems and has been called Chemically Initiated Electron Exchange Luminescence – CIEEL [106].



**Scheme 13** General mechanism for the peroxyoxalate chemiluminescence using imidazole (IMI-H) as base catalyst [95].

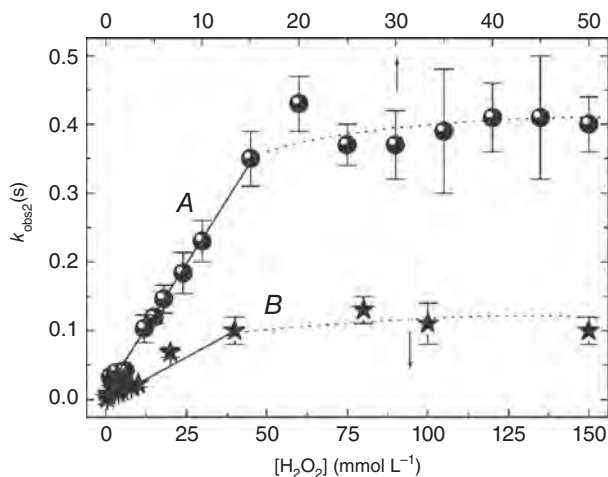


**Figure 20** Dependence of  $k_{\text{obs}2}$  on  $[\text{H}_2\text{O}_2]$  at different imidazole concentrations [97].

It has been possible also to observe this reaction step by direct kinetic measurements, using a reaction system in which the HEI can be accumulated in the absence of the ACT (Figure 21). Addition of the ACT with a delay time to a system consisting of oxalyl chloride and hydrogen peroxide leads to the observation of an intense flash of light with a fast decay

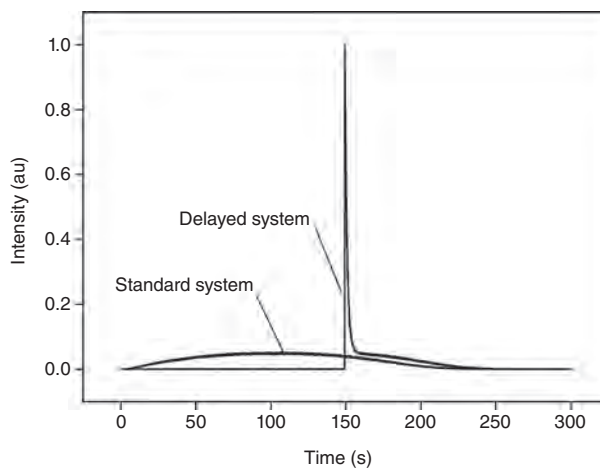


**Figure 21** Delayed addition of an ACT to the reaction of oxalyl chloride with hydrogen peroxide [100].

constant (in the order of seconds at room temperature). The decay constant of this emission intensity depends on the concentration of the added ACT, allowing the calculation of bimolecular rate constants ( $k_{\text{cat}}$ ) for different ACTs. These rate constants showed a linear Gibbs energy correlation with the ACT's one-electron oxidation potentials, confirming the above-mentioned conclusions with respect to the mechanisms of this reaction step [100].

In summary, we have shown that the kinetics can be followed by measuring the light emission intensity, which is generally proportional to the concentration of a limiting reagent; at the same time, this intensity is also proportional to the overall reaction rate. Thus, the mechanism of this complex reaction is elucidated via conventional kinetic studies by observing the influence of the reaction conditions on the time course of the CL emission intensity. Furthermore, the activation parameters of the CL reaction are determined from the effect of temperature on the emission intensity. In addition, delayed reagent addition contributed to mechanistic elucidation. Finally, the usefulness a photophysical approach to obtain rate constants for the interaction of the CL activator with an HEI formed during the reaction is illustrated.

## 4 OBTAINING QUALITY KINETIC DATA

### 4.1 Avoiding Pitfalls in Kinetic Experiments

As mentioned in Introduction, the improvement of both hardware and software has contributed to reduce much of the labor involved in doing chemical kinetics. However, this is no guarantee, *a priori*, that reliable results will be obtained because of possible pitfalls that neophytes (and the not so neophytes as well!) may fall into, as shown in the following illustrative examples.

**4.1.1 Temperature Control** Consider the apparently “trivial” task of controlling the reaction temperature. Some will be satisfied by assuming that the temperature of the reaction is the same as that indicated on the digital display of the attached thermostat, that

is, without taking into consideration heat losses, for example, during the flow of the heating fluid between the thermostat and the equipment. This problem can be avoided using a temperature sensor placed in or next to the reaction cell. When a spectrophotometer is employed, this can be conveniently done by placing the sensor inside a silicone-oil-filled cuvette in the (multiple) cuvette holder. With a conductivity meter, the sensor can be inserted into an NMR tube containing silicone oil and placed inside the reaction solution. The heating device is then adjusted to give the required temperature *inside* the reaction cell. Much better temperature control is achieved if a PC controls the thermostat. One would be surprised by the relatively long time required to achieve thermal equilibrium before the experiment can be initiated.

**4.1.2 Concentration and pH Control** Preparing solutions of known concentration and pH is straightforward [107]. Several problems may arise, however, if the conditions under which the solutions were prepared are noticeably different from those used for the reaction. These include changes of concentration, pH, or both. Consider an aqueous solution that has been prepared at room temperature, and then employed at higher temperatures (60–80 °C). The change in the density of water between 25 °C (0.9978) and 80 °C (0.9718) is 2.53%. Due to this relatively large thermal expansion coefficient, the molar concentration at 80 °C will be reduced by the same factor. Therefore, the *molal* – not the molar concentration scale – should be employed. This implies that solutions should be prepared by *volume and weight*. Furthermore, unless tightly stoppered reaction cells are employed, solvent evaporation can result at high temperatures, especially if the medium contains a volatile organic solvent, such as acetone or methanol, leading to changes in the concentration. Evaporation of a volatile component from a binary solvent mixture leads to changes in both the reagent concentration and the medium properties. In this regard, cuvettes with PTFE stoppers (not those with lids) should be employed in kinetics experiments, *slow or fast*.

Many reactions are acid–base catalyzed; therefore, the use of buffer to control the solution pH is necessary. However, the buffer should be chosen carefully because the reaction may be catalyzed by the components of the buffer. For example, imidazole, MOPS (3-morpholinopropane-1-sulfonic acid), and *o*-iodosobenzoic acid all have  $pK_a$ s in water of about 7. Therefore, they may be employed, *a priori*, to control the reaction pH at about 7. As discussed previously in the hydrolysis of substituted phenyl benzoates, imidazole and *o*-iodosobenzoic acid buffers will also act as nucleophiles, leading to fast ester hydrolysis via a nucleophilic catalysis mechanism (Scheme 7); [88, 108]. The components of MOPS, on the other hand, only participate in acid–base catalysis.

Other aspects that should be considered include the use of buffers in aqueous organic solvents; the capacity of the buffer to maintain the solution (initial) pH during the reaction; the real pH if there is a large difference between the temperatures of buffer preparation and that of the reaction. Although a detailed discussion of the use of buffers and the meaning of the pH reading in mixed (aqueous) solvents is beyond the scope of this text, the following example shows the practical problem faced in these media. Consider the effect of adding methanol to a dilute aqueous buffer whose pH is 5.0. The conditions of the starting solution mean that the pH equals or very nearly equals to  $(-\log a_H)$ . After the addition of methanol, the pH reading will be higher, for example, 7, although the solution cannot be neutral; in fact, it is not. Several factors contribute to the overestimated pH reading, including a change in the buffer  $pK_a$ , a change in the electrode junction potential, and a change in the autoionization constant of the medium, that is, a change

from  $pK_w = 14$  of water to a value somewhere between that of water and methanol (the equivalent  $pK_{\text{MeOH}} = 16.7$ ; where neutral is defined as  $[\text{CH}_3\text{O}^-] = [\text{CH}_3\text{OH}_2^+]$  at  $\text{pH} = 8.35$ ).

Methods for measuring the pH in partially aqueous solutions (where the glass electrode is still responsive) have been published elsewhere [109–113]. One important practical tip is that the glass electrode should be conditioned in the binary solvent mixture for an adequate time before it is used to measure the pH. This conditioning is reversible, that is, the response in aqueous solution is readily restored after reconditioning in water or dilute acid solution.

The power of the buffer to maintain its buffering capacity is related to its concentration and the difference between the pH and the  $pK_a$  of the buffer. The buffering capacity is maximum at its  $pK_a$  value; for practical purposes, the useful range of the buffer is  $\text{pH} = pK_a \pm 1$ . Using dilute buffer solutions (in the mmol range) at pH value outside the  $pK_a \pm 1$  range is not prudent. Furthermore, the ionic strength can play a major role in reaction kinetics [114]. A good practice is to measure the pH at the end of the kinetic run to verify that the solution initial pH has been maintained.

The temperature effect on pH is another experimental variable whose importance should not be overlooked. Temperature affects the  $pK_a$  of the buffer, hence the buffer pH, leading to the so-called buffer temperature coefficient, which is the change in  $\text{pH}/^\circ\text{C}$ . Although this coefficient may vary only slightly over a wide range of temperatures in the acid region, it can be quite dramatic in the alkaline region. Thus, the differences  $\Delta\text{pH} = \text{pH}(\text{at } 10^\circ\text{C}) - \text{pH}(\text{at } 60^\circ\text{C})$  are  $-0.08$  (acetate buffer,  $\text{pH}$  at  $10^\circ\text{C} = 4.00$ ),  $0.11$  (phosphate buffer,  $\text{pH}$  at  $10^\circ\text{C} = 7.07$ ), and  $0.43$  (phosphate buffer,  $\text{pH}$  at  $10^\circ\text{C} = 10.18$ ). A simple method has been suggested in order to correct the effect of  $T$  (up to  $100^\circ\text{C}$ ) on the pH of several extensively employed buffers [115].

**4.1.3 Reliability of the “Infinity” Reading** The determination of rate constants using the least squares method is mostly based on the minimization of the sum of the square of residuals ( $\Sigma Q^2$ ); a residual is the difference between an observed value and the fitted value provided by a model. For simple exponential growth models, the calculation routine starts by the estimation of an “infinity” reading, for example, ( $A_\infty$ ) in spectrophotometry. Consecutive iterations vary the value of this (and the other) parameter of the model in order to minimize the value of  $\Sigma Q^2$ . When following product formation, a saturation curve is expected and data fitting will converge after a few iterations. However, if there are side reactions, for example, precipitation of a sparingly soluble product or light-induced color fading, the experimental determination of ( $A_\infty$ ) will become unreliable. Figure 22 shows some examples of difficulties in the determination of ( $A_\infty$ ) and the effect of the uncertainty of this parameter on the rate constant.

For a problem-free reaction (Figure 22a), the adjusted determination coefficient ( $\text{Adj-}R^2$ ) is close to unity, the value of  $\chi^2$  is reduced, and the  $\Sigma Q^2$  is randomly distributed over time. Figure 22b shows the effect of, for example, the precipitation of the product, causing a slight decrease in the absorption at the end of the reaction. Conversely, Figure 22c depicts an increase in absorption at the end of the reaction, caused for example by the slow formation of a coproduct absorbing at the same wavelength as the product. As shown by the corresponding residuals (lower part), curve fitting becomes unsatisfactory toward the end of the reaction in both cases, compared to the problem-free reaction.

Visual inspection of the solution or a check for light scattering using a very low power laser source at the end of the reaction should detect the formation of any precipitate. A

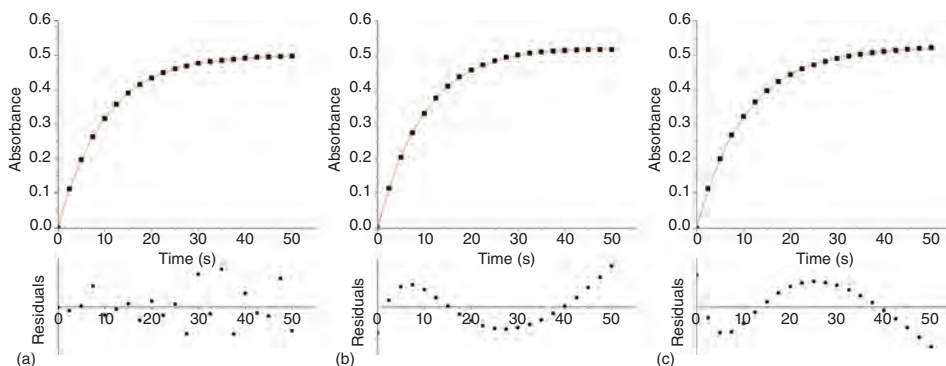


**Figure 22** (a–c) Simulated effect of side reactions on the kinetic profile of a simple first-order reaction. The red lines correspond to the monoexponential fit of the data. The lower part of each plot shows the dependence of the square of the residuals ( $\Sigma Q^2$ ) on time.

simple control to check for the occurrence of photoinduced side reactions is to compare the spectrum of the kinetic experiment with an authentic freshly prepared mixture of products. Using a spectrophotometer that irradiates the sample only during data acquisition can minimize photochemical processes. Deoxygenation of the reaction solution and flushing the cuvette with an inert gas should reduce photooxidation. Another potential problem may occur when the reaction is irradiated with “white” light (entire spectral range including the UV; as in most spectrophotometers with diode-array detection) and not light with the appropriate wavelength. In this case, sample irradiation with the entire spectrum may lead to, for example, photooxidation or light-induced color fading. Therefore, depending on the photosensitivity of the reaction components, it is recommended to check the configuration of the spectrophotometer.

For some reactions, determination of the changes in the concentrations of the reactants/products or the corresponding physicochemical properties is not practical/feasible, for example, the extremely slow hydrolysis of phosphate esters. Even with efficient intramolecular catalysis, at 60 °C, these reactions take from 4 to 14.7 days, at pH = 0.3 and 7.98, respectively [116]. Under these conditions, dedication and extreme care should be exercised in order to avoid solvent evaporation and side reactions. Because most of these problems occur toward the end of the reaction, it is more practical to calculate the infinity reading by nonlinear curve fitting based on initial-rate kinetics (Section 5.2.1) or the Guggenheim method [117].

The Guggenheim method has been used for the determination of the rate-constant ( $k$ ) of first-order or monoexponential reactions [117, 118]. Although this ingenious method has now been surpassed by nonlinear regression analysis, we include it as a historical note. The difference between pairs of readings, taken at a time  $t$  and  $t + \Delta t$  (where  $\Delta t$  is a constant time interval that must be at least 2 or 3 times the half-life) are plotted against  $t$  in a semilogarithmic plot, since it can be shown that

$$\ln([B]_{t+\Delta t} - [B]_t) = c - kt \quad (81)$$

where  $c$  is a constant.

The value of ( $k$ ) corresponds to the slope of the plot and the use of the integrated equation  $[B]_{\infty} - [B]_t = ([B]_{\infty} - [B]_0)e^{-kt}$  allows the determination of the “infinite time” concentrations of B.

## 4.2 Techniques Employed for the Determination of Rate Constants

There are many questions that must be answered before an experimental approach can be selected to obtain kinetic data [119]. The crucial aspects are the reaction timescale, the stability of the reactants/products and the range of temperature. In the following section, we describe the most common experimental techniques and detection methods, classified according to the application.

### 4.2.1 Slow to Moderately Fast Reactions

*Batch Mixing* The progress of the classical stir-in-a-pot reactions (reaction half-time ( $\tau$ )  $\approx$  10 s) can be monitored by removing samples at intervals to determine the change in reactant or product concentration using a myriad of techniques (see the following discussion). Furthermore, it may be convenient to stop the reaction by freezing, neutralization, and so on before the analysis. The reaction can also be monitored directly on-line or *in situ* using, for example, optical absorption, polarimetry, ion-selective electrodes, and conductivity.

*Flow Experiments* For faster reactions, say  $\tau \approx$  0.1 s, the kinetics can be studied by combining the reactants continuously in a mixing chamber, then allowing them to react while flowing down a tube [120]. Although this approach requires large amounts of reagents, it is very convenient because the concentrations are constant at each point along the tube and, thus, signals can be averaged to get good signal-to-noise ratio [121, 122]. Measurements at different distances along the flow tube yield concentrations at different reaction times. Conversely, a change in flow velocity allows the study of chemical reactions occurring at different rates [120, 123]. Spectroscopic detection along the length of the tube, or mass spectrometry using a moveable injector to vary the flow distance, is the most popular detection technique. In addition, mixing of supersonic fluid jets allows mixing times of microseconds.

*Stopped-Flow Technique* For fast reactions occurring on the millisecond timescale, the stopped-flow technique is indicated [119]. In this method, solutions of reactants are mixed rapidly in a special chamber (typical mixing, or “dead” time of a few ms) and flowed through a detection cell. As long as the reactants are flowing steadily, no change in the composition of the mixture in the detection chamber appears [121, 122]. When the flow is suddenly stopped, the composition begins to change and this is monitored as a function of time by a fast-response detector. The stopped-flow technique is limited to timescales of a millisecond or longer due to the hydrodynamics of most solvents. For faster reactions, it is necessary to produce one reactant *in situ* or to use near-equilibrium techniques.

**4.2.2 Fast Reactions** Fast reactions can be difficult to follow and often require the use of near-equilibrium techniques, such as relaxation methods (e.g., jump techniques), NMR analysis [124], and flash photolysis [4, 17, 125]. Jump techniques rest on the fact that, when a chemical equilibrium is perturbed due to a sudden change in temperature, pressure, or pH, the system will relax to a new equilibrium state. The kinetics of this relaxation can be followed for reactions with half-lives from micro- to milliseconds [119]. Flash photolysis is

one of the several methods used to create a nonequilibrium mixture of reactants within a very short time scale [126, 127]. The pump-probe approach is the most conventional method to produce and analyze reactive intermediates and species in the electronically excited state. A very fast intense light pulse is used to create the species of interest, which are then monitored using a spectroscopic technique, including absorbance or fluorescence [128]. The duration of the light pulse should be shorter than the lifetime of the species probed. More information  $q(t)dt$  on this subject can be found in the specialized literature [119].

**Integral and Differential Measurements** Integral measurements are based on the relationship between a measurable parameter and species concentration, that is, any technique able to relate signal intensity to temporal changes in reactant or product concentrations. For example, reaction progress can be monitored by following characteristic vibrations or specific electronic transitions of reactant or product molecules (e.g., absorption spectroscopy). The change in signal intensity with time is related to temporal changes in reactant or product concentrations; thus, with integral methods, the rate is termed the “processed” parameter derived from the “primary” parameter of concentration or conversion of the substrate (Table 2) [57].

Differential (or derivative) methods measure the reaction rate directly. For example, reaction calorimetry measures the instantaneous heat flow upon conversion of reactants to products, which is inherently related to the  $\Delta H$  of the reaction. In this case, the measured rate is the primary parameter, while the concentration or conversion is the processed parameters, proportional to the integral of the rate versus the time (Table 2) [57].

**4.2.3 Conventional Monitoring Methods** This section presents some theoretical and practical information on three of the most common methods for monitoring chemical reactions: conductance, absorption spectroscopy, and fluorescence emission. For a comprehensive description of the methods available for the study of the kinetics of chemical processes, one should refer to these sources [3, 22].

**Measurement of Conductance** These are useful when the reaction studied involves the formation or disappearance of ions or where an ion is replaced with another ion of different mobility. Examples of such reactions are the solvolysis of RCl (neutral reagent  $\rightarrow$  neutral product +  $H^+$  +  $Cl^-$ ; the conductance,  $\Lambda$  increases with time), formation of water by the reaction ( $H^+$  +  $HO^- \rightarrow H_2O$ ;  $\Lambda$  decreases with time), and the hydroxide ion-mediated

**TABLE 2 Integral and Differential Measurements of Reaction Progress [57]**

FTIR spectroscopy as an example of an integral measurement <sup>a</sup>	Reaction calorimetry as an example of a differential measurement <sup>b</sup>
$A = \epsilon bc$	$q = \Delta H_{\text{rxn}} \times \text{volume} \times \text{rate}$
$\text{Rate} = \frac{dc}{dt}$	$\text{Conversion} = \int_{t=0}^{t=t} q(t)dt / \int_{t=0}^{t=t(\text{end})} q(t)dt$
$\text{Conversion} = 1 - \frac{A}{A_0}$	
Measured parameter: conversion	Measured parameter: reaction rate
Processed parameter: reaction rate	Measured parameter: conversion

<sup>a</sup> $A$  = absorbance,  $c$  = concentration,  $\epsilon$  = extinction coefficient, and  $b$  = cell path length.

<sup>b</sup> $q$  = reactant heat flow and  $\Delta H_{\text{rxn}}$  = heat of reaction.

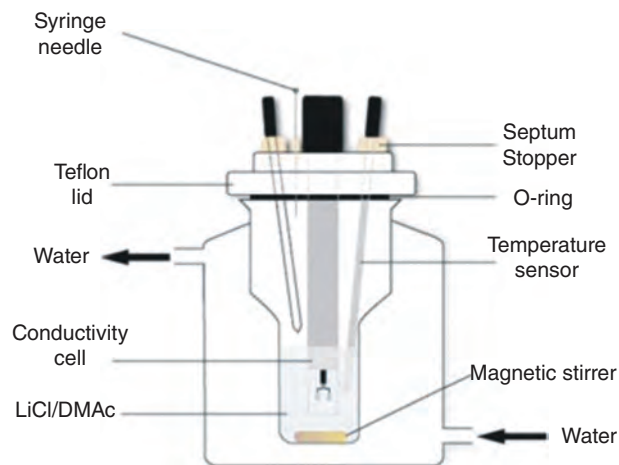


**Figure 23** Setup of a double-wall conductivity cell with temperature sensor.

hydrolysis of ethyl acetate ( $\text{CH}_3\text{CO}_2\text{Et} + \text{NaOH} \rightarrow \text{CH}_3\text{CO}_2\text{Na} + \text{EtOH}$ ;  $\Lambda$  decreases with time because the order of ionic mobility is  $\text{HO}^- > \text{H}_3\text{CCO}_2^-$ ). Figure 23 shows a typical setup of a conductivity cell for measurement of reaction kinetics. Water from a thermostat is circulated in the double-wall cell, the temperature of the reaction solution is continuously monitored by a PT-100 sensor inserted in the reaction solution, and the solution is magnetically stirred.

Reactions in which there is a change in the pH can be easily followed by a pH meter using a glass electrode sensitive to an increase or decrease in  $[\text{H}_3\text{O}^+]$ . An example is the hydrolysis of alkyl chloroformate [129]:  $\text{ClCO}_2\text{Et} + \text{H}_2\text{O} \rightarrow \text{HCl} + \text{CO}_2 + \text{EtOH}$ . Ion-selective electrodes sensitive to ions other than  $\text{H}_3\text{O}^+$ , for example, halides, sulfide, or cyanide, can be used to follow the kinetics of reactions in which ions form (solvolysis of halides) or disappear, for example, by complex formation. Care should be taken because the response time of electrodes can be slow.

A variant to measuring the reaction pH as a function of time ( $t$ ) is to use a pH-stat device. In this case, the reaction is monitored at constant pH, achieved by automatically adding either ( $\text{H}_3\text{O}^+$ ) or ( $\text{HO}^-$ ) during the reaction, depending on which species is liberated or consumed. The volume of solution added is continuously recorded as a function of ( $t$ ) and employed to calculate the rate constant. Besides being a very useful method for carrying out routine experiments, pH-stat, or any other type of “stat” are employed for studying reactions under pseudo-first-order conditions.

Unlike spectroscopic methods, where reaction progress can be unequivocally demonstrated by the disappearance/appearance of characteristic peaks, the change in solution conductivity or pH is *insufficient* evidence to confirm that what is being followed is the reaction of interest. Because these methods merely indicate the formation/disappearance of ions, an independent proof should be given, for example, by isolation of the reaction product *under the conditions of the kinetic run*. This approach was followed in acylation of cellulose in  $\text{LiCl}/N,N$ -dimethylacetamide where the cellulose esters formed were isolated at the end of the kinetic experiments [130].

*Measurement of Absorbance* The absorption of electromagnetic radiation of different wavelengths (e.g., in the microwave, infrared, and visible and ultraviolet regions) is an intrinsic property of all polyatomic chemical species. Therefore, it is possible to monitor the intensity of light absorption by a given species during a chemical reaction. The Beer–Lambert law (also known as the Lambert–Beer, Beer–Lambert–Bouguer law, or simply Beer’s law) correlates the absorption of monochromatic light by a single species of concentration ( $c$ ):

$$A = \log \frac{I_0}{I_t} = \epsilon \cdot c \cdot d \quad (82)$$

where ( $A$ ) is the absorbance, ( $I_0$ ) and ( $I_t$ ) the intensity of incident- and transmitted light, respectively, ( $\epsilon$ ) the molar absorptivity, and ( $d$ ) the optical path length (in cm) through the solution. Note that solution absorption of light is *the sum* of the individual absorption of all chemical species present that absorb light at that wavelength. That is, absorbance and molar absorptivity are additive parameters, a fact that complicates determination of concentrations in samples with more than one absorbing species. Consequently, a given band in the spectrum of a reaction mixture does not necessarily represent a single substance and, therefore, the intensity at the maximum absorption wavelength ( $\lambda_{\max}$ ) cannot, *a priori*, be related to the concentration of a single species in solution [131]. Some practical suggestions related to the study of reaction kinetics by absorption spectroscopy are compiled below.

1. *Importance of Acquiring the Entire Spectrum.* Light absorption is very often used to follow reaction kinetics by monitoring a single wavelength or the whole absorption spectrum over time; therefore, it can be classified as an integral technique [57]. For a preliminary study of a reaction, it is important to first acquire the spectra of the pure reactants and, if possible, pure products; monitor spectral changes after their mixing; and identify intermediates and products as well as eventual changes in the baseline. For example, a dispersive UV–vis spectrophotometer takes from several seconds to a few minutes to scan a range of 400 nm; however, some instruments equipped with rapid scanning and detection can record the whole spectrum very quickly (millisecond scale), which is convenient to monitor reaction kinetics. Only after the changes in the absorption profiles are understood should systematic studies be carried out at fixed wavelength(s).
2. *Proper Choice of Solvent and Cuvette Material.* The choice of proper solvent and cuvettes are fundamental for the acquisition of reliable data. Tables 3 and 4 present the spectral cutoff of common solvents and the wavelength range of some optical materials used to make cuvettes, respectively. These lists are not comprehensive; they give an idea of the properties of most common materials. In addition, although some commercial names are listed, this does not imply recommendation of the particular brand cited.
3. *Importance of the Optical Path Length.* Although the optical path in UV–vis absorption measurements is usually 1 cm, it is important to realize that the path length directly influences the absorption. Thus, if the concentration of a given substance is too low to be measured in a 1 cm cuvette, the use of a cuvette with a longer path length (e.g., 10 cm) may solve the problem. This is also a very valuable approach in case of aggregation, where the concentration of the analyte should be maintained low. Unfortunately, many UV–vis spectrophotometers are provided with cell holders that accepts only 1 cm path cuvette.

4. *Light Scattering and Baseline.* Some applications are not based on the measurement of the absorption but rather on light scattering. In turbid samples (e.g., bacterial cultures), the *apparent absorbance* (also called *attenuance*) is recorded. In this case, the observed parameter is called the optical density (OD). However, light scattering can change the baseline, leading to undesirable results, for example, when measuring the absorbance of chemical species in complex samples. In suspensions, scattering effects increase the absorbance since the scattered light does not reach the light detector. The absorbance recorded by the spectrophotometer is thus overestimated and needs to be corrected [135]. In some applications, though, changes in the baseline over time can be interpreted as the result of the process being monitored, for example, growth or changes in the morphology of nanoparticles. Figure 24 depicts the effect of the increase in the baseline on the absorption band (simulated Gaussian curve) with maximum around 450 nm. As the baseline rises, the absorption maximum shifts (in this example to shorter wavelengths) and the measure of absorbance is not quantitative. This example is much more dramatic than expected for baseline change due to scattering effects and may be due, for example, to precipitation (as observed in nanoparticle formation).
5. *Solutions for High Background Signal and Band Superposition.* Several approaches are available to minimize the effects of background absorption and band superposition. These include monitoring absorption at several  $\lambda$ , and use of difference and differential absorption spectroscopy. Ideally, UV–vis absorption is useful to monitor the progress of a chemical reaction if only the reagent or only the product absorb light. However, most often both reagents and products absorb light in the wavelength range of interest. It is desirable that the  $\lambda_{\text{max}}$  of the reactant and product be well separated, but in practice, the progress of the reaction can still be monitored provided that the respective values of  $\epsilon$  are significantly different. If reagents and products absorb at different wavelengths and are converted directly, there should be a wavelength lying between these positions, known as the isosbestic point, at which the absorbance should remain constant throughout the reaction (Figure 25).

1. *Beer's Law is Additive.* Considering a mixture in solution containing two components at concentrations  $c_A$  and  $c_B$ , the absorbance at any wavelength,  $\lambda$ , is, for unit path length, given by

$$A(\lambda) = c_A \epsilon_A(\lambda) + c_B \epsilon_B(\lambda) \quad (83)$$

Consequently, it is possible to determine the concentration of the components A and B by measuring the absorbance at two or more wavelengths and using the equations:

$$A_{\lambda_1} = c_A \epsilon_{A,\lambda_1} + c_B \epsilon_{B,\lambda_1} \quad (84)$$

$$A_{\lambda_2} = c_A \epsilon_{A,\lambda_2} + c_B \epsilon_{B,\lambda_2} \quad (85)$$

where  $A_{\lambda_1}$  and  $A_{\lambda_2}$  represent the absorbance at  $\lambda_1$  and  $\lambda_2$ ,  $\epsilon_A$  and  $\epsilon_B$  are the respective molar absorptivities of A and B at wavelengths  $\lambda_1$  and  $\lambda_2$ , and  $C_A$  and  $C_B$  are the unknown concentrations of these substances. In solutions containing ( $n$ ) absorbing components, it is possible, in principle, to determine the concentration of all ( $n$ ) components by measuring the absorbance and molar absorption coefficients at ( $n$ ) wavelengths. However, the accuracy of such determinations is usually low when many overlapping absorptions are present.

**TABLE 3 UV Absorbance Cutoff<sup>a</sup> of Typical Solvents Used in the Kinetic Study of Chemical Reactions**

Solvent	UV absorbance cutoff (nm)
Acetone	329
Acetonitrile	190
Benzene	278
Dimethylformamide (DMF)	267
1,4-Dioxane	215
Ethanol	210
Ethyl acetate	256
Hexane	195
Methanol	205
Toluene	285
Water	180

<sup>a</sup>Abs = 1 in a 1.00 cm path length.

**TABLE 4 Properties of Common Materials Used in Absorption Cuvettes [132–134]**

Material	Abbreviations	Wavelength range (nm)
BK7 glass		380–2100
Optical glass	OG	360–2500
Special optical glass	OS	320–2500
Borofloat <sup>®</sup> glass	BF	330–2500
HOQ 310H, Herasil <sup>®</sup> quartz	QH or UV	260–2500
Plastic (PS)	PS	340–800
Plastic (PMMA)	PMMA	300–800
Plastic	BRAND <sup>™</sup> UV	220–900
Plastic	Eppendorf <sup>®</sup> UVette <sup>®</sup>	220–1600
Fused quartz	UVFS	195–2100
Suprasil <sup>®</sup> quartz	QS	200–2500
Suprasil <sup>®</sup> 300 quartz	QX	200–3500
Extrasil quartz	ES	170–2500

2. *Use of Difference Spectroscopy.* This approach measures small changes in systems with high background absorbance. Difference spectra are obtained by subtracting one absorption spectrum from another (with a PC, or using a double-beam spectrophotometer; the latter approach is preferred). Difference spectra may contain negative  $\Delta$ Abs values, and the absorption maxima and minima can be displaced. Furthermore, ( $\epsilon$ ) values are different from the parent spectra. Points of  $\Delta$ Abs = 0 indicate isosbestic points and may be used to check for the presence of interfering substances (Figure 26).

It is clear from the analysis of Figure 26 that it should be possible sometimes to find a wavelength, often different from the absorption maxima, at which the absorbance is a function of concentration of a single component of the reaction mixture. Often, such a wavelength will correspond to the long-wavelength tail of an absorption band. Sometimes, the optimum wavelength corresponds to a minimum of the initial spectrum [3].

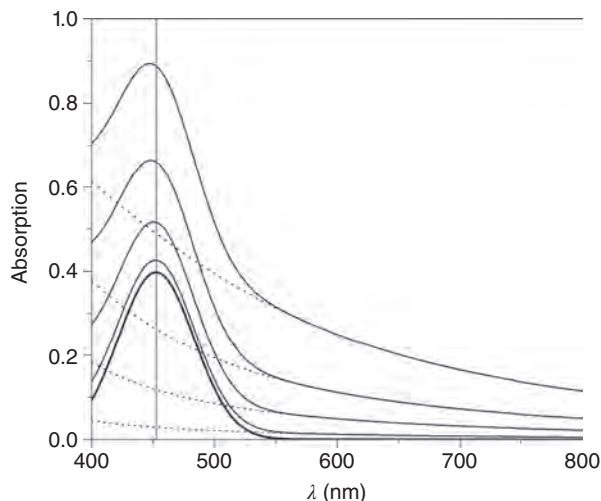


**Figure 24** Effect of the baseline rise (dashed line) on the observed absorption and  $\lambda_{\max}$  of a simulated Gaussian curve in a static hypothetical system were the concentration of the compound of interest is constant and the baseline is deliberately increased.

3. *Use of Derivative Spectroscopy.* In this method, the absolute absorption spectrum of a sample is differentiated using numerical methods with appropriate software and the differential ( $\delta^x \text{Abs} / \delta \lambda^x$ ) is plotted against the wavelength. For example, Figure 27 shows that differentiation of the spectra in Figure 24 eliminate baseline effects on both absorption intensity and maxima; therefore, all curves superimpose, contrasting with the spectral profile depicted in Figure 24.

The usefulness of this approach depends on many factors, such as the noise generated by differentiation. The signal-to-noise ratio decreases as the order of differentiation increases, requiring the use of mathematical smoothing, for example, Savitzky-Golay or fast Fourier transform (FFT) filters. As a result, the absorption maxima and minima can be displaced compared to the original spectra. Figure 28 depicts the effect of the differentiation order on the spectral profile for (a) a single absorption band and (b) a spectrum composed by two superimposing bands. As shown in part (a), differentiation of a single peak spectrum is useful for the precise determination of  $\lambda_{\max}$ . Differentiation of the spectrum composed of superimposed bands allows their separation and, therefore, the determination of the absorption maxima and the degree of band superposition (Figure 28b).

An example of this method is the use of second derivative absorption spectroscopy to monitor the kinetics of thermal decomposition of the main pigment in the beetroot juice, *betanin* [136], in the presence of other components (Figure 29) [137].

4. *The Problem of Weakly or Nonabsorbing Reagents and Products.* It is possible to follow reaction kinetics in cases where the reactants and products absorb weakly or do not absorb light if one of the components of the reaction reacts very quickly with another substance to produce a stable color that is proportional to the concentration of the studied component. An example is the formation of ascorbic acid, which can be monitored by the change in color of 2,6-dichlorophenolindophenol added to the

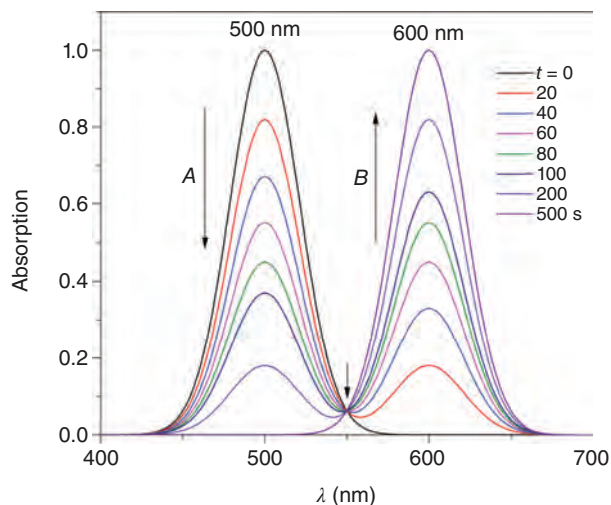


**Figure 25** Ideal situation for reaction monitoring by UV–vis spectroscopy where a reagent *A* is converted to the product *B* with  $k = 0.01 \text{ s}^{-1}$  and the superposition of the absorption bands is negligible. Spectra were simulated by considering Gaussian bands and  $\epsilon_A = \epsilon_B$ . The longer arrows indicate the dependence of the absorption with time and the shorter one shows the isosbestic point.

reaction mixture [3]. Another example is the hydrolysis of methyl chloroformate to produce HCl, methanol, and  $\text{CO}_2$ . This reaction was studied in the presence of an acid–base indicator in its basic (blue) form. Protonation of this form due to formation of HCl decreased the indicator absorbance [129].

*Spectrofluorimetry* Fluorimetry is theoretically at least 100 times more sensitive than spectrophotometry [14]. This technique is based on the measurement of luminescence from a sample during irradiation because most substances are promoted to an electronically excited state after the absorption of a photon. Fluorescence has been a useful method for the study of many systems [138–141], including those involving supramolecular aggregation [142]. The deactivation of this energetic state by fluorescence is fast (around 10 ns) and usually results in photons with lower energy content, that is, the emitted light has longer wavelength than the absorbed radiation. The efficiency of the process is termed fluorescence quantum yield ( $\Phi_{\text{FL}}$ ), which is equal to the ratio between the number of quanta emitted and absorbed and, therefore, less than or equal to unity. The fluorescence of solutions is usually measured at right angles to the excitation source against a dark background, and a drift of 5% in the excitation intensity leads to a 5% change in the detected signal. On the other hand, absorbance measurements involve detecting a small change in the transmitted light, that is, the effect of the background light is very high. Any fluctuation is magnified and a change of 5% in the light intensity corresponds to a variation of 0.02 in the absorbance [135]. Although the intensity of the fluorescence emission depends on the amount of emitting species present, it is proportional to the intensity of the excitation beam. However, it is not possible to compensate indefinitely because the solvent scatters light, via Rayleigh scattering (at the same wavelength of excitation) and Raman scattering (longer wavelength),

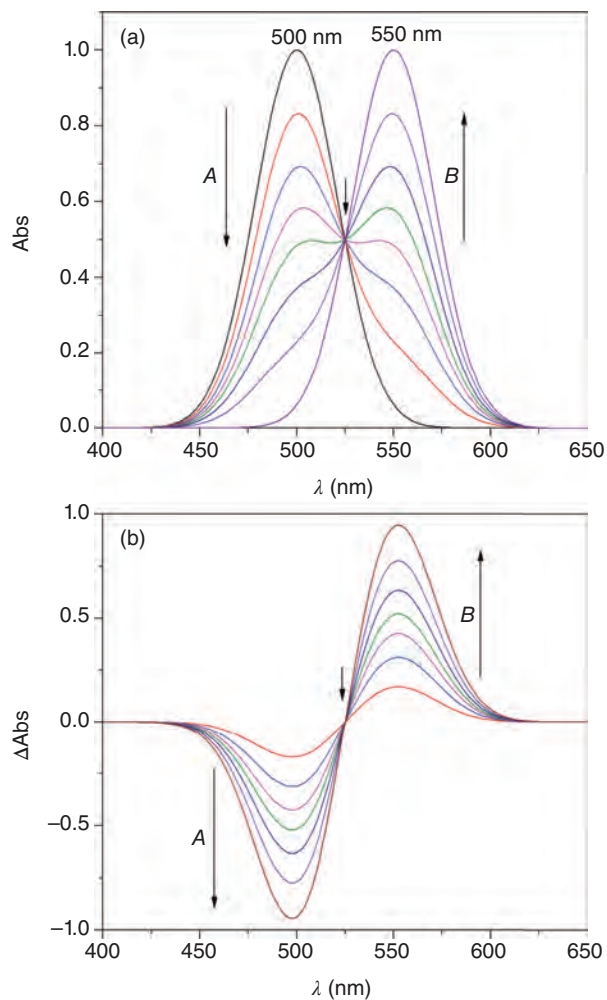


**Figure 26** Simulated spectra for a chemical reaction. In the upper part, the reagent (*A*) is converted to the product (*B*) with  $k = 0.01 \text{ s}^{-1}$ . The lower plot shows the corresponding difference spectra, produced by subtracting the spectrum acquired at a time ( $t$ ) from the reagent spectrum at time ( $t_0$ ). The longer arrows indicate the dependence of the absorption with time and the shorter one shows the isosbestic point.

and eventually swamps the emitted light. Furthermore, increasing the excitation intensity may lead to photolysis of the sample.

Errors in fluorescence measurements can arise through several types of quenching, frequently including concentration quenching. The relation between fluorescence intensity and absorption is given in the following equation:

$$I_{\text{ave}} = I_0 \times 10^{-0.5A} \quad (86)$$

The true fluorescence may be calculated from the above equation, from more sophisticated correction formulae, or from standard curves [135].

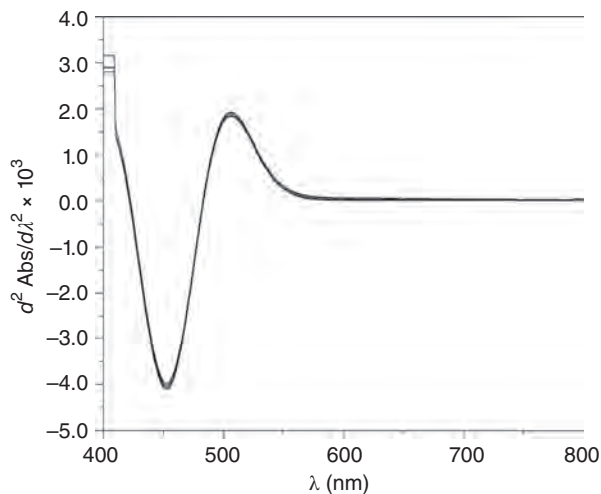


**Figure 27** Second derivative spectra of the simulated spectra in Figure 24 (in the absence of chemical reaction). The effect of the baseline rise is fully eliminated by differentiation.

## 5 ANALYSIS OF KINETIC DATA

For clarity, we have subdivided the following section in two topics: methods for the determination of the reaction order and methods for the determination of reaction kinetics.

### 5.1 Determination of the Reaction Order

**5.1.1 From Reactions Carried Out under Pseudo-First-Order Conditions** For a given reaction with the following rate law:

$$\text{Rate} = k[A]^n[B]^m[C]^p \quad (87)$$

The reaction order can be determined by means of the empirical rate equations as described in Section 2.2.1 for pseudo-first-order conditions. Experiments should be carried out by changing the concentration of the reactants, *one at a time*, while keeping the concentration of the other reactants fixed. This is the so-called isolation method, which is probably the best procedure to study chemical kinetics.

A very convenient variety of this approach is when the reactant concentrations are adjusted in order to change the (higher) order of the reaction into a pseudo-order one. This approach simplifies both the experimental procedure and the subsequent calculations. Consider a typical second-order reaction, for example, hydrolysis of carboxylic acid esters, or an  $S_N2$  reaction. The order in one of the reactants ( $A$ ) is “isolated” using the other ( $B$ ) in large excess (in practice  $[B]_0 \geq 10 [A]_0$ ). A linear plot of  $\ln(\text{experimental quantity})$ , for example, the change in absorbance or the conductivity, versus time, means that the reaction is first order in ( $A$ ). The experiment is then carried out at different ratios of ( $[B]_0/[A]_0$ ), for example, 10, 15, 20, 25, and 30, leading to the corresponding values of  $k_{\text{obs}}$ . A linear plot of  $k_{\text{obs}}$  versus  $[B]$  indicates that the reaction is also first order in ( $B$ ), that is, the total order is two; the slope of such plot is the second-order rate constant. The same approach is essentially applied to third-order reactions.

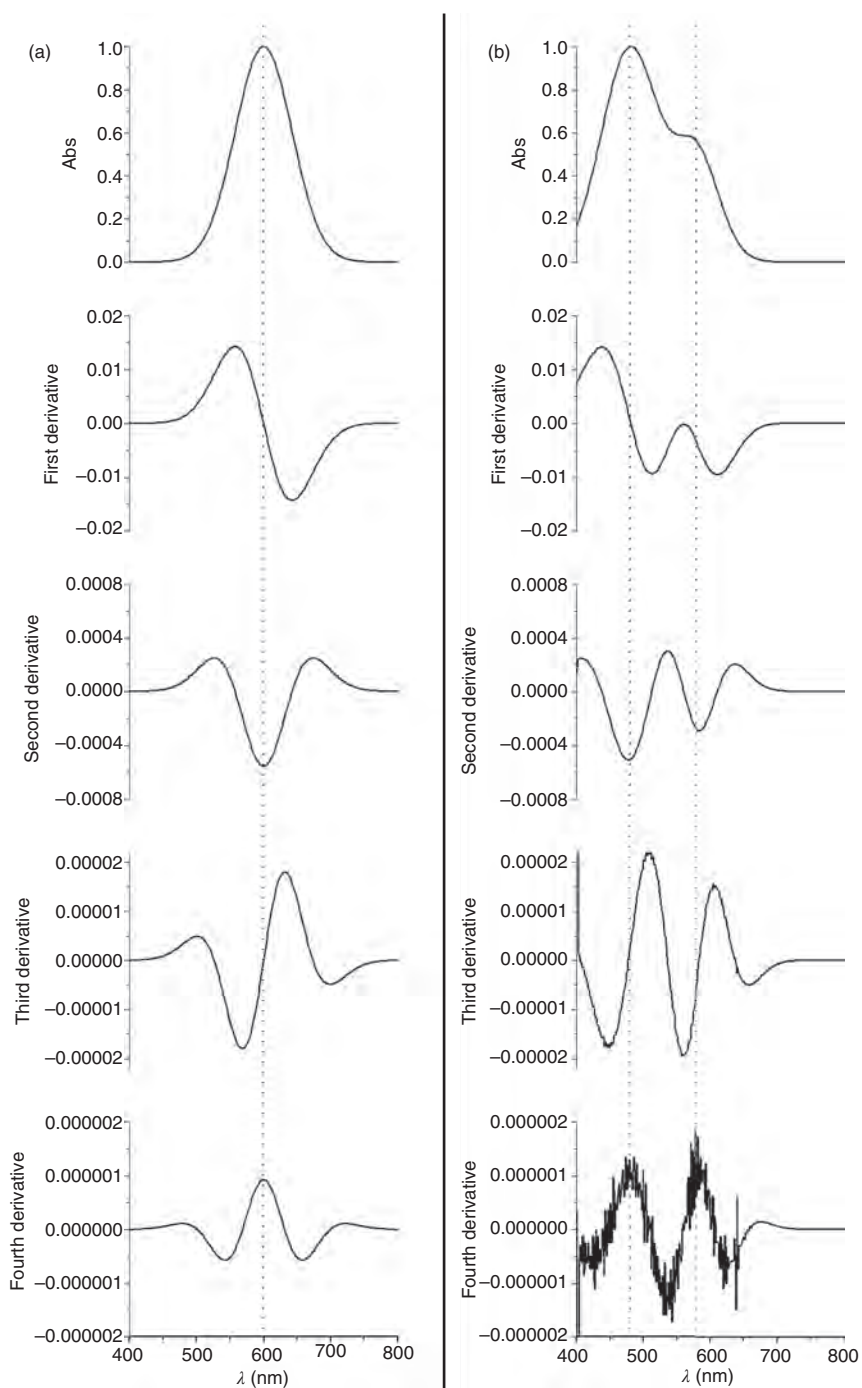


**Figure 28** Effect of the order of differentiation on the spectral profile (a) for a hypothetical Gaussian-shaped absorption band and (b) for a simulated spectrum showing two superimposing bands.

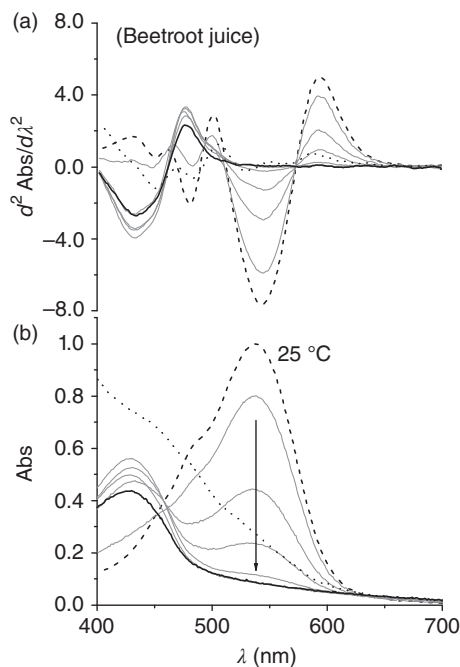


**Figure 29** Effect of microwave heating on the absorption (b) and second-derivative spectra (a) of solutions of fresh beetroot juice in phosphate buffer (pH = 7.4) with absorbance = 1.0 at 536 nm. Dashed lines indicate the absorption at room temperature. Arrows indicate the decrease in absorption intensity at 536 nm with time. The dotted line corresponds to the absorption profile of microwave-dried (1 atm) beetroot juice [137].

Another approach is to, again, keep the concentration of all reagents except one high but measure the concentration change only of the limiting reagent [3]. This procedure is particularly advantageous if the concentration change of this component follows first-order kinetics. The observed rate constants  $k'$  are determined for individual kinetic runs at varying the concentration of one of the components present in excess. For example, if  $[A]_0$  is kept small when compared to  $[B]_0$  and  $[C]_0$ , the observed rate constant  $k'$  can be obtained from Equation 89, and when the value of  $m = 1$ , the plot of  $k'$  versus  $[B]_0$  is linear; otherwise, the value of  $m$  is best determined from the dependence of  $\log k'$  on  $\log [B]_0$ . If the initial concentration of one of the components in excess,  $B$ , for example, is increased by a factor  $j$  with the concentration of all other components kept constant, the resulting observed rate constant ( $k_2'$ ) is related to  $j$  according to

$$j^m = \frac{k_2'}{k'} \quad (88)$$

or from

$$m = \frac{\log k_2' - \log k'}{\log j} \quad (89)$$

The reliability of the result is much improved when the value of the observed rate constant  $k'$  is determined not only for two but also for several values of  $[B]_0$ .

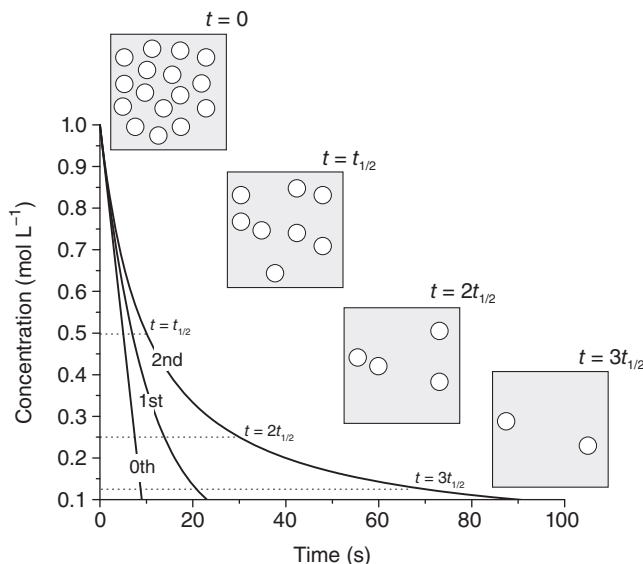


**Figure 30** Graphical illustration of the half-life determination for zero-, first-, and second-order reactions.

**5.1.2 Using the Half-Life Method** As indicated earlier, the half-life,  $t_{1/2}$ , is the time required for the concentration of the reactant to decrease to half its original value; this time depends on reaction order (Figure 30). The value of  $t_{1/2}$  for a first-order reaction is a constant, that is, half-life is independent of initial concentration; whereas for second-order reaction (in  $A$ , or where  $[A_0] = [B_0]$ ), the  $t_{1/2}$  is inversely proportional to the initial concentration. Therefore, the first step is to determine the dependence of  $t_{1/2}$  on time, as shown by the following two examples, for a first- and second-order reactions in ( $A$ ), respectively. After the reaction order is found, the rate constant is calculated from the appropriate equations, for example,  $k = \ln 2/t_{1/2}$  for the first-order reaction, or  $k_2 = 1/t_{1/2} [A]_0$  for the second-order reaction.

## 5.2 Calculation of Rate Constants

**5.2.1 Initial-Rate Method** This method is useful when the reaction is too slow to be followed over its complete time course, or in which there are complicating side reactions. The initial rate ( $v_0$ ) for the reaction of  $A$  to the product ( $P$ ) is given by

$$v_0 = k_f[A]_0 \quad (90)$$

The value of  $k_f$  is determined by dividing  $v_0$  by the change in reagent concentrations:

$$k_f = \frac{v_0}{\Delta[A]_0} \quad (91)$$

At the very beginning of the reaction, the change in concentration of ( $A$ ) is small, as a result, we can assume that  $[A] \approx [A]_0$ . This means that  $d[P]/dt$  is essentially a constant equal to  $k[A]_0$ . Plotting  $[P]$  versus ( $t$ ) over the first few percent of the reaction gives a line whose

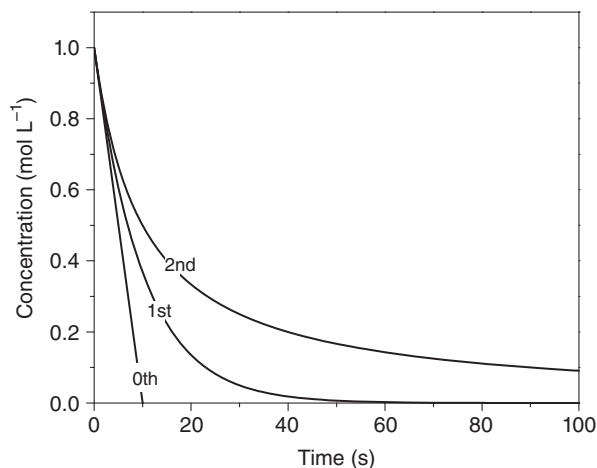


**Figure 31** Dependence of reagent concentration ( $1.0 \text{ mol L}^{-1}$ ) on time for *irreversible* reactions of one reagent A with different kinetic orders. The values of  $k$  employed to generate these curves are  $0.1 \text{ mol L}^{-1} \text{ s}^{-1}$  (zero order),  $0.1 \text{ s}^{-1}$  (first order), and  $0.1 \text{ L mol}^{-1} \text{ s}^{-1}$  (second order).

slope is  $k[A]_0$ . This is a simple way to determine first-order rate constants as long as one can accurately measure early in the reaction a low concentrations of products, or the small decrease in reactant concentration. It also allows the determination of the kinetic order by measuring initial rates for different initial reagent concentrations ( $[A]_0$ ) [5].

**5.2.2 Use of Integrated Rate Equation** In mechanistic studies, the rate law is an essential piece of information because it contains the concentration of species necessary to convert the reactants into products by the lowest energy pathway. Consequently, measurement of the variation of reactant or product concentration (or any experimental variable proportional to the concentration, see above) versus time is the basis of any kinetic study. A particular rate law is a differential equation, which must be reduced to one concentration variable and then integrated [143]. The following section introduces only the integrated rate laws for irreversible reactions; more complex situations will be dealt with later (Table 5). More details are available in advanced textbooks on chemical kinetics [4].

Figure 31 depicts the dependence of concentration on time for the reaction of one reagent (A) occurring with different kinetic orders, all started at the same initial reagent concentration of  $1.0 \text{ mol L}^{-1}$ , using the rate constants of  $0.1 \text{ mol L}^{-1} \text{ s}^{-1}$  (zero order),  $0.1 \text{ s}^{-1}$  (first order), and  $0.1 \text{ L mol}^{-1} \text{ s}^{-1}$  (second order). When the zero-order reaction is complete, the concentrations in the first- and second-order reactions have reached  $1/e$ , and half of their initial values, respectively [87]. The difference between the first- and second-order reactions becomes increasingly marked after that point.

**5.2.3 The Graphical Method** We include these methods because they are didactic, and because of their historic importance, before the advent of sophisticated calculators and the introduction of the computer in the laboratory. The method is based on the (graphical) determination of which rate-law fits the experimental data best [144]. For example, a linear plot of  $\ln [\text{species}]$  (reactant or product) versus time indicates a first-order reaction whose slope is given by  $(-k, \text{ reactant followed; or } k, \text{ product followed})$ . Similarly, for the

**TABLE 5** Some Special Cases of Integral Forms of Equations for the Rate of Reaction  $aA + bB + cC \rightarrow \dots$  Corresponding to Differential Equation  $dx/dt = k(A_0 - x)^m(B_0 - \frac{b}{a}x)^n(C_0 - \frac{c}{a}x)^o$ , Taking Place in Constant Volume and at Constant Pressure

Type	Order			Stoichiometric coefficient			Differential Equation	Infinite Integral	Limited Integral	$\tau_{1/2}$	Units of $k$
	$m$	$n$	$o$	$a$	$b$	$c$					
A	1	0	0	1	—	—	$dx/dt = k(A_0 - x)$	$\ln(A_0 - x) = C - kt$	$\ln A_0/(A_0 - x) = kt$	$1/k \ln 2$	$s^{-1}$
2A	2	0	0	2	—	$a$	$dx/dt = k(A_0 - x)^2$	$1/(A_0 - x) = C + kt$	$x/A_0(A_0 - x) = kt$	$1/kA_0$	$s^{-1} L \text{ mol}^{-1}$
A + B	1	1	0	1	1	—	$dx/dt = k(A_0 - x)(B_0 - x)$	$1/(B_0 - A_0) \ln \frac{B_0 - x}{A_0 - x} = C + kt$	$\frac{1}{B_0 - A_0} \ln \frac{A_0(B_0 - x)}{B_0(A_0 - x)} = kt$	$\frac{k(B_0 - A_0)}{2B_0 - A_0} \times \ln \frac{B_0}{B_0 - A_0}$	$s^{-1} L \text{ mol}^{-1}$
A + 2B	1	1	0	1	2	—	$dx/dt = k(A_0 - x)(B_0 - 2x)$	$\frac{1}{B_0 - 2A_0} \ln \frac{B_0 - 2x}{A_0 - x} = C + kt$	$\frac{1}{B_0 - 2A_0} \ln \frac{A_0(B_0 - 2x)}{B_0(A_0 - x)} = kt$	$\frac{1}{k} \times \ln \frac{B_0}{2(B_0 - A_0)}$	$s^{-1} L \text{ mol}^{-1}$
3A	3	0	0	3	—	$b$	$\frac{dx}{dt} = k(A_0 - x)^3$	$\frac{1}{(A_0 - x)^2} = C + 2kt$	$\frac{2A_0x - x^2}{A_0^2(A_0 - x)^2} = 2kt$	$3/(2k A_0^2)$	$s^{-1} L^2 \text{ mol}^{-2}$
A + B + C	1	1	1	1	1	$c$	$\frac{dx}{dt} = k(A_0 - x)(B_0 - x)(C_0 - x)$	$\frac{C_0 - B_0}{C_0 - A_0} \ln(A_0 - x) + \frac{A_0 - C_0}{B_0 - A_0} \ln(B_0 - x) + \frac{B_0 - A_0}{C_0 - B_0} \ln(C_0 - x) = C + kt$	$\frac{2A_0x - x^2}{A_0^2(A_0 - x)^2} = 2kt$ $\frac{C_0 - B_0}{T} \ln \frac{A_0}{A_0 - x} + \frac{A_0 - C_0}{T} \ln \frac{B_0}{B_0 - x} + \frac{B_0 - A_0}{T} \ln \frac{C_0}{C_0 - x} = kt$	$\frac{B_0 - C_0}{kT} \ln 2 + \frac{C_0 - A_0}{kT} \ln \times \ln \frac{B_0}{B_0 - A_0/2} + \frac{A_0 - B_0}{kT} \ln \frac{C_0}{C_0 - A_0/2}$	$s^{-1} L^2 \text{ mol}^{-2}$
mA	$m > 1$	0	0	$m$	—	—	$\frac{dx}{dt} = k(A - x)^m$	$\frac{1}{(A_0 - x)^{m-1}} = (m - 1)kt + C$	$\frac{1}{(A_0 - x)^{m-1}} - \frac{1}{A_0^{m-1}} = (m - 1)kt$	$\frac{2^{m-1} - 1}{kA_0^{m-1}}$	$s^{-1} L^{m-1} \text{ mol}^{1-m}$
0	0	0	0	1	—	—	$\frac{dx}{dt} = k$	$-(A_0 - x) = kt + C$	$x = kt$	$A_0/2k$	$s^{-1} L^{-1} \text{ mol}$
1/2A	$1/2$	0	0	1	—	—	$\frac{dx}{dt} = k(A_0 - x)^{1/2}$	$-(A_0 - x)^{1/2} = \frac{kt}{2} + C$	$A_0^{1/2}(A_0 - x)^{1/2} = \frac{kt}{2} + C$	$\frac{kt}{2} \times 3A_0^{1/2}/2k$	$s^{-1} L^{-1/2} \text{ mol}^{1/2}$

<sup>a</sup>Valid also for  $A + B \rightarrow$  if  $[A] = [B]$ .

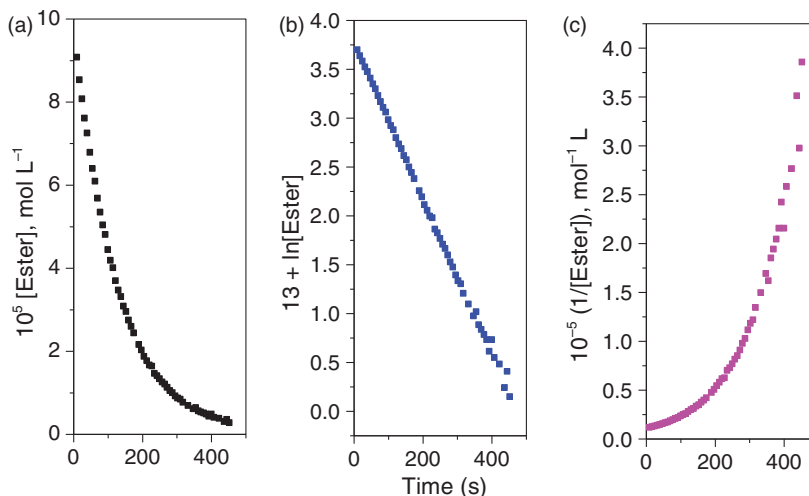
<sup>b</sup>Valid also for  $A + 2B \rightarrow$  if  $2[A] = [B]$  and  $A + B + C \rightarrow$  for  $[A] = [B] = [C]$ .

<sup>c</sup> $T = A_0B_0(A_0 - B_0) + A_0C_0(C_0 - A_0) + B_0C_0(B_0 - C_0)$ .

Note: Table modified from R. Livingstone, Evaluation and Interpretation of Rate Data, in *Investigation of Rates and Mechanisms of Reactions* (S. L. Friess, E. S. Lewis, and A. Weissberger, Eds.), 2nd ed., Part I, Interscience, New York, 1961, p. 114.

**TABLE 6** Rate Laws in their Differential and Integrated Forms, Property that is Plotted to Calculate the Rate Constant, and Half-Lives for Simple, Irreversible Reactions

	Zero order	First order	Second order
Rate law	$-\frac{d[A]}{dt} = k$	$-\frac{d[A]}{dt} = k[A]$	$-\frac{d[A]}{dt} = k[A]^2$
Integrated form	$[A] = [A]_0 - kt$	$[A] = [A]_0 e^{-kt}$	$\frac{1}{[A]} = \frac{1}{[A]_0} + kt$
Units of $k$	$\frac{\text{mol}}{\text{L} \cdot \text{s}}$	$\frac{1}{\text{s}}$	$\frac{\text{L}}{\text{mol} \cdot \text{s}}$
Linear plot to determine $k$	$[A]$ versus $t$	$\ln([A])$ versus $t$	$\frac{1}{[A]}$ versus $t$
Half-life	$t_{1/2} = \frac{[A]_0}{2k}$	$t_{1/2} = \frac{\ln(2)}{k}$	$t_{1/2} = \frac{1}{k[A]_0}$

**Figure 32** Determination of kinetic order of the hydrolysis of DNPC in acetonitrile reaction in the presence of 30 mol L<sup>-1</sup> water with 0.01 mol L<sup>-1</sup> of HCl at 25 °C. The reaction was followed at 360 nm. Plots (a–c) are for zero-, first-, and second-order reactions, respectively.

reaction of a species ( $A$ ), or ( $A + B$ ) ( $[A]_0 = [B]_0$ ), a linear plot of  $1/[A]$  versus time indicates a second-order reaction, whose slope is  $k_2$ .

As shown in Table 6, the use of integrated rate equation to fit experimental data is suitable for the determination of the reaction order of simple reactions from the corresponding linear plot. However, the reaction order is not necessarily an integer and, therefore, the use of integrated rate equations is unwarranted for these cases.

An example of the application of this method is the reaction of a reactive ester, namely the pH-independent hydrolysis of 4-nitrophenyl chloroformate (DNPC) in acetonitrile as solvent and water (30 mol L<sup>-1</sup>). Figure 32 shows attempts to apply zero- ( $A$  vs.  $t$ ) first- ( $\ln(A)$  vs.  $t$ ) and second-order rate law ( $1/A$  vs.  $t$ ) to the experimental data. Only the first-order law gives a straight line; therefore, this reaction is pseudo-first order which is reasonable, as water is present in excess.

For a simple reaction ( $R \rightleftharpoons P$ ) first-order kinetics, the rate constant can be determined by

$$\ln \left( \frac{A_{\infty} - A_0}{A_{\infty} - A_t} \right) = k_1 t \quad (92)$$

where ( $A_0$ ), ( $A_t$ ), and ( $A_{\infty}$ ) refer to the signal proportional to the initial-, time  $t$ -, and final concentration, respectively. The rate constant  $k_1$  can be calculated from the slope of the plot of  $\ln \left( \frac{A_{\infty} - A_0}{A_{\infty} - A_t} \right)$  versus time.

**5.2.4 Nonlinear Regression Analysis** There are many computer programs useful for fitting theoretical rate equations to experimental kinetic data. The main advantage of using such software packages is the possibility of fit nonlinear curves to the data, including those requiring complex equations. The nonlinear fitting of data avoids the transformation of data to linear equations and, consequently, do not compromise the statistics. However, the data are fitted using mathematical functions selected by the user and, as a result, nonlinear regression analysis can be misleading if not used properly. The following suggestions are useful to avoid the most common errors in fitting a certain model to experimental data.

*No Manipulation Will Extract a Reliable Rate Constant from a Bad Set of Data* Kinetic analysis depends on (i) an accurate method for detection of reaction progress; preferably with continuous data acquisition with adequate signal strength and resolution and (ii) adequate computational support for acquiring and manipulating the data [57].

*Checking the Residuals is a Reliable Approach to Judge Kinetic Data Quality* The residuals plot (the  $y_{\text{calculated}} - y_{\text{observed}}$  against  $x$ ) should be always checked. The residuals should be randomly distributed around the  $x$ -axis; any systematic or periodic deviation is an evidence of lack-of-fit. For example, the nonlinear fitting of the curve describing the formation of the product  $C$  in Figure 12 is shown in Figure 33. In this example, the use of a two-exponential function (Equation 93) results in  $k_1 = 0.01 \text{ s}^{-1}$  and  $k_2 = 0.1 \text{ s}^{-1}$  and  $y_0 = 1$ , the exact values used to simulate the data. The precision of the fitting using a monoexponential function depends on the interval selected, that is,  $k_1 = 0.00942 \text{ s}^{-1}$  ( $t_0 = 40 \text{ s}$ ) versus  $k_1 = 0.00998 \text{ s}^{-1}$  ( $t_0 = 0 \text{ s}$ ).

The corresponding regular residuals plots are given in Figure 34. Only the fitting using the two-exponential function (Equation 93) results in random residual profile; the use of the monoexponential function gives a trend line indicating lack-of-fit.

*The Size of the Dataset is Important* The number of experimental points and both the number of half-lives monitored and the acquisition time interval are crucial parameters. Figure 35 shows the effect of the number of points on the determination of rate constants. Although the reduction of the number of data point by a factor of 6 does not compromise the value of the rate constants for either the disappearance of ( $A$ ) or formation of ( $B$ ), the rate constants related to the intermediate species ( $C$ ) have been appreciably affected.

*Noise is Not always a Problem* Consider, for example, the function  $\text{signal} = e^{-0.1t}$ . This plot is shown as a solid line in Figure 36a. To it has been added random error, which hereafter will be referred to as *noise*.

Table 7 shows that the application of smooth functions to the kinetic data with different noise levels does not necessarily lead to any increase in the exactness of the obtained kinetic

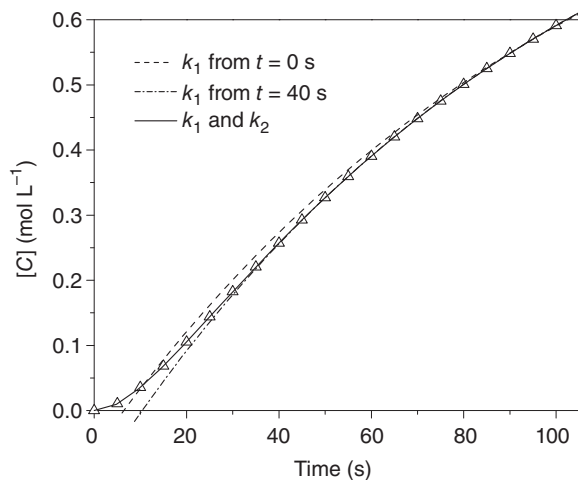


**Figure 33** Nonlinear curve fitting of the data presented in a first-order consecutive reaction following Equation 48. The data were fitted to a two-exponential function and with a monoexponential function from  $t_0 = 0$  s or 40 s.

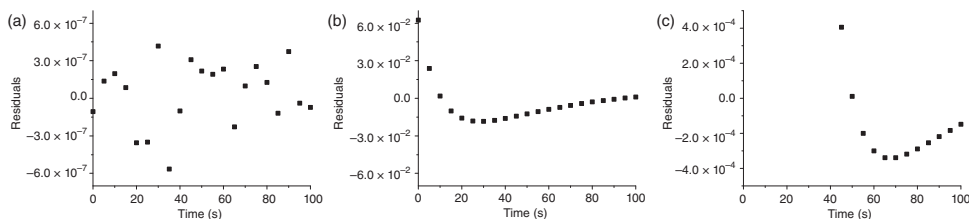


**Figure 34** Plots of residuals corresponding to (a) two-exponential function, (b) monoexponential function from  $t_0 = 0$  s, and (c) monoexponential function from  $t_0 = 40$  s.

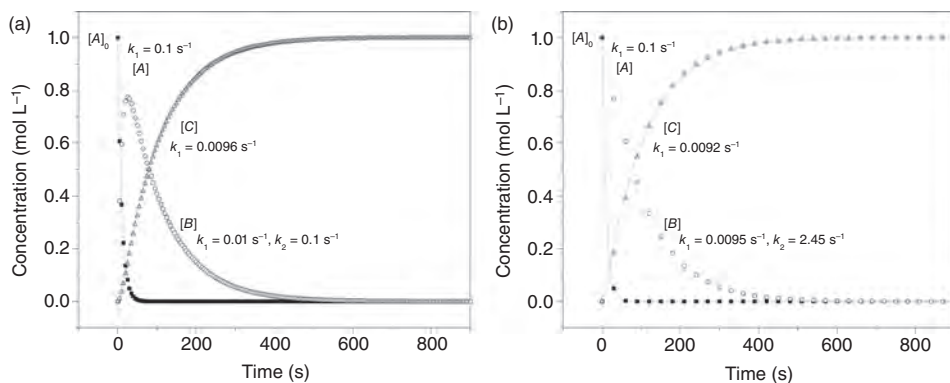


**Figure 35** Comparison of data resolution on fitting. Plots (a) and (b) have 180 and 30 data points, respectively, that is, one point every 5 or 30 s. The changes in concentration of (A) and (C) with time were fitted using a monoexponential model, whereas the change in concentration of (B) was fitted using a two-exponential model.

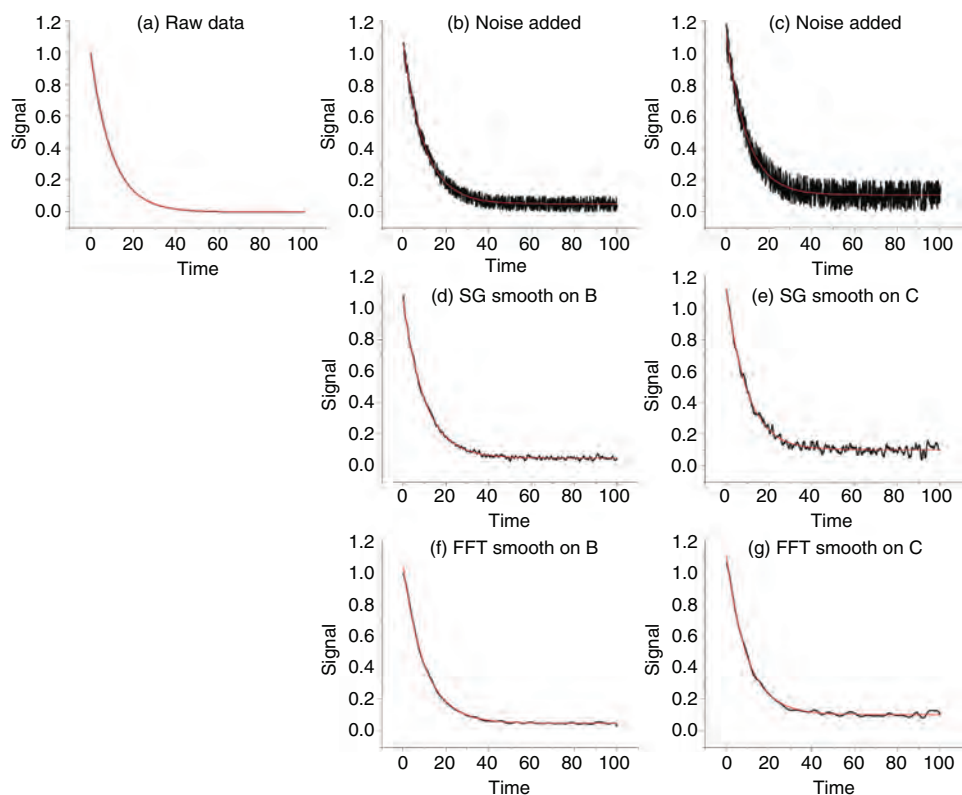


**Figure 36** Effect of noise on data fitting. (a) Dataset obtained using a monoexponential function parameterized as follows:  $y_0$  (offset) = 0,  $A = 1$ ,  $k = 0.1 \text{ time}^{-1}$ . In (b) and (c), random numbers have been added to the dataset to simulate low and high intensity noise, respectively. Curves (d) and (e) show the effect of smoothing the data in (b) and (c) using the Savitzky–Golay (SG) algorithm with 20 points of window in a second-order polynomial. Plots (f) and (g) show the effect of smoothing the data in (b) and (c) using a fast Fourier transform (FFT) filter with 20 points of window and a cutoff of unity.

**TABLE 7** Parameters Determined by Nonlinear Fitting of Data Presented in Figure 36

Plot	$y = y_0 + Ae^{-(kt)}$		
	$y_0$	$A$	$k$
<b>(A) Original dataset</b>	<b>0</b>	<b>1</b>	<b>0.1</b>
<b>(B) Dataset + Low intensity noise</b>	<b>0.04916</b>	<b>1.00132</b>	<b>0.10004</b>
(D) SG smooth of (B)	0.04911	1.00107	0.10001
(F) FFT smooth of (B)	0.04868	0.99015	0.09846
<b>(C) Dataset + High intensity noise</b>	<b>0.10263</b>	<b>1.01788</b>	<b>0.10431</b>
(E) SG smooth of (C)	0.10267	1.01906	0.10443
(G) FFT smooth of (C)	0.10216	1.00641	0.10263

parameters. In the previous example, the large number of points decreases the effect of noise on the kinetic parameters; however, noise and data smoothing may influence the value of the rate constant.

*The Fitting Function must be Chosen with Care* Equations with a larger number of variables are likely to provide a better fit to the data as compared to simpler ones. However, the combination of a large number of independent variables and a small dataset may compromise the statistical significance of the resulting fitting parameters. More importantly, however, the kinetic model chosen and the corresponding fitting function have to be based on a plausible reaction mechanism. If this is not the case, the fitting parameters will not have any mechanistic meaning. For example, even so a first-order kinetic decay can be fitted using, for example, a polynomial function; this fitting does not give rise to any kinetic parameters that can be utilized for mechanistic interpretation.

*Check Variables for Dependence* One must check the dependence of the variables to prevent collinearity (or multicollinearity), which is the mutual dependence (close to unity) of two or more “independent” variables. This effect is particularly important if the kinetic model used to rationalize the experimental data has several rate- and, eventually, equilibrium constants. Reducing the number of variables or selecting a different fitting function avoids this high dependence.

*Verify the Fitting with the Appropriate Parameter* The coefficient of determination ( $R^2$ ) and common chi-squared ( $\chi^2$ ) tests for goodness of fit do not guarantee that a given model fits the data better than another! The F-test and Akaike Information Criterion (AIC) test should be used to decide which of the two models is the better one to fit the same dataset (instead of the  $R^2$  parameter). The F-test assumes that the models are nested (one model is the simplified version of the other). In case the models are not nested, the model with the lower AIC is the best to fit a given dataset. There are some examples that discuss the balance between chemical relevance and fitting quality [145].

*Limitations of the Fitting Algorithm* Specific mathematic algorithms are required in the least squares curve fitting. One of the most common is the Levenberg–Marquardt algorithm (LMA), which is widely utilized for regression analysis by software packages [146, 147]. However, the LMA finds only a local minimum, which is not necessarily the global minimum. Consequently, the initial guess of fitting parameters becomes very important when using the LMA, and when in doubt, one must check the effect of the initial value of the regression parameters on the final convergence. The use of heuristic algorithms minimize the problem, but critical analysis of the parameters obtained fitting the model to the data seems to be enough for most cases [148].

*Determination of Rate Constants of Similar Magnitude in Consecutive Processes* In consecutive processes, the determination of the rate constant for the slow process is straightforward. However, the difficulty in the determination of the other rate constant is determined by the ratio between  $k_1$  and  $k_2$ , that is, the value of the first-order constants  $k_1$  and  $k_2$  can be determined using Equation 93 if the rate constants are different, for example,  $k_1 \gg k_2$ .

$$[B] = A_1 e^{-k_1 t} - A_2 e^{-k_2 t} \quad (93)$$

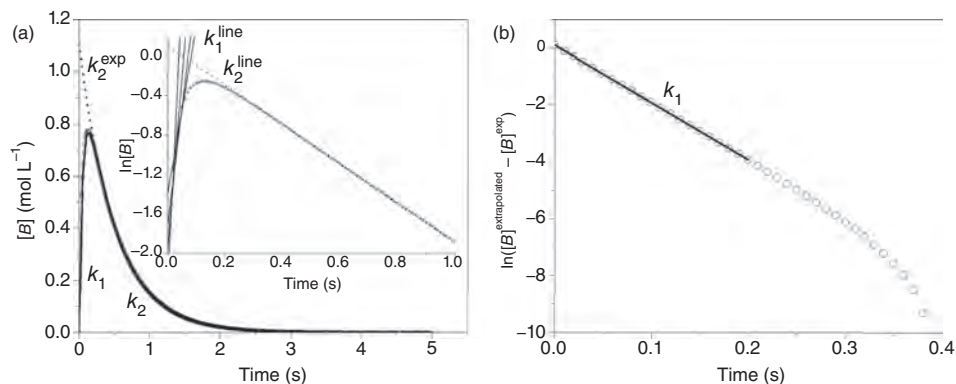


**Figure 37** Graphical method for the determination of rate constants in consecutive first-order reactions. The nonlinear fitting of  $[B]$  against time was used to determine  $k_1$  and  $k_2$  directly from simulated data ( $k_1 = 2 \text{ s}^{-1}$ ;  $k_2 = 20 \text{ s}^{-1}$ , thick black line in (a)). The inset plot in (a) shows the  $\ln([B])$  against time. Plot (b) allows the determination of  $k_1$  from the linear fitting of the residuals.

In cases where the intermediate can be isolated (or obtained by means of chemical synthesis), the value of  $k_2$  can be determined directly. However, there are several approaches to determine the rate constants  $k_1$  and  $k_2$ . For example, the rate constant for the slower process can be obtained from the slope of the linear region after the faster process has died out. In Figure 37a, this condition is achieved after ca. 0.3 s ( $k_2^{\text{line}} = 0.199$ ); however, the rate constant of the fast process (upto 0.3 s) cannot be obtained accurately by the same approach because the kinetic data is not linear (i.e., the value of  $k_1^{\text{line}}$  obtained by linear fitting of data in different intervals varies from 17 to  $59 \text{ s}^{-1}$ , Figure 37a, inset). The rate constant  $k_1$  can be determined by plotting the  $\ln$  of the difference between the value of  $[B]$  (not  $\ln([B])!$ ) at a particular time ( $[B]^{\text{exp}}$ ) and the value of  $[B]$  extrapolated back from the value of  $k_2$  ( $[B]^{\text{extrapolated}}$ , Figure 37b). A  $k_1$  of  $20.1 \text{ s}^{-1}$  was determined by linear fitting of the data in Figure 37b. Again, the graphic method is useful if  $k_1$  and  $k_2$  are very different, for example, the second process starts 5–10 half-lives after the first. If the rate constants are not separated by this factor, it is easier to change the experimental conditions in order to achieve a more convenient  $k_1/k_2$  ratio than to try to fit the data using the least squares method.

However, a similar result can be obtained from a nonlinear least squares fit of the data to Equations 94 and 95:

$$[B] = \frac{[A]_0 k_1}{(k_2 - k_1)} (e^{-k_1 t} - e^{-k_2 t}) \quad (94)$$

$$[C] = [A]_0 \left[ 1 + \frac{1}{(k_1 - k_2)} (k_2 e^{-k_1 t} - k_1 e^{-k_2 t}) \right] \quad (95)$$

Alternatively, in more complex cases (i.e., if  $k_1$  and  $k_2$  are similar), one should consider that when  $[B]$  reaches its maximum,  $[B]^{\text{max}}$ ,  $d[B]/dt = 0$ ; thus,  $k_2$  can be determined from  $k_1$  and the ratio of the concentration of  $A$  at the time that the concentration of  $B$  reaches its maximum (Equation 96).

$$k_2 = k_1 \frac{[A]_t^{\text{max}}}{[B]^{\text{max}}} \quad (96)$$

where  $[A]_t^{\max}$  is the concentration of  $A$  at time  $t_{\max}$ , when  $[B] = [B]^{\max}$ .

Differentiation of Equation 95 with respect to  $t$ , and equating to zero, shows that the conditions relating to the maximum allow the evaluation of  $k_2$  (Equations 97 and 98).

$$t_{\max} = \frac{\ln(k_1/k_2)}{k_1 - k_2} \quad (97)$$

$$[B]^{\max} = [A]_0 \left( \frac{k_1}{k_2} \right)^{\frac{k_2}{k_1 - k_2}} \quad (98)$$

## ACKNOWLEDGMENTS

We thank our students and collaborators who have done some of the kinetic work reported here. OAS thanks Dr. Paulo A. R. Pires because his competence in developing software has turned doing chemical kinetics easy. We thank FAPESP (State of São Paulo Research Foundation, grant #2014/22136-4) and CNPq (National Council for Scientific and Technological Research, fellowship 307022/2014-5) for their continuous financial support and research productivity fellowships to OAS and ELB.

## REFERENCES

1. Clark, J.D. (1924) The kinetic theory – an example of right thinking. *J. Chem. Educ.*, **1** (4), 75.
2. Laidler, K.J. (1996) A glossary of terms used in chemical kinetics, including reaction dynamics. *Pure Appl. Chem.*, **68** (1), 149–192.
3. Zuman, P. and Patel, R. (1992) *Techniques in Organic Reaction Kinetics*, Krieger Publishing, Malabar, FL.
4. Marin, G.B. and Yablonsky, G.S. (2011) *Kinetics of Chemical Reactions: Decoding Complexity*, Wiley-VCH Verlag, Weinheim, Germany.
5. Anslyn, E.V. and Dougherty, D.A. (2006) *Modern Physical Organic Chemistry*, University Science, Sausalito, CA.
6. Arnaut, L., Formosinho, S., and Burrows, H. (2007) *Chemical Kinetics: from Molecular Structure to Chemical Reactivity*, 1st edn, Elsevier, Amsterdam; Boston.
7. Benson, S.W. (1982) *The Foundations of Chemical Kinetics*, R.E. Krieger, Malabar, FL.
8. Billing, G.D. and Mikkelsen, K.V. (1996) *Introduction to Molecular Dynamics and Chemical Kinetics*, John Wiley & Sons, Inc., New York.
9. Billing, G.D. and Mikkelsen, K.V. (1997) *Advanced Molecular Dynamics and Chemical Kinetics*, John Wiley & Sons, Inc., New York.
10. Compton, R.G. (1989) *Reactions at the Liquid-Solid Interface*, Elsevier, Amsterdam, New York.
11. Connors, K.A. (1990) *Chemical Kinetics: The Study of Reaction Rates in Solution*, VCH, New York, NY.
12. Èmanuël', N.M. (1981) *Problems in Chemical Kinetics* (Rev. from the 1979 Russian ed.), MIR Publishers, Moscow.
13. Espenson, J.H. (1981) *Chemical Kinetics and Reaction Mechanisms*, McGraw-Hill, New York.
14. Fersht, A. (1999) *Structure and Mechanism in Protein Science: A Guide to Enzyme Catalysis and Protein Folding*, W.H. Freeman, New York.

15. Houston, P.L. (2001) *Chemical Kinetics and Reaction Dynamics*, 1st edn, McGraw-Hill, Dubuque, Iowa.
16. Masel, R.I. (2001) *Chemical Kinetics and Catalysis*, Wiley-Interscience, New York.
17. Mauser, H. and Gauglitz, G. (1998) *Photokinetics: Theoretical Fundamentals and Applications*, Elsevier, Amsterdam; New York.
18. Reichardt, C. and Welton, T. (2011) *Solvents and Solvent Effects in Organic Chemistry* (4th, updated and enl. ed.), Wiley-VCH, Weinheim, Germany.
19. Wojciechowski, B.W. and Rice, N.M. (2003) *Experimental Methods in Kinetic Studies*, Rev. edn, Elsevier, Amsterdam; Boston.
20. Laidler, K.J. (1987) *Chemical Kinetics*, 3rd edn, Harper & Row, New York.
21. Laidler, K.J. and Glasstone, S. (1948) Rate, order and molecularity in chemical kinetics. *J. Chem. Educ.*, **25** (7), 383.
22. Halpern, A.M. and McBane, G.C. (2006) *Experimental Physical Chemistry: A Laboratory Textbook*, 3rd edn, W. H. Freeman, New York.
23. Laidler, K.J. (1988) Rate controlling step: a necessary or useful concept? *J. Chem. Educ.*, **65** (3), 250.
24. McBane, G.C. (2013) <http://faculty.gvsu.edu/mcbane/chem875.pdf> (accessed 23 March 2016).
25. McNaught, A.D. and Wilkinson, A. (1997) *IUPAC. Compendium of Chemical Terminology (the "Gold book")*, 2nd edn, Blackwell Scientific Publications, Oxford.
26. Buskirk, A. and Baradaran, H. (2009) Can reaction mechanisms be proven? *J. Chem. Educ.*, **86** (5), 551.
27. Lewis, D.E. (2009) Response to "Can Reaction Mechanisms Be Proven?". *J. Chem. Educ.*, **86** (5), 554.
28. Wade, P.A. (2009) Response to "Can Reaction Mechanisms Be Proven?". *J. Chem. Educ.*, **86** (5), 558.
29. Yoon, T. (2009) Response to "Can Reaction Mechanisms Be Proven?". *J. Chem. Educ.*, **86** (5), 556.
30. Andraos, J. (1999) A streamlined approach to solving simple and complex kinetic systems analytically. *J. Chem. Educ.*, **76** (11), 1578.
31. Baginski, E. and Zak, B. (1962) Experiment demonstrating first order kinetics. *J. Chem. Educ.*, **39** (12), 635.
32. Kemp, D.S., Cox, D.D., and Paul, K.G. (1975) Physical organic-chemistry of benzisoxazoles .4. Origins and catalytic nature of solvent rate acceleration for decarboxylation of 3-carboxybenzisoxazoles. *J. Am. Chem. Soc.*, **97** (25), 7312–7318.
33. Kemp, D.S. and Paul, K.G. (1975) Physical organic-chemistry of benzisoxazoles .3. Mechanism and effects of solvents on rates of decarboxylation of benzisoxazole-3-carboxylic acids. *J. Am. Chem. Soc.*, **97** (25), 7305–7312.
34. Grate, J.W., McGill, R.A., and Hilvert, D. (1993) Analysis of solvent effects on the decarboxylation of benzisoxazole-3-carboxylate ions using linear solvation energy relationships – relevance to catalysis in an antibody-binding site. *J. Am. Chem. Soc.*, **115** (19), 8577–8584.
35. Pace, R.D. and Regmi, Y. (2006) The Finkelstein reaction: quantitative reaction kinetics of an S<sub>N</sub>2 reaction using nonaqueous conductivity. *J. Chem. Educ.*, **83** (9), 1344.
36. Tobey, S.W. (1962) Determining second order rate constants. *J. Chem. Educ.*, **39** (9), 473.
37. Esteb, J.J., Magers, J.R., McNulty, L. *et al.* (2009) A simple S<sub>N</sub>2 reaction for the undergraduate organic laboratory. *J. Chem. Educ.*, **86** (7), 850.
38. Horowitz, G. (2009) A safer, discovery-based nucleophilic substitution experiment. *J. Chem. Educ.*, **86** (3), 363.

39. Ryan, J.J. and Humffray, A.A. (1966) Rate correlations involving the linear combination of substituent parameters. Part I. Hydrolysis of aryl acetates. *J. Chem. Soc. B Phys. Org. (O)*, 842–845.
40. Winkler, C.A. and Hinshelwood, C.N. (1935) The factors determining the velocity of reactions in solution. The formation of quaternary ammonium salts in benzene solution. *J. Chem. Soc. (Resumed)*, (0), 1147–1151.
41. Deming, H.G. (1935) The kinetic derivation of the mass action expression. *J. Chem. Edu.*, **12** (4), 195.
42. Alvaro, C.E.S. and Nudelman, N.S. (2010) The “Dimer Nucleophile Mechanism” for reactions with rate-determining first step: derivation of the whole kinetic law and further treatment of kinetic results. *Int. J. Chem. Kinet.*, **42** (12), 735–742.
43. Nawaz, H., Pires, P.R., Bioni, T. *et al.* (2014) Mixed solvents for cellulose derivatization under homogeneous conditions: kinetic, spectroscopic, and theoretical studies on the acetylation of the biopolymer in binary mixtures of an ionic liquid and molecular solvents. *Cellulose*, 1–12.
44. Corbett, J.F. (1972) Pseudo first-order kinetics. *J. Chem. Educ.*, **49** (10), 663.
45. Katritzky, A.R. and Musumarra, G. (1984) New insights into aliphatic nucleophilic substitution reactions from the use of pyridines as leaving groups. *Chem. Soc. Rev.*, **13** (1), 47–68.
46. Arnáiz, F.J. (1999) Mice in the box for zero-order kinetics. *J. Chem. Educ.*, **76** (10), 1458.
47. Hindmarsh, K. and House, D.A. (1996) An easily demonstrated zero-order reaction in solution. *J. Chem. Educ.*, **73** (6), 585.
48. O'Neill, S., Tipton, K.F., Prichard, J.S., and Quinlan, A. (1984) Survival after high blood alcohol levels. Association with first-order elimination kinetics. *Arch. Intern. Med.*, **144** (3), 641–642.
49. Holford, N.G. (1987) Clinical pharmacokinetics of ethanol. *Clin. Pharmacokinet.*, **13** (5), 273–292.
50. Dunford, H.B., Baader, W.J., Bohne, C., and Cilento, G. (1984) On the mechanism of peroxidase-catalyzed chemiluminescence from isobutyraldehyde. *Biochem. Biophys. Res. Commun.*, **122** (1), 28–32.
51. Bastos, E.L., Ciscato, L.F.M.L., Bartoloni, F.H. *et al.* (2007) Studies on PVP hydrogel-supported luminol chemiluminescence: 1. Kinetic and mechanistic aspects using multivariate factorial analysis. *Luminescence*, **22** (2), 113–125.
52. Bartoloni, F.H., Ciscato, L.F.M.L., Peixoto, M.M.D. *et al.* (2011) Light: a rare reaction product. *Quim. Nova*, **34** (3), 544–554.
53. Bechara, E.J.H., Oliveira, O.M.M.F., Duran, N. *et al.* (1979) Peroxidase catalyzed generation of triplet acetone. *Photochem. Photobiol.*, **30** (1), 101–110.
54. Sasso, M.G., Quina, F.H., and Bechara, E.J.H. (1986) Ruthenium(II) tris(bipyridyl) ion as a luminescent probe for oxygen uptake. *Anal. Biochem.*, **156** (1), 239–243.
55. Quijano, C., Alvarez, B., Gatti, R.M. *et al.* (1997) Pathways of peroxydinitrite oxidation of thiol groups. *Biochem. J.*, **322** (1), 167–173.
56. House, D.A. (1962) Kinetics and mechanism of oxidations by peroxydisulfate. *Chem. Rev.*, **62** (3), 185–203.
57. Blackmond, D.G. (2005) Reaction progress kinetic analysis: a powerful methodology for mechanistic studies of complex catalytic reactions. *Angew. Chem. Int. Ed.*, **44** (28), 4302–4320.
58. El Seoud, O.A., Ruasse, M.F., and Rodrigues, W.A. (2002) Kinetics and mechanism of phosphate-catalyzed hydrolysis of benzoate esters: comparison with nucleophilic catalysis by imidazole and o-iodosobenzoate. *J. Chem. Soc. Perkin Trans.*, **2** (6), 1053–1058.
59. Laurie, S.H. (1972) Kinetic stability versus thermodynamic stability. *J. Chem. Educ.*, **49** (11), 746.

60. El Seoud, O.A., El Seoud, M.I., and Farah, J.P.S. (1997) Kinetics of the pH-Independent hydrolysis of bis(2,4-dinitrophenyl) carbonate in acetonitrile–water mixtures: effects of the structure of the solvent. *J. Org. Chem.*, **62** (17), 5928–5933.
61. Dawber, J.G. and Crane, M.M. (1967) Keto-enol tautomerization: a thermodynamic and kinetic study. *J. Chem. Educ.*, **44** (3), 150.
62. Nichols, M.A. and Waner, M.J. (2010) Kinetic and mechanistic studies of the deuterium exchange in classical keto–enol tautomeric equilibrium reactions. *J. Chem. Educ.*, **87** (9), 952–955.
63. Howell, S.J., Ashton, P.R., Spencer, N., and Philp, D. (2001) Exploiting the Curtin–Hammett principle – recognition-mediated acceleration of an aldol reaction. *Org. Lett.*, **3** (3), 353–356.
64. Seeman, J.I. (1983) Effect of conformational change on reactivity in organic chemistry. evaluations, applications, and extensions of Curtin–Hammett Winstein–Holness kinetics. *Chem. Rev.*, **83** (2), 83–134.
65. Seeman, J.I. (1986) The Curtin–Hammett principle and the Winstein–Holness equation: new definition and recent extensions to classical concepts. *J. Chem. Educ.*, **63** (1), 42.
66. Pyun, C.W. (1971) Steady-state and equilibrium approximations in chemical kinetics. *J. Chem. Educ.*, **48** (3), 194.
67. NIST (2013) *NIST, Chemical Kinetics Database*, <http://kinetics.nist.gov/kinetics/index.jsp> (accessed 23 June).
68. Hoops, S., Sahle, S., Gauges, R. *et al.* (2006) COPASI—a COMplex PATHway SIMulator. *Bioinformatics*, **22** (24), 3067–3074.
69. Laidler, K.J. (1984) The development of the Arrhenius equation. *J. Chem. Educ.*, **61** (6), 494.
70. Leenson, I.A. (1999) Old rule of thumb and the Arrhenius equation. *J. Chem. Educ.*, **76** (10), 1459.
71. Carroll, H.F. (1998) Why the Arrhenius equation is always in the exponentially increasing region in chemical kinetic studies. *J. Chem. Educ.*, **75** (9), 1186.
72. Dewar, M.J. and Storch, D.M. (1985) Alternative view of enzyme reactions. *Proc. Natl. Acad. Sci. U.S.A.*, **82** (8), 2225–2229.
73. Dewar, M.J.S. and Storch, D.M. (1989) Anionic substitution at carbonyl carbon. Implications for the chemistry of ions in solution. *J. Chem. Soc. Perkin Trans.*, **2** (7), 877–885.
74. Leffler, J.E. and Grunwald, E. (1989) *Rates and Equilibria of Organic Reactions as Treated by Statistical, Thermodynamic, and Extrathermodynamic Methods*, Dover Publications, New York.
75. Mozurkewich, M. and Benson, S.W. (1984) Negative activation energies and curved Arrhenius plots. I. Theory of reactions over potential wells. *J. Phys. Chem.*, **88** (25), 6429–6435.
76. Singh, T.D. and Taft, R.W. (1975) Novel activation parameters and catalytic constants in aminolysis and methanolysis of p-nitrophenyl trifluoroacetate. *J. Am. Chem. Soc.*, **97** (13), 3867–3869.
77. Swart, E.R. and Leroux, L.J. (1956) The effect of solvent on a simple ion-dipole reaction I. The order and mechanism of the methyl iodide-iodide ion exchange reaction in different solvents. *J. Chem. Soc.*, 2110–2114.
78. El Seoud, O.A. (2007) Solvation in pure and mixed solvents: some recent developments. *Pure Appl. Chem.*, **79** (6), 1135–1151.
79. El Seoud, O.A. (2009) Understanding solvation. *Pure Appl. Chem.*, **81** (4), 697–707.
80. Duggleby, R.G. (1984) Regression analysis of nonlinear Arrhenius plots: an empirical model and a computer program. *Comput. Biol. Med.*, **14** (4), 447–455.
81. Masgrau, L., González-Lafont, À., and Lluch, J.M. (2003) The curvature of the Arrhenius plots predicted by conventional canonical transition-state theory in the absence of tunneling. *Theor. Chem. Acc.*, **110** (5), 352–357.

82. Silvius, J.R. and McElhaney, R.N. (1981) Non-linear Arrhenius plots and the analysis of reaction and motional rates in biological membranes. *J. Theor. Biol.*, **88** (1), 135–152.
83. Truhlar, D.G. and Kohen, A. (2001) Convex Arrhenius plots and their interpretation. *Proc. Natl. Acad. Sci. U. S. A.*, **98** (3), 848–851.
84. Sen, A. and Kohen, A. (2009) Quantum effects in enzyme kinetics, in *Quantum Tunnelling in Enzyme Catalyzed Reactions* (eds R. Allemann and N. Scrutton), Royal Society of Chemistry, London, pp. 164–181.
85. Blackmond, D.G., Rosner, T., and Pfaltz, A. (1999) Comprehensive kinetic screening of catalysts using reaction calorimetry. *Org. Proc. Res. Dev.*, **3** (4), 275–280.
86. Valera, F.E., Quaranta, M., Moran, A. *et al.* (2010) The flow's the thing ... or is it? Assessing the merits of homogeneous reactions in flask and flow. *Angew. Chem. Int. Ed.*, **49** (14), 2478–2485.
87. Logan, S.R. (1996) *Fundamentals of Chemical Kinetics*, Longman, Harlow.
88. El Seoud, O.A. and Martins, M.F. (1995) Kinetics and mechanism of the hydrolysis of substituted phenyl benzoates catalyzed by the o-Iodosobenzoate anion. *J. Phys. Org. Chem.*, **8** (10), 637–646.
89. Quina, F.H. and Bastos, E.L. (2014) Fundamental aspects of quantitative structure-reactivity relationships, in *Encyclopedia of Physical Organic Chemistry* (ed E.J. Cosio).
90. Fjerbaek, L., Christensen, K.V., and Norddahl, B. (2009) A review of the current state of biodiesel production using enzymatic transesterification. *Biotechnol. Bioeng.*, **102** (5), 1298–1315.
91. Baader, W.J., Stevani, C.V., and Bastos, E.L. (2006) Chemiluminescence of organic peroxides, in *PATAI'S Chemistry of Functional Groups*, vol. **2** (ed Z. Rappoport), John Wiley & Sons, Ltd, pp. 1211–1278.
92. Segal, E. (1989) Nonisothermal kinetic analysis-some current problems. *Thermochim. Acta*, **148** (0), 127–135.
93. Vyazovkin, S. and Sbirrazzuoli, N. (2003) Estimating the activation energy for non-isothermal crystallization of polymer melts. *J. Therm. Anal. Calorim.*, **72** (2), 681–686.
94. Stevani, C.V., Campos, I.P.D., and Baader, W.J. (1996) Synthesis and characterisation of an intermediate in the peroxyoxalate chemiluminescence: 4-chlorophenyl O,O-hydrogen monoperoxyoxalate. *J. Chem. Soc. Perkin Trans.*, **2** (8), 1645–1648.
95. Stevani, C.V., Lima, D.F., Toscano, V.G., and Baader, W.J. (1996) Kinetic studies on the peroxyoxalate chemiluminescent reaction: imidazole as a nucleophilic catalyst. *J. Chem. Soc. Perkin Trans.*, **2** (5), 989–995.
96. Albertin, R., Arribas, M.A.G., Bastos, E.L. *et al.* (1998) Organic chemiluminescence: some classroom demonstration experiments. *Quim. Nova*, **21** (6), 772–779.
97. Silva, S.M., Casallanovo, F., Oyamaguchi, K.H. *et al.* (2002) Kinetic studies on the peroxyoxalate chemiluminescence reaction: determination of the cyclization rate constant. *Luminescence*, **17** (5), 313–320.
98. Silva, S.M., Wagner, K., Weiss, D. *et al.* (2002) Studies on the chemiexcitation step in peroxyoxalate chemiluminescence using steroid-substituted activators. *Luminescence*, **17** (6), 362–369.
99. Ciscato, L.F.M.L., Bartoloni, F.H., Bastos, E.L., and Baader, W.J. (2006) Kinetic observation of the chemi-excitation step in peroxyoxalate chemiluminescence. *Luminescence*, **21** (5), 273–273.
100. Ciscato, L.F.M.L., Bartoloni, F.H., Bastos, E.L., and Baader, W.J. (2009) Direct kinetic observation of the chemiexcitation step in peroxyoxalate chemiluminescence. *J. Org. Chem.*, **74** (23), 8974–8979.
101. Augusto, F.A., Bartoloni, F.H., and Baader, W.J. (2012) Peroxyoxalate chemiluminescence in aqueous medium: concurrence between hydrolysis and perhydrolysis. *Luminescence*, **27** (2), 97–97.

102. Baader, W.J., Augusto, F.A., Bartoloni, F.H., and Ciscato, L.F.M.L. (2012) Peroxyoxalate chemiluminescence: mechanisms and applications. *Luminescence*, **27** (2), 98–98.
103. Ciscato, L.F.M.L., Augusto, F.A., Weiss, D. *et al.* (2012) The chemiluminescent peroxyoxalate system: state of the art almost 50 years from its discovery. *Arkivoc*, **391-430**.
104. de Oliveira, M.A., Bartoloni, F.H., Augusto, F.A. *et al.* (2012) Revision of singlet quantum yields in the catalyzed decomposition of cyclic peroxides. *J. Org. Chem.*, **77** (23), 10537–10544.
105. Stevani, C.V., Silva, S.M., and Baader, W.J. (2000) Studies on the mechanism of the excitation step in peroxyoxalate chemiluminescence. *Eur. J. Org. Chem.*, **24**, 4037–4046.
106. Schuster, G.B. (1979) Chemi-luminescence of organic peroxides – conversion of ground-state reactants to excited-state products by the chemically-initiated electron-exchange luminescence mechanism. *Acc. Chem. Res.*, **12** (10), 366–373.
107. Schmitz, G. (1994) The uncertainty of pH. *J. Chem. Educ.*, **71** (2), 117.
108. Seoud, O.A.E., Menegheli, P., Pires, P.A.R., and Kiyan, N.Z. (1994) Kinetics and mechanism of the imidazole-catalysed hydrolysis of substituted N-benzoylimidazoles. *J. Phys. Org. Chem.*, **7** (8), 431–436.
109. Roses, M. (2004) Determination of the pH of binary mobile phases for reversed-phase liquid chromatography. *J. Chromatogr. A*, **1037** (1-2), 283–298.
110. Porras, S.P. and Kenndler, E. (2004) Capillary zone electrophoresis in non-aqueous solutions: pH of the background electrolyte. *J. Chromatogr. A*, **1037** (1-2), 455–465.
111. Bates, R.G. (1969) Practical measurement of pH in amphiprotic and mixed solvents. *Pure Appl. Chem.*, **18** (3), 419–425.
112. Buck, R.P., Rondinini, S., Covington, A.K. *et al.* (2002) Measurement of pH. Definition, standards, and procedures: (IUPAC Recommendations 2002). *Pure Appl. Chem.*, **74** (11), 2169–2200.
113. Bamford, C.H. and Compton, R.G. (eds) (1986) *Electrode Kinetics: Principles and Methodology*, Elsevier, Amsterdam; New York.
114. Bauer, J., Tomišić, V., and Vrkljan, P.B.A. (2012) The effect of temperature and ionic strength on the oxidation of iodide by iron(III): a clock reaction kinetic study. *J. Chem. Educ.*, **89** (4), 540–544.
115. Rolim, G.L., Simoni, J.d.A., Airoidi, C., and Chagas, A.P. (1990) Thermodynamics of interaction between zinc chloride and N,N-dimethylacetamide in 1,2-dichloroethane solution. *J. Braz. Chem. Soc.*, **1** (3), 95–98.
116. Kirby, A.J., Lima, M.F., da Silva, D. *et al.* (2006) Efficient intramolecular general acid catalysis of nucleophilic attack on a phosphodiester. *J. Am. Chem. Soc.*, **128** (51), 16944–16952.
117. Guggenheim, E.A. (1926) On the determination of the velocity constant of a unimolecular reaction. *Philos. Mag.*, **2** (9), 538–543.
118. Barnard, P.W.C. and Smith, B.V. (1981) The Menshutkin reaction: a group experiment in a kinetic study. *J. Chem. Educ.*, **58** (3), 282.
119. Kalidas, C. (2005) *Chemical Kinetic Methods: Principles of Fast Reaction Techniques and Applications*, New Age International.
120. Howard, C.J. (1979) Kinetic measurements using flow tubes. *J. Phys. Chem.*, **83** (1), 3–9.
121. Clark, C.R. (1997) A stopped-flow kinetics experiment for advanced undergraduate laboratories: formation of iron(III) thiocyanate. *J. Chem. Educ.*, **74** (10), 1214.
122. Morelli, B. (1976) A kinetic experiment using a spring powered, stopped-flow apparatus. *J. Chem. Educ.*, **53** (2), 119.
123. Kaufman, F. (1984) Kinetics of elementary radical reactions in the gas phase. *J. Phys. Chem.*, **88** (21), 4909–4917.
124. Socrates, G. (1967) Kinetic study by NMR. *J. Chem. Educ.*, **44** (10), 575.

125. Swinehart, J.A. (1967) Relaxation kinetics: an experiment for physical chemistry. *J. Chem. Educ.*, **44** (9), 524.
126. Christoff, M., Toscano, V.G., and Baader, W.J. (1996) Influence of methoxy substitution on flavonoid photophysics: a steady state and laser flash photolysis study. *J. Photochem. Photobiol. A*, **101** (1), 11–20.
127. Maçanita, A.L., Moreira, P.F., Lima, J.C. *et al.* (2002) Proton transfer in anthocyanins and related flavylum salts. Determination of ground-state rate constants with nanosecond laser flash photolysis. *J. Phys. Chem. A*, **106** (7), 1248–1255.
128. Hippler, M. (2005) Does a photochemical reaction have a kinetic order? *J. Chem. Educ.*, **82** (1), 37.
129. El Seoud, O.A. and Takashima, K. (1998) The spontaneous hydrolysis of methyl chloroformate – a physical chemistry experiment for teaching techniques in chemical kinetics. *J. Chem. Educ.*, **75** (12), 1625–1627.
130. Nawaz, H., Casarano, R., and El Seoud, O. (2012) First report on the kinetics of the uncatalyzed esterification of cellulose under homogeneous reaction conditions: a rationale for the effect of carboxylic acid anhydride chain-length on the degree of biopolymer substitution. *Cellulose*, **19** (1), 199–207.
131. Goldstein, J.H. and Day, R.A. (1954) A kinetic interpretation of the Bouguer-Beer law. *J. Chem. Educ.*, **31** (8), 417.
132. Optical Properties of Cell Window Materials (2013) <http://www.hellma-analytics.com/text/283/en/material-and-technical-information.html> (accessed 13 June).
133. UVFS (2013) <http://www.newport.com/Optical-Materials/144943/1033/content.aspx> (accessed 13 June 13).
134. ES quartz (2013) <http://www.precisioncells.com/extrasil-es-quartz> (accessed 13 June).
135. Wilson, K. and Walker, J.M. (2009) *Principles and Techniques of Biochemistry and Molecular Biology*, 7th edn, Cambridge University Press, Cambridge, UK New York.
136. Goncalves, L.C.P., Trassi, M.A.D., Lopes, N.B. *et al.* (2012) A comparative study of the purification of betanin. *Food Chem.*, **131** (1), 231–238.
137. Goncalves, L.C.P., Di Genova, B.M., Dorr, F.A. *et al.* (2013) Effect of dielectric microwave heating on the color and antiradical capacity of betanin. *J. Food Eng.*, **118** (1), 49–55.
138. Bartoloni, F.H., Goncalves, L.C.P., Rodrigues, A.C.B. *et al.* (2013) Photophysics and hydrolytic stability of betalains in aqueous trifluoroethanol. *Monatsh. Chem.*, **144** (4), 567–571.
139. Bower, N. (1982) Kinetic fluorescence experiment for the determination of thiamine. *J. Chem. Educ.*, **59** (11), 975.
140. Calderon-Ortiz, L.K., Tauscher, E., Bastos, E.L. *et al.* (2012) Hydroxythiazole-based fluorescent probes for fluoride ion detection. *Eur. J. Org. Chem.*, **13**, 2535–2541.
141. Coutinho, A. and Prieto, M. (1993) Ribonuclease T1 and alcohol dehydrogenase fluorescence quenching by acrylamide: a laboratory experiment for undergraduate students. *J. Chem. Educ.*, **70** (5), 425.
142. Barros, T.C., Toma, S.H., Toma, H.E. *et al.* (2010) Polymethine cyanine dyes in beta-cyclodextrin solution: multiple equilibria and chemical oxidation. *J. Phys. Org. Chem.*, **23** (10), 893–903.
143. Berberan-Santos, M.N. and Martinho, J.M.G. (1990) The integration of kinetic rate equations by matrix methods. *J. Chem. Educ.*, **67** (5), 375.
144. Birk, J.P. (1976) The use of log-log plots in the determination of reaction orders. *J. Chem. Educ.*, **53** (11), 704.
145. Gandour, R.D., Coyne, M., Stella, V.J., and Schowen, R.L. (1980) Proton inventory of phthalic anhydride hydrolysis. Comments on analysis of proton-inventory data. *J. Org. Chem.*, **45** (10), 1733–1737.

146. Marquardt, D. (1963) An algorithm for least-squares estimation of nonlinear parameters. *J. Soc. Ind. Appl. Math.*, **11** (2), 431–441.
147. Moré, J. (1978) The Levenberg-Marquardt algorithm: implementation and theory, in *Numerical Analysis*, vol. **630** (ed G.A. Watson), Springer, Berlin Heidelberg, pp. 105–116.
148. Deavor, J.P. (1987) Simplex optimization: a computer program for instrumental analysis. *J. Chem. Educ.*, **64** (9), 792.